TESIS DOCTORAL

Caracterización del material particulado atmosférico y el ozono en un entorno de alta montaña en la cuenca mediterránea occidental

RUBÉN SOLER MORENO

LABORATORIO DE CONTAMINACIÓN
ATMOSFÉRICA

DEPARTAMENTO DE AGROQUÍMICA Y MEDIO AMBIENTE
UNIVERSIDAD MIGUEL HERNÁNDEZ DE ELCHE

El Dr. D. **IGNACIO GÓMEZ LUCAS**, como director del Departamento de Agroquímica y Medio Ambiente de la Universidad Miguel Hernández de Elche,

DOY MI CONFORMIDAD

Para que la presente memoria titulada “Caracterización del material particulado atmosférico y el ozono en un entorno de alta montaña en la cuenca mediterránea occidental”, realizada bajo la dirección del Dr. D. José Francisco Nicolás Aguilera y el Dr. D. Eduardo Yubero Funes, sea presentada por D. Rubén Soler Moreno para optar al grado de Doctor.

Elche, marzo de 2017

El director del Departamento

Dr. D. IGNACIO GÓMEZ LUCAS

El Dr. D. **JOSÉ FRANCISCO NICOLÁS AGUILERA** y el Dr. D. **EDUARDO YUBERO FUNES**, del Departamento de Física y Arquitectura de Computadores,

AUTORIZAN

Que la presente memoria titulada "Caracterización del material particulado atmosférico y el ozono en un entorno de alta montaña en la cuenca mediterránea occidental", realizada en este departamento bajo su dirección, sea presentada por D. Rubén Soler Moreno para optar al grado de Doctor.

Elche, marzo de 2017

Los directores

Dr. D. JOSÉ FRANCISCO NICOLÁS AGUILERA

Dr. D. EDUARDO YUBERO FUNES

AGRADECIMIENTOS

Tras estos últimos años, marcados por grandes cambios, dudas y difíciles elecciones, me queda el buen recuerdo de todas esas personas de excelencia personal, académica y profesional que, de una manera u otra, me han acompañado y ayudado en esta intensa etapa. Me siento especialmente afortunado por la buena voluntad y bondad que ha habido detrás de cada gesto de apoyo recibido. Muchas gracias de todo corazón.

A mis directores José Nicolás y Eduardo Yubero por su paciencia, apoyo y comprensión. Por ese inmejorable ambiente de trabajo.

Al Laboratorio de Contaminación Atmosférica, en especial a Javier, Nuria, Montse y Sandra por haber estado en momentos clave en los que necesité consejo, tomar decisiones o simplemente un empujón. Agradecer, además, el aporte de otros estudiantes y becarios que, de algún modo u otro, han colaborado en la realización de este trabajo.

A Laura y Pau por su ayuda con la parte de la tesis en inglés.

A mi familia por haber sido siempre un ejemplo de constancia, sacrificio y perseverancia.

A Vik y Paula por haber copado todos estos años de risas, ánimos y buenos momentos que, sin duda, me han ayudado siempre a retomar este trabajo con energía. Sin olvidar tan valiosa ayuda con el diseño y formato de la tesis.

A Bea, gran ejemplo de autosuperación y crecimiento personal, por estar siempre a mi lado y ayudarme a buscar la mejor perspectiva a lo inevitable. Esta tesis es tan tuya como mía.

ÍNDICE

RESUMEN

Durante las últimas décadas, se han llevado a cabo numerosos estudios sobre la caracterización del material particulado atmosférico y el ozono, debido principalmente a sus efectos sobre la salud humana, clima, ecosistemas, visibilidad, materiales y patrimonio cultural. No obstante, no en todo tipo de entornos han sido estos contaminantes caracterizados por igual. De hecho, debido al reducido número de estaciones de alta montaña instaladas, se presentan ciertas incertidumbres referentes a su caracterización físico-química, así como en la influencia que determinados procesos de transporte de masas de aire tienen sobre ellos en este tipo de ambientes. Por todo ello, el presente estudio utiliza como plataforma de trabajo una estación de alta montaña de reciente instalación ubicada en el punto más alto de la provincia de Alicante (Pico Aitana, 1558 msnm).

La investigación realizada presenta dos vías de actuación. En primer lugar, la determinación de las concentraciones másica y en número de partículas, así como de sus evoluciones temporales y especiación química en un entorno de elevada altitud y escasa actividad antrópica. Gracias a ello, las concentraciones obtenidas podrían establecerse como referente de fondo para toda la provincia. Para este propósito, además de la estación de montaña, se han empleado estaciones de carácter urbano como marco comparativo de referencia. A este respecto, se ha podido constatar que la concentración en número de partículas finas (N_f) obtenida en las áreas urbanas es el doble que la registrada en la estación de alta montaña, mientras que la relativa a las partículas gruesas (N_c) es similar en ambos entornos. Por su parte, la concentración másica (PM_1) registrada en la estación urbana es unas tres veces mayor a la obtenida en el entorno de montaña.

El análisis y la caracterización de los diferentes transportes de masas de aire que inciden en la estación de alta montaña constituyen la segunda vía de actuación de este trabajo. El objetivo de la misma es determinar la influencia que estas circulaciones presentan sobre el aerosol atmosférico y el ozono. Se ha hecho especial hincapié en el estudio de dos eventos: los episodios de alta contaminación durante los meses más fríos, relacionados con periodos de elevada estabilidad atmosférica, y las intrusiones de polvo sahariano. En relación a los primeros, se han determinado que, aunque complejo, se puede dar un transporte a nivel mesoescalar efectivo de contaminantes desde zonas costeras urbanas hacia la cima si el régimen de brisas es suficientemente intenso y la cumbre reside dentro de la capa límite planetaria. Respecto a las intrusiones de polvo sahariano, se ha cuantificado el descenso en los niveles de O_3 (alcanzando reducciones en su concentración por encima del 15%) y el incremento en las concentraciones de PM_1 y en algunos de sus componentes químicos.

ABSTRACT

Over the last few decades, a great number of studies about the characterization of atmospheric particulate matter and ozone have been performed due to their negative effects on human health, climate, ecosystems, visibility, materials and cultural patrimony. However, these pollutants have not been characterized equally in every type of environment. Due to the lack of high-mountain stations, there are still uncertainties surrounding these pollutants' physical and chemical properties, as well as the influence that the transport of air masses has on their concentration and behaviour in these types of environments. As such, the present study uses as its measuring platform a recently installed high-altitude station (MS), which is located at the highest point in the province of Alicante (Aitana Peak, 1558 m a.s.l.)

The studies we have carried out have two main objectives. Firstly, the particle number and mass concentration of particulate matter, including temporal variations and chemical speciation in a high-altitude environment with scarce anthropic activity, have been determined. These concentrations could be used as a background reference level for the whole province. In order to do this and in addition to the mountain station, urban stations were used as a comparative framework. Results show that fine particle number concentration (N_f) at urban areas was double the concentration registered at the high-mountain station. However, the coarse particle number concentration (N_c) was similar at both urban and high-altitude stations. Regarding particle mass concentration (PM_1), the concentration at an urban station was three times more than the level registered at the mountain station.

The second objective of these studies was the analysis and characterization of the different transports of air masses that had an effect on the mountain station. We aimed at determining the influence of these air mass transports on atmospheric aerosol and the ozone. Two transport events should be highlighted: the severe winter pollution episodes (WREGs) caused by stagnant weather conditions and the Saharan dust outbreaks (SDOs). With regard to the WREGs, results suggest that effective pollutant transport from urban coastal areas inland to the top of the mountain range could take place, particularly when there is sufficient sea-breeze development and the summit is within the planetary boundary layer. Regarding SDOs, ozone reductions were measured that appear to be related to its interaction with mineral dust (reaching reductions in concentration of over 15%). An increase in particle mass concentration (PM_1) and some of its chemical compounds has also been quantified.

1. Introducción

El presente trabajo de investigación se centra en la caracterización del material particulado atmosférico y el ozono en un entorno de alta montaña ubicado en la cuenca mediterránea occidental. Los niveles y evolución temporal de los contaminantes atmosféricos en enclaves de elevada altitud difieren de los registrados en otros ambientes de menor altura y de carácter más urbano. Así mismo, la cuenca mediterránea occidental se caracteriza por una peculiar dinámica atmosférica que da lugar a ciertos episodios de transporte de masas de aire de distinto origen y características. Para proporcionar un marco de referencia a la hora de interpretar los resultados obtenidos en la investigación, a continuación se hará hincapié, tanto en la caracterización de entornos de alta montaña, como en el estado del arte del material particulado y el ozono troposférico. A su vez, se describirán los principales episodios de transporte de masas de aire que tienen lugar en la cuenca mediterránea occidental.

1.1. Estaciones de alta montaña

Aunque es todavía escasa, la instalación de estaciones de medida que caracterizan entornos de fondo regional a elevada altitud está permitiendo afrontar estudios atmosféricos de interés científico, los cuales son difícilmente abordables en estaciones ubicadas a menor altura. Este tipo de estaciones son particularmente adecuadas para estudiar los procesos de transporte a larga distancia, pues la interferencia de fuentes antrópicas es extremadamente baja (Ripoll et al. 2014; Moroni et al. 2015). Así por ejemplo, estas instalaciones son idóneas para determinar de forma nítida el impacto que las intrusiones de polvo procedentes del Sahara tienen sobre los niveles de concentración de partículas (Marinoni et al. 2008) o sobre la reducción en los niveles de ozono troposférico (Bonasoni et al. 2004). Otra de las utilidades que presenta en particular la medición del material particulado atmosférico (PM) en estos enclaves es la obtención de perfiles temporales de concentración, bien en nº de partículas (N) o másica (PM_x), que nos pueden ayudar a discriminar cuál es la verdadera carga de concentración atribuible a un determinado entono urbano o de tráfico.

En el estudio de los componentes atmosféricos en este tipo de ubicaciones, un parámetro a tener en cuenta, cuyo valor puede determinar una mayor o menor conectividad entre la estación de montaña y las zonas urbanas ubicadas a menor altitud, es la altura de la capa de mezcla (MH). El valor de este parámetro puede condicionar un mayor o menor aporte de PM y gases procedentes de focos urbanos al punto de muestreo. Por otra parte, si la estación de montaña está emplazada a suficiente altitud, brinda la posibilidad de describir la troposfera libre, de la cual se posee una caracterización menos extensa. De esta forma, la evolución temporal de MH puede determinar la variabilidad de las concentraciones del PM o de gases como el ozono (O_3) en un determinado enclave de alta montaña, y puede ser determinante para explicar sus cambios estacionales (Segura et al. 2016).

En Europa se cuenta con cierto número de estaciones de alta montaña, en las cuales se miden una gran variedad contaminantes y parámetros físicos y meteorológicos. No obstante, algunas de ellas actualmente no se encuentran operativas, o simplemente no se centran en el estudio del PM y el O_3. Muchas de estas estaciones, junto con otras a nivel mundial, forman parte, bien como estaciones regionales (~400) o globales (31), de la red de

centros de investigación atmosférica pertenecientes al programa GAW (Global Atmospheric Watch). Éste tiene como misión principal entender y controlar el incremento de la influencia de la actividad humana sobre la atmósfera a través de diversos proyectos y programas de investigación. Parte de estas estaciones proporcionan largas series temporales de propiedades ópticas, físicas y químicas del aerosol.

Así mismo, a nivel europeo cabe destacar el Programa ACTRIS-2 (2015-2019) (Aerosols, Clouds, and Trace gases Research InfraStructure), el cual tiene como principal objetivo la integración de las distintas estaciones de medición europeas vanguardistas para la observación a largo plazo de las nubes, aerosol y gases traza en la atmósfera (incluyendo superficie, troposfera y estratosfera). El ACTRIS-2 recibe financiación del programa europeo Horizonte2020 y cuenta con 31 miembros y 79 asociados, la gran mayoría dentro del territorio Europeo. Entre los miembros, se identifican 8 entidades españolas, destacando el Consejo Superior de Investigación Científicas (CSIC), el Centro de Investigaciones Energéticas, Medioambientales y Tecnológicas (CIEMAT) y el centro de investigación atmosférica en Izaña de la Agencia Estatal de Meteorología (AEMET). Además, entre los miembros asociados se encuentran el Laboratorio de Contaminación Atmosférica de la Universidad Miguel Hernández (LCA-UMH), el Centro de Estudios Ambientales del Mediterráneo (CEAM) y la Universidad de Valencia (UA). Más información sobre el programa ACTRIS-2 en su página web oficial: http://actris2.nilu.no/Home.aspx

Como resultado de esta continua monitorización, y dentro del marco de programas como los anteriormente citados, varios estudios han sido llevados a cabo en este tipo de emplazamientos en las últimas décadas. De esta forma, se ha posibilitado la caracterización cualitativa y cuantitativa de contaminantes atmosféricos en estaciones europeas de alta montaña, como en Monte Cimone y Monte Martano en Italia (Van Dingenen et al. 2005; Marenco et al. 2006; Moroni et al. 2015), puy de Dôme en Francia (Sellegri et al. 2003; Freney et al. 2011), Jungfraujoch en Suiza (Cozic at al. 2008; Sjogren et al. 2008) o Izaña y Montsec en España (Alastuey et al. 2005; Ripoll et al. 2014, 2015b).

A modo de síntesis, la tabla 1 recoge las estaciones de alta montaña (h>1400 msnm) europeas operativas de la red GAW, en las que se estudia aerosoles y O_3 actualmente. No obstante, aunque no figuren en la tabla debido a su menor altitud, estaciones como Hohenpeissenberg (HPB) y Schauinland (SIL), en Alemania, son localizaciones de gran interés en las cuales se llevan a cabo investigaciones sobre estos contaminantes. Destacar a su vez estaciones no pertenecientes a la red en las cuales también se realiza una monitorización de contaminantes, como es el caso de la estación de Monte Martano (MTO) en Italia.

El programa EMEP (The European Monitoring and Evaluation Programme) cuenta con diversas estaciones en España consideradas como de fondo regional emplazadas a elevada altitud. Estos emplazamientos son: la estación de Víznar (37°14' N, 3°28' W; 1260 msnm), la cual pertenece a la red GAW, aunque actualmente figura como 'non-reporting station'; Risco Llano (39°31' N, 4°21' W, 1241 msnm) y Campisábalos (41°16' N, 3°09' W; 1360 msnm) en el Centro Peninsular; Peñausende (41°17' N, 5°52' W) en el noroeste; Coratxar (40°41'N, 0°05' E, 1200 msnm), Tagamanent (41°44' N, 02°16' E, 990 msnm) y Morella (40°38' N, 0°05' W, 1150 msnm) en el Este-Nordeste de la península ibérica.

Tabla 1: Información relativa a estaciones de alta montaña europeas de la red GAW en las que se estudia el PM y O_3.

Abreviatura	Estación de montaña	Localización; País	Altitud (msnm)
ZSF	Zugspitze-Schneefernerhaus	47°24'59'' N, 10°58'46'' E; Alemania	2671
ZUG	Zugspitze-Gipfel	47°25'16'' N, 10°59'09'' E; Alemania	2962
BEO	Beo Moussala	42°10' N, 23°35' E; Bulgaria	2925
SUM	Summit	72'34' N, 38°48' W; Dinamarca	3238
CHO	Chopok	48°58' N, 19°36' E; Eslovaquia	2008
MSA	Montsec	42°30' N, 0°43' E; España	1570
IZA	Izaña	28°18' N, 16°30' E; España (I. Canarias)	2400
PDD	Puy de Dôme	45°46' N, 02°57' E; Francia	1450
CMN	Monte Cimone	44°11' N, 10°42' E; Italia	2165
SNZ	Sniezka	50°43' N, 15°43' E; Polonia	1603
JFJ	Jungfrauhoch	46°19' N, 7°35' E; Suiza	3580

La figura 1 ilustra la localización espacial de las estaciones de alta montaña anteriormente mencionadas. Así, se incluye la estación del Monte Aitana (AIT), localización de este estudio, que será descrita posteriormente.

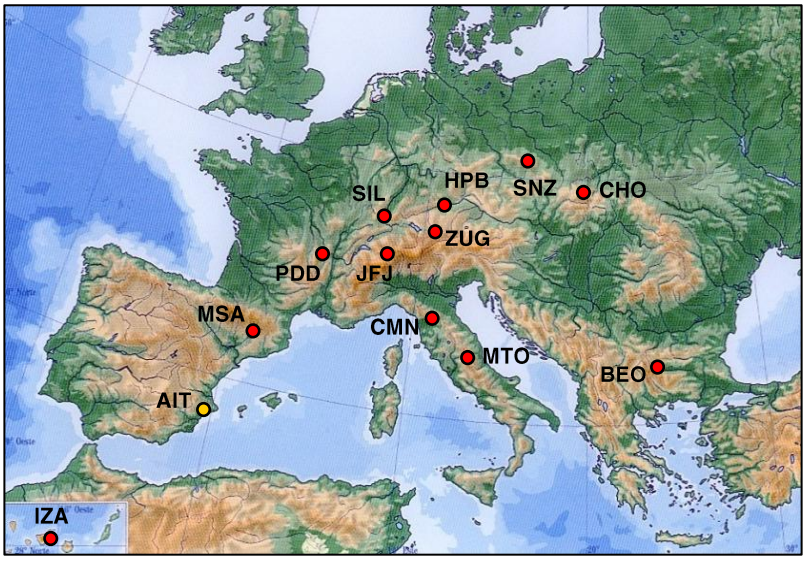

Figura 1: Localización geográfica de diversas estaciones de alta montaña en Europa en las que se monitorizan PM y O_3.

Como se puede observar en la figura 1, Centro Europa cuenta con una gran cantidad de estaciones de alta montaña, en las que se muestrea aerosoles y O_3, localizadas principalmente en Los Alpes, mientras que Europa del Este y la cuenca mediterránea

occidental (Western Mediterranean Basin, WMB) presentan un menor número de estaciones de estas características. Centrándonos en la cuenca mediterránea, se observa que la ubicación geográfica de la estación Aitana hace de este enclave una localización ideal para el estudio de las intrusiones de polvo saharianas (SDOs), debido a su elevada altitud (1558 msnm) y proximidad al continente africano.

1.2. Principales episodios de transporte de masas de aire característicos de la cuenca mediterránea occidental

Aunque todas las estaciones de montaña presentan características comunes (escasez de actividad antrópica, elevada altura sobre el nivel del mar, niveles bajos de concentración en la mayoría de contaminantes respecto a otros tipos de estaciones…), también es cierto que, en función de su particular localización geográfica, pueden verse afectadas por diferentes aportes de contaminantes atmosféricos dependiendo del origen de las masas de aire que los transporten. Por ello, las dinámicas atmosféricas y las fuentes propias de cada región pueden determinar los valores de concentración registrados en estas estaciones así como su variabilidad estacional. En este sentido, el área que nos ocupa en este trabajo, la WMB, se caracteriza por presentar una dinámica atmosférica peculiar que genera una clara estacionalidad en los niveles registrados en este tipo de estaciones. En Querol et al. 2009 se enumeran los principales factores que afectan la característica y compleja dinámica atmosférica del mediterráneo occidental. De forma breve podemos resumirlos en: a) la influencia del anticiclón de las Azores en la meteorología; b) la existencia de cadenas montañosas próximas a la costa mediterránea; c) los débiles gradientes de presión sobre el mediterráneo como consecuencia de las bajas térmicas sobre el Sahara y la península ibérica; d) las intensas brisas favorecidas por condiciones de poca advección y e) la escasa precipitación durante el verano y, en general, el contraste estacional de temperaturas y humedad. De esta forma, en la WMB, el aerosol y gases como el O_3 pueden estar sometidos tanto a efectos producidos por dinámicas de circulaciones de masas de aire a nivel mesoescalar (p.ej. brisas de mar y montaña) como de transporte a nivel sinóptico (p.ej. advecciones de masas de aire procedentes del Atlántico).

Resumimos, a continuación, los principales procesos de transporte que tiene lugar en la región de estudio. Podemos establecer que durante los meses más cálidos las condiciones atmosféricas propician la recirculación de masas de aire (SREG) provocadas por la escasa advección bajo las cuales el PM y los gases (primarios y secundarios), procedentes de áreas urbanas ubicadas en la costa, pueden alcanzar la estación de montaña gracias al régimen de brisas. Esta circulación mesoescalar es usual en la cuenca mediterránea occidental y ha sido ampliamente documentada (Millán et al. 1996; Rodríguez et al. 2002; Jorba et al. 2013). La explicación del proceso recirculatorio se explicará posteriormente con mayor detalle al ilustrar la dinámica del O_3. Así mismo, durante los meses más cálidos, se registran las mayores frecuencias de entradas de polvo procedentes del norte de África. Este transporte, que constituye el principal responsable de las superaciones del valor límite del PM en las estaciones de fondo (Escudero et al. 2007), presenta una tendencia estacional definida por máximos durante el final de la primavera, verano e inicio del otoño y mínimos en el invierno. Un estudio donde se detalla las regiones fuente, así como los patrones atmosféricos que originan estas entradas de polvo mineral sobre la península ibérica, puede verse en Salvador et al. 2014. Aunque estas entradas de masas de aire

tienen lugar a lo largo de todo el año, es durante los meses más fríos cuando la influencia de las advecciones atlánticas (AA) es mayor. Esta circulación trae aire limpio que elimina las masas de aire envejecidas. Del mismo modo, se generan durante los meses de otoño-invierno situaciones de estancamientos de masas de aire asociados a sistemas de altas presiones y débiles gradientes de presión superficiales (WREG). Esta situación favorece la acumulación de contaminantes primarios, además de la formación fotoquímica de aerosoles secundarios. Bajo estas condiciones, el PM registrado en ubicaciones de fondo regional o montaña también puede verse afectado por un proceso de transporte similar al presentado durante los meses cálidos. Un trabajo que ilustra el efecto de este tipo de episodios sobre el PM se puede ver en Pey et al. 2010a. Finalmente, también pueden llegar al área de estudio masas de aire contaminadas procedentes del centro y norte de Europa (EE), aunque su mayor o menor influencia dependerá de la situación geográfica de la estación de medida. En nuestro caso particular, la influencia de este tipo de transporte es mínima.

A continuación, se muestra en la figura 2 las direcciones de transporte preferentes, según el episodio diferencial del que se trate, que pueden llegar a la estación de Aitana.

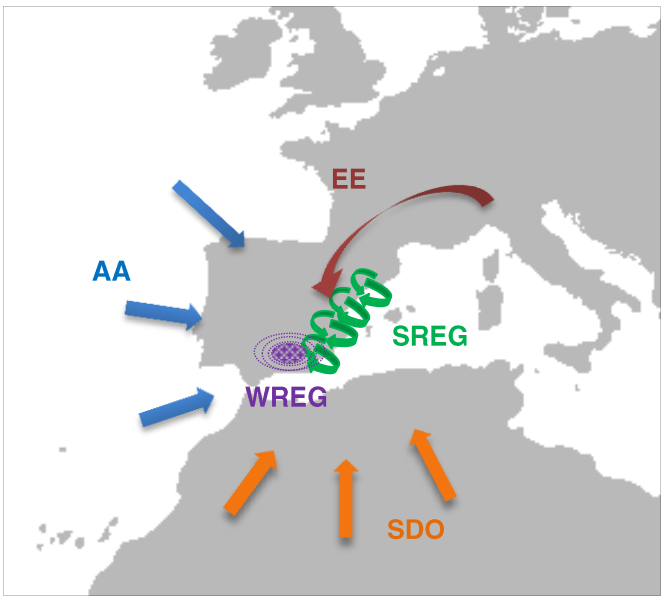

Figura 2: Orígenes de masas de aire que pueden llegar al área de estudio.

En Escudero et al. 2007 y Ripoll et al. 2015a se pueden observar interesantes trabajos relacionados con el efecto de estos episodios atmosféricos sobre el PM realizados en la WMB en estaciones de fondo regional y de montaña.

1.3. Material particulado atmosférico

1.3.1. Generalidades

El material particulado atmosférico en suspensión o aerosol se define como la suspensión de partículas sólidas o líquidas, a excepción del agua pura, en la atmósfera (Mészáros, 1999). El concepto aerosol, o simplemente partícula, hace referencia a una entidad

individual sólida o líquida que contiene gran cantidad de moléculas que permanecen unidas gracias a fuerzas intermoleculares y con tamaños que inicialmente son mayores a las dimensiones de éstas, es decir, aproximadamente superiores a 0,001 micras (µm) de diámetro. También se consideran partículas a dos o más de las anteriores entidades estructurales que permanecen unidas gracias a fuerzas de adhesión entre ellas, de forma que se comportan como una entidad individual en suspensión (Seinfeld y Pandis, 1998). Así, las partículas pueden llegar a presentar diámetros de hasta varias decenas de µm, considerando que a partir de entre 50 o 100 µm se establece la distinción entre material particulado en suspensión y sedimentable. Por tanto, el tamaño de la partícula es un parámetro decisivo que condiciona su tiempo de residencia en la atmósfera.

Las partículas atmosféricas pueden ser emitidas por una gran variedad de fuentes de origen natural (producción biogénica, aerosol marino…) o antropogénico (tráfico, industria…). Respecto a los mecanismos de formación, las partículas pueden ser emitidas como tales a la atmósfera (primarias) o bien ser generadas por reacciones químicas tras su emisión (reacciones secundarias). Dichas reacciones químicas pueden consistir en la interacción entre gases precursores en la atmósfera para formar una nueva partícula por condensación, o entre un gas y una partícula atmosférica para dar lugar a un nuevo aerosol por adsorción o coagulación (Warneck, 1988).

Existen varias formas de cuantificar el PM, en función de que se quiera expresar su concentración por unidad de volumen de aire en: masa ($\mu g \cdot m^{-3}$), volumen ($cm^3 \cdot cm^{-3}$), superficie ($cm^2 \cdot cm^{-3}$) o número de partículas (cm^{-3}).

Los mecanismos de formación y crecimiento de las partículas condicionan la distribución de tamaño de las mismas. Esta distribución suele presentar tres modas características, formadas por la combinación de tres distribuciones log-normal (Whitby, 1978) denominadas modas de Nucleación ($d<0,1$ µm), Acumulación ($0,1<d<1$ µm) y Gruesa ($d>1$ µm). No obstante, también cabe la posibilidad de identificar una cuarta moda, “Aitken” ($0,02<d<0,1$ µm) (Seinfeld y Pandis, 1998). Generalmente, la granulometría, composición química y distribución del material particulado suelen ser característicos del foco emisor.

En función del ámbito de estudio se suele adoptar distintas rangos granulométricos dentro de los grupos de partículas diferenciados. De este modo, en ciencias atmosféricas se engloba como “partículas finas” a todas aquellas cuyo diámetro es inferior a 1 µm y como “partículas gruesas” a las que posean un diámetro superior a 1 µm. En cambio, en el ámbito epidemiológico, esta distinción entre partículas finas y gruesas se encuentra en torno a 2,5 µm de diámetro.

La figura 3 (Viana, 2003) representa las distintas modas identificadas dentro del material particulado atmosférico y los tamaños de partículas que abarcan. La figura hace referencia al n° de partículas en función de las modas. Aunque depende del entorno muestreado, por lo general el n° de partículas como podemos apreciar en la figura, suele distribuirse preferentemente en las modas de acumulación y nucleación, mientras que en la moda gruesa, que registra el menor número de concentración de partículas, se distribuye la mayor proporción de la masa. Las fracciones PM_{10}, $PM_{2.5}$ y PM_1 (recogidas también en la figura 3 y empleadas ampliamente en estudios relacionados con la calidad del aire) se definen como el conjunto de partículas que pasan a través del cabezal de tamaño selectivo para un diámetro aerodinámico de 10, 2.5 y 1 µm, respectivamente, con una eficiencia de corte del 50%.

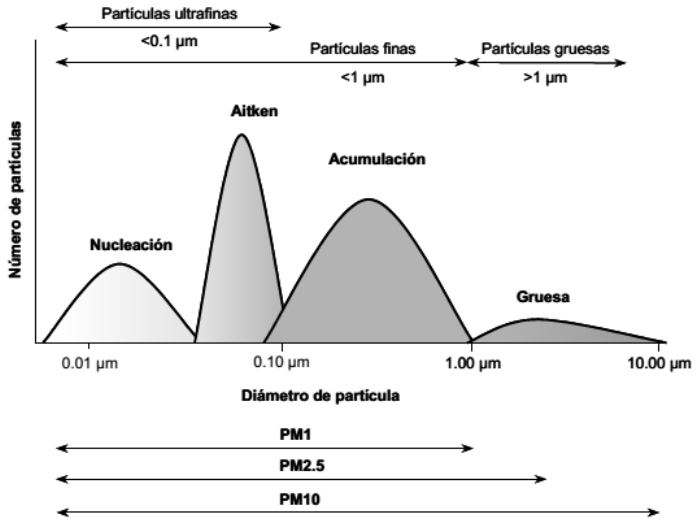

Figura 3: Distribución del número de partículas en función del diámetro (Viana, 2003).

1.3.2. Composición química y fuentes de emisión de PM

El aerosol atmosférico se compone de una gran variedad de compuestos, cuya composición química está relacionada directamente con su origen. La materia particulada está formada en mayor medida de elementos procedentes de la corteza terrestre y del mar, compuestos de carbono, iones secundarios como sulfatos, nitratos y amonio y elementos traza (principalmente metales). A continuación, se describe brevemente estos componentes indicando cuáles son sus principales fuentes de emisión.

Materia crustal

La presencia de partículas minerales en la atmósfera, procedentes de la corteza terrestre, puede ser debido a la resuspensión a escala local o por transporte desde regiones áridas y semiáridas (por ejemplo, las SDOs). Esta componente del PM se caracteriza por una granulometría predominantemente gruesa. El material crustal está principalmente formado por Si, Al, Fe, Na, K, Ca y Mg.

Sales marinas

El aerosol marino es el material resuspendido de océanos y mares. Está compuesto principalmente por cloruro sódico (NaCl) y otras formas de cloruros y sulfatos (MgCl, $MgSO_4$ o Na_2SO_4). Su formación se produce cuando una burbuja de aire en agua estalla, produciendo unas 10 partículas de diámetro entre 2 y 4 µm y unas 200 de tamaño submicrométrico. Únicamente el 10% del aerosol marino es transportado e introducido en el aire continental, el resto se deposita sobre los océanos (debido a su tiempo de residencia).

Compuestos de carbono

Los compuestos de carbono cubren un amplio abanico de especies tanto naturales como antropogénicas. Generalmente, se distingue entre carbono elemental (EC) o Black Carbon y

carbono orgánico (OC). El EC suele ser emitido directamente a la atmósfera por procesos de combustión incompleta, por lo que su origen es principalmente antropogénico. Sin embargo, los compuestos de carbono orgánico pueden ser emitidos directamente a la atmósfera o formarse por condensación de compuestos orgánicos semivolátiles. En ambos casos, su origen puede ser natural o antropogénico. Los compuestos de carbono suelen distribuirse dentro del rango de las partículas más finas.

Compuestos inorgánicos secundarios

Los compuestos inorgánicos mayoritarios son el sulfato, el nitrato y las sales de amonio. Éstos se forman a partir de reacciones de oxidación (en mayor medida por los radicales de OH·) de sus precursores, SO_2 y NO_2, emitidos tanto por fuentes biogénicas como antropogénicas.

Partículas biogénicas

Definen un amplio espectro de partículas biológicas de variados tamaños, en el que se pueden incluir restos vegetales, granos de polen, algas y hongos, etc.

Elementos traza

La emisión de elementos traza a la atmósfera, no incluidos en los anteriores grupos, puede ser de forma natural o antropogénica. Cabe destacar, como otras fuentes de emisión naturales, la resuspensión de polvo, emisiones volcánicas, fuentes biogénicas e incendios forestales.

1.3.3. Efectos del PM

El PM tiene un impacto nocivo sobre la salud humana, el clima, los ecosistemas, la visibilidad, los materiales y el patrimonio cultural, además de consecuencias económicas derivadas. Todos estos efectos están extensamente documentados (WHO, 2013a, 2013b, 2016; EPA, 2016a; IPCC 2013; Pope III y Dockery, 2006; Horemans et al. 2011; Eliseev, 2015; Fuzzi et al. 2015; Singh et al. 2016).

Quizás el más acuciante por sus consecuencias inmediatas sea el impacto sobre la salud humana. De hecho, el material particulado está asociado con un aumento en la morbilidad y mortalidad en núcleos urbanos (WHO, 2013a, 2016). El sistema respiratorio supone la principal vía de entrada del material particulado en el organismo. El alcance y peligrosidad de las partículas, una vez dentro del cuerpo, depende del tamaño, la forma, la densidad, la composición química, el tiempo de exposición, la susceptibilidad y estado de salud del individuo. En este contexto, se le presta gran atención a las partículas de la fracción $PM_{2.5}$ e inferiores, puesto que son capaces de alcanzar la región alveolar y poseen mayor reactividad química que las partículas de mayor tamaño (EPA, 2002).

Los efectos más significativos del PM sobre el clima son la dispersión y la absorción de las longitudes de onda cortas (espectro visible), que tienen como consecuencia la modificación del balance radiativo global (Fuzzi et al. 2015), la reducción de la visibilidad y modificación del albedo (EPA 2002; Zhao et al. 2017; Liu et al. 2014).

1.3.4. Fracción másica PM_1: importancia y composición

La fracción másica PM_1 ha cobrado importancia en los últimos tiempos debido a que, como hemos comentado anteriormente, son las partículas atmosféricas en suspensión de menor tamaño las responsables directas de efectos adversos sobre la salud.

Debemos tener en cuenta que la mayoría de las fuentes de contaminación antropogénica están relacionadas con procesos de combustión de carburantes fósiles y generan partículas con diámetros inferiores a 1 µm. No obstante, las concentraciones elevadas de PM en áreas urbanas provienen, no sólo de dicha emisión directa de fuentes contaminantes, sino también de la formación en la atmósfera de nuevos aerosoles.

Aunque una gran variedad de trabajos se han publicado en las últimas décadas sobre composición química urbana del PM_{10} y $PM_{2.5}$, hay un menor número de investigaciones hasta el momento sobre PM_1, y menos aún si el entorno donde se lleva a cabo el muestreo es un enclave de alta montaña. Además, los estudios sobre especiación de PM_1 son escasos, especialmente en el sur de Europa, y limitados a campañas cortas de medida y/o a emplazamientos de captación singulares, normalmente urbanos (Putaud et al. 2002; Vecchi et al. 2004; Ariola, et al. 2006).

Los resultados experimentales existentes permiten establecer que la fracción PM_1 está casi exclusivamente asociada a fuentes antropogénicas, con componentes carbonosos primarios (EC+OC) y compuestos secundarios, inorgánicos y orgánicos que constituyen la mayor parte (70-80%) de la masa de PM_1 muestreada (Pérez et al. 2008). No obstante, se han encontrado diferencias tanto en masa, como en composición química y en los patrones estacionales dependiendo de las características de los distintos emplazamientos en donde se ha estudiado.

La figura 4 muestra, a modo de ejemplo, la composición química de la fracción PM_1 obtenida en un enclave urbano (ciudad de Barcelona, Pérez et al. 2008).

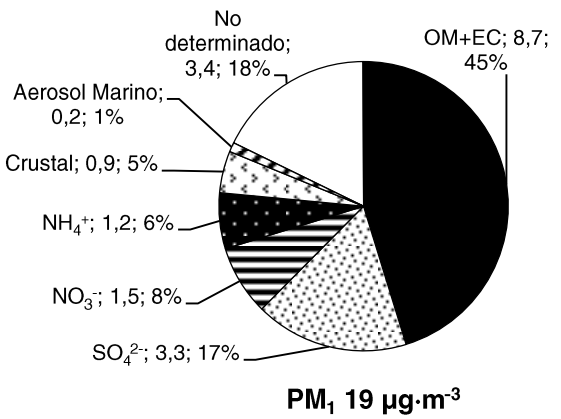

Figura 4: Ejemplo de la composición química de la fracción PM_1 en un entorno urbano.

Otro punto de interés con respecto a la fracción PM_1 es que ~33% de su masa es aerosol orgánico secundario (SOA) (Coury y Dillner, 2009). El SOA está constituido por compuestos

particulados generados a partir de transformaciones atmosféricas de especies orgánicas, cuyo origen es tanto biogénico como antrópico.

1.3.5. Características del PM_1 en estaciones de alta montaña

Los estudios llevados a cabo sobre la tendencia estacional de la fracción PM_1 en ambientes de alta montaña muestran máximos durante el verano y mínimos durante el invierno. La misma tendencia presenta la concentración de partículas finas. Varias son las razones que llevan a este comportamiento estacional, pero, entre ellas, cabe destacar que, durante el invierno, este tipo de estaciones suelen permanecer en la troposfera libre. Además, durante el periodo estival, sobre todo en las estaciones situadas más al sur del continente europeo, los periodos de SDOs son más frecuentes y los de precipitación más escasos.

Por ello, la mayoría de estudios implican a las variaciones estacionales de la capa límite planetaria (Planetary Boundary Layer, PBL) y el diferente origen de las masas de aire, que llegan a los puntos de muestreo según sean invierno o verano, como los principales factores que modulan la estacionalidad de las concentraciones de PM_1. Como ejemplo, a raíz de lo comentado anteriormente sobre la oscilación estacional de las concentraciones de PM_1, las concentraciones en Mt. Cimone/Montsec varían de 1,2/4,1 $\mu g \cdot m^{-3}$, durante el invierno, a los 5,0/7,5 $\mu g \cdot m^{-3}$, de valor promedio durante el verano (Carbone et al. 2014; Ripoll et al. 2015b).

La tabla 2 muestra algunas concentraciones másicas registradas por esta fracción en este tipo de enclaves. Se puede apreciar una reducción de valores bastante ostensible si los comparamos con valores de concentración media de PM_1 obtenidos en entornos urbanos o de tráfico en ciudades mediterráneas como Atenas (19,3 $\mu g \cdot m^{-3}$ promedio primavera-verano; Pateraki et al. 2012) o Elche (12 $\mu g \cdot m^{-3}$ en verano y 16 $\mu g \cdot m^{-3}$ en invierno; Yubero et al. 2015).

Tabla 2: Valores de PM_1 en diversas estaciones de montaña europeas.

Estación de Montaña	Altitud (msnm)	PM_1 ($\mu g \cdot m^{-3}$)	Referencia
Montsec (España)	1570	4.9	Ripoll et al. 2015b
Puy de Dôme (Francia)	1465	3.9	Bourcier et al. 2012
Mt. Martano (Italia)	1100	10.9[a]	Moroni et al. 2015
Mt. Cimone (Italia)	2165	2.4	Carbone et al. 2014

[a]: Valor de $PM_{2.5}$

El patrón horario de la fracción PM_1 en entornos de montaña es poco definido. Éste únicamente presenta un máximo, no muy pronunciado y ancho, entre las 12:00 UTC y las 16:00 UTC aproximadamente, coincidiendo con el periodo de mayor radiación solar y la mayor producción fotoquímica. Esta variabilidad también tiene que ver con el desarrollo de la brisa que puede transportar PM procedente de enclaves urbanos al punto de muestreo. Igualmente, las especies químicas que lo conforman presentan dicha evolución horaria a lo largo del día. Únicamente los aerosoles orgánicos muestran ese máximo de una forma más definida (Ripoll et al. 2015b). La variabilidad horaria descrita anteriormente también es

válida para la concentración en número de partículas finas, como puede verse en Marinoni et al. 2008.

En cuanto a la especiación química del PM_1 en ambientes de alta montaña, se debe comentar que es la materia orgánica su principal constituyente seguido del sulfato y las sales de amonio. Por lo general, todos estos constituyentes presentan valores superiores en verano que en invierno.

En relación a la influencia de los distintos episodios diferenciales sobre el PM_1, comentar que, aunque sabemos que las SDOs afectan principalmente a la fracción gruesa del material particulado, el PM_1 también puede verse afectado, sobre todo si se evalúa en entornos de alta montaña, puesto que el transporte sahariano suele tener lugar a elevadas alturas. Evidentemente el impacto será mayor cuanto más próxima este la estación de medida con el norte de África. De esta forma, en Ripoll et al. 2015 se estima un incremento neto de 2,9 $\mu g \cdot m^{-3}$ en la estación de Montsec. Este incremento está asociado principalmente al aumento de la materia mineral, SO_4^{-2}, NH_4^+, NO_3^-, materia orgánica y EC. Igualmente, se pueden observar incrementos de la concentración de PM_1 durante el transcurso de episodios regionales registrados en periodos cálidos, gracias al mayor desarrollo de la PBL que facilita el transporte de PM hasta enclaves montañosos. Los análisis muestran principalmente incrementos en sulfato, materia orgánica, EC y ciertos elementos traza. Por el contrario, las advecciones atlánticas generan el efecto contrario en las concentraciones de PM_1 que los dos anteriores eventos, puesto que renuevan las masas de aire envejecido y suelen ir acompañadas de precipitaciones. Finalmente, durante los WREG los niveles de concentración también pueden incrementarse aunque no de una manera tan intensa como en los entornos urbanos. En Pey et al. 2010b se establece un incremento promedio en la estación de fondo regional Montseny (720 msnm en dirección NNE de Barcelona) de unos 3 $\mu g \cdot m^{-3}$.

1.4. El ozono

1.4.1. Generalidades

El ozono es una sustancia gaseosa compuesta por tres átomos de oxígeno (O_3), de color azulado, olor penetrante y muy inestable. El O_3 se descompone fácilmente liberando oxígeno molecular y oxígeno atómico. Esto hace de éste un compuesto altamente oxidante y agresivo.

En la atmósfera, el 90% del O_3 se encuentra en la estratosfera, alcanzando concentraciones máximas en torno a 10 $mg \cdot m^{-3}$ a una altitud de 25-30 km. Este ozono estratosférico conforma la denominada capa de ozono, la cual actúa como barrera de radiaciones nocivas para la vida en la tierra, la radiación UV-B y UV-C ($200<\lambda<320$ nm), procedentes del sol. En la estratosfera, la formación de ozono tiene lugar por combinación del oxígeno atómico, liberado por fotólisis ($\lambda<242$ nm, UV) en capas superiores, y el oxígeno molecular (Seinfeld y Pandis, 1998) siguiendo las siguientes reacciones fotoquímicas (hv es la radiación solar y M un compuesto que absorbe la energía liberada, generalmente N_2 u O_2):

$$O_2 + hv \rightarrow O + O$$

$$O + O_2 + M \rightarrow O_3 + M$$

En la troposfera, en ausencia de otros contaminantes, se produce un equilibrio entre la producción y destrucción de O_3, siguiendo el siguiente ciclo estacionario (figura 5):

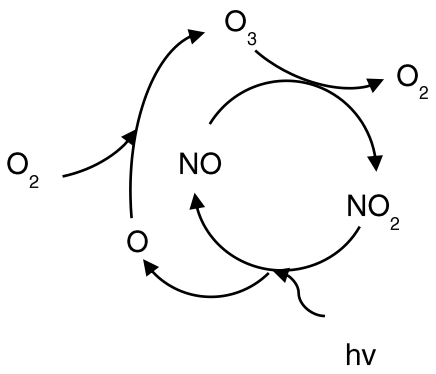

Figura 5. Ciclo natural del ozono en la troposfera.

No obstante, el O_3 troposférico, es un contaminante secundario que se produce principalmente por las reacciones fotoquímicas entre óxidos de nitrógeno, compuestos orgánicos volátiles (COV) y oxígeno (Seinfeld y Pandis, 1998). Los COVs alteran el ciclo del O_3 puesto que desencadenan la formación de radicales hidroperoxi HOO· y peroxi ROO·. Éstos son capaces de oxidar el NO, dando lugar a una acumulación de O_3 en la troposfera. La siguiente figura representa la interferencia de los COVs en el ciclo del O_3 y su consecuente acumulación (figura 6).

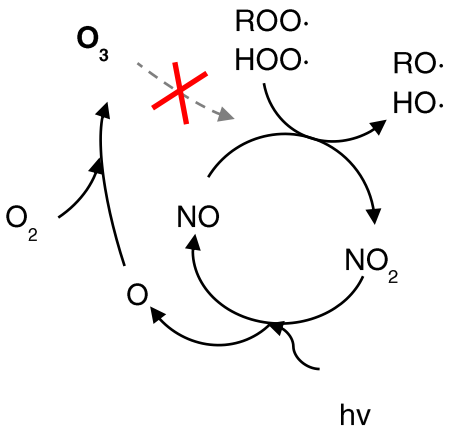

Figura 6. Alteración del ciclo natural del O_3 y su acumulación.

La formación del O_3 troposférico se produce principalmente en entornos urbanos, donde la contaminación por óxidos de nitrógeno y COVs es mayor debido a fuentes antropogénicas como el tráfico rodado, quema de combustibles fósiles, la actividad industrial y empleo de disolventes, o en áreas donde los precursores han sido transportados por el viento. Así mismo, cabe destacar la emisión de COVs, como el isopreno, por fuentes biogénicas. La

fuerte dependencia de los ciclos del nitrógeno y O_3 a la radiación solar y la importancia de la dinámica atmosférica en el transporte de las masas de aire, hacen que la radiación solar y los parámetros meteorológicos sean de gran relevancia para el estudio del O_3 en zonas de alta montaña.

1.4.2. Efectos del ozono

Numerosos estudios e informes documentan el efecto que tienen elevados niveles de O_3 sobre la salud humana, la vegetación natural, cultivos y los materiales (WHO, 2016; EPA, 2016b; Yan et al. 2016; Bromberg, 2016; Paoletti, 2006; Ashmore, 2015; Mills et al. 2016; Druzik, 1985; Cass et al. 1989).

Según la Organización Mundial de la Salud (OMS-WHO) un exceso de ozono en aire ambiente puede causar problemas respiratorios, desarrollar asma, reducir la actividad pulmonar y otras enfermedades pulmonares (WHO 2013b, 2016, EPA, 2016b). La alteración de los ciclos del nitrógeno y O_3, con la consecuente producción y acumulación de agentes oxidantes como el O_3, PAN, aldehídos y HNO_3 pueden desembocar en episodios nocivos para la salud y el medio ambiente como son el smog fotoquímico y lluvia ácida.

1.4.3. Caracterización del ozono en ambientes de elevada altitud

En entornos de alta montaña, los niveles de O_3 presentan un ciclo estacional caracterizado por valores elevados a lo largo de la primavera y verano, y mínimos en otoño. Los acusados incrementos en los niveles de O_3 registrados durante la primavera están vinculados, por un lado, a la intensa producción fotoquímica de O_3 por la acumulación de precursores durante el invierno y el incremento de radiación solar y, por otro, al aumento de la frecuencia de intrusiones de ozono estratosférico. La figura 7 recoge los valores medios mensuales de concentración de O_3 en diferentes estaciones de alta montaña.

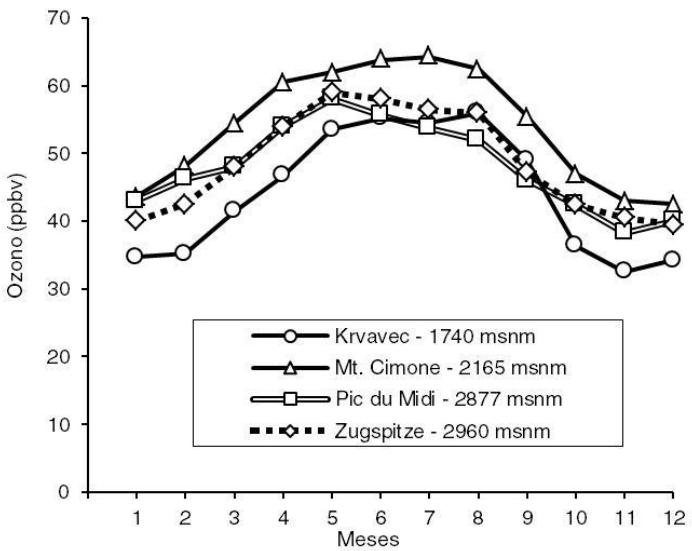

Figura 7. Concentraciones mensuales medias de O_3 en varias estaciones de alta montaña europeas (Adaptado de Scheel et al. 1997).

El ciclo diario del O_3 se caracteriza por valores de concentración máximos a mediodía (mayor producción fotoquímica debido a una mayor radiación solar), un descenso por la tarde y mínimos durante la noche (ausencia de producción fotoquímica). La figura 8 ilustra, a nivel horario, las variaciones estacionales del O_3 obtenidas en la localidad de Buitrago de Lozoya en Madrid, en una estación situada a 975 m de altitud (Alonso et al. 2009).

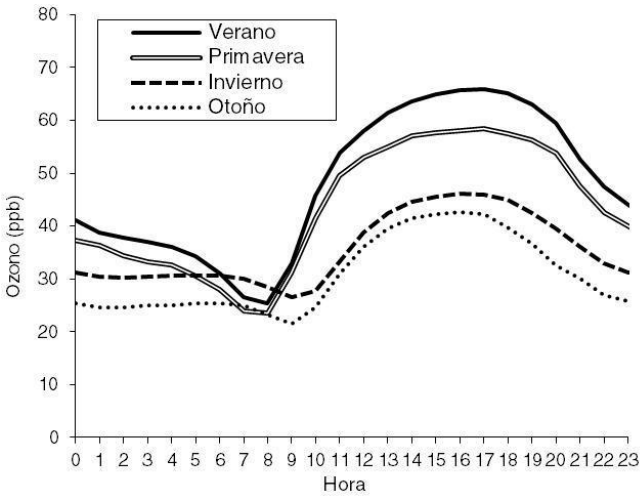

Figura 8: Variación diaria y estacional de la concentración de O_3 troposférico. Ciclo diario medio obtenido en la localidad de Buitrago del Lozoya (975 m de altitud, Madrid) durante las distintas estaciones del año (promedio 2004-2006). (Fuente CIEMAT, adaptado de Alonso et al. 2009).

En cuanto a la distribución espacial, el O_3 se encuentra en mayores concentraciones en las zonas rurales frente a las urbanas, difiriendo con el resto de contaminantes atmosféricos. Esto es debido a que, por un lado, las elevadas emisiones de NOx, procedentes del tráfico rodado, promueven el consumo de O_3 en las zonas urbanas y, por otro, a la producción fotoquímica de O_3 en el proceso de transporte y dispersión de otros contaminantes como los COVs hacia zonas rurales.

En escenarios costeros, la concentración de O_3 y su distribución espacial se encuentra fuertemente condicionada por la topografía, el régimen de brisas y los procesos de recirculación. Así, durante el día, las brisas marinas, junto con vientos de ladera, transportan contaminantes emitidos por los núcleos urbanos costeros hacia el interior, siguiendo la orografía. Durante este transporte, además, tiene lugar una producción fotoquímica del O_3 por reacción entre sus precursores, que tienden a acumularse en las capas atmosféricas más elevadas. Al atardecer, se produce una inversión en la dirección de las brisas dominantes y un descenso en la altura de capa de mezcla que da lugar a un desplazamiento de las capas ricas en O_3 ladera abajo hacia el mar, acumulándose a cierta altitud. Al amanecer, estas capas estratificadas enriquecidas en O_3 son, de nuevo, transportadas por las brisas marinas hacia el interior. La prolongación de este proceso de recirculación conduce a un incremento paulatino de los niveles de O_3. Las capas en altura enriquecidas en ozono pueden además desplazarse largas distancias desembocando en problemas de contaminación a escala regional (Millán et al. 2006).

En cuanto a su distribución en vertical, las concentraciones de O_3 aumentan con la altitud alrededor de 30 ppb a lo largo del primer kilómetro y, a partir de éste, continua el incremento con un gradiente medio alrededor de 3 ppb·km^{-1}. Esto se debe por un lado a la influencia de las masas de aire desde la estratosfera (Chevalier et al. 2007) y el régimen de viento de ladera en las zonas montañosas que hace que se produzcan las reacciones fotoquímicas durante el transporte en altura. Así mismo, el perfil diario del O_3 también se ve afectado por la altitud. Éste se caracteriza, a medida que aumenta la altitud, por mayores niveles de O_3, una menor oscilación diaria, un desplazamiento de los máximos hacia las últimas horas de la tarde y una menor disminución de las concentraciones. Esta moderada caída de los niveles de O_3 durante la noche se debe al descenso vertical de la masa de aire cuando se invierte la dirección del viento. La figura 9 recoge los valores horarios medios de O_3 durante el mes de junio 2006 en tres emplazamientos a distinta altitud en la comunidad de Madrid.

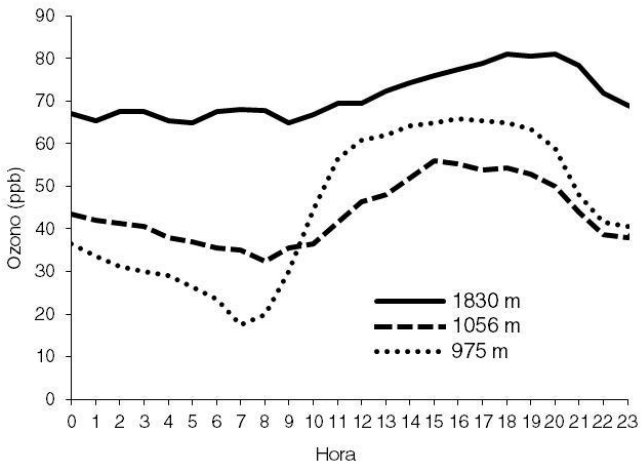

Figura 9: Variaciones diarias de O_3 troposférico con la altitud en la Comunidad de Madrid durante el mes de junio de 2006. (Fuente: Ministerio de Agricultura, Alimentación y Medio Ambiente. Informe sobre el O_3 troposférico y sus efectos en la vegetación).

1.4.4. Influencia de las SDOs sobre el O_3

Numerosos estudios (Prospero et al. 1995; Dentener et al. 1996; Dickerson et al. 1997; Bauer et al. 2004) han analizado los mecanismos por los que el aerosol mineral puede influir, directa o indirectamente, sobre las concentraciones de gases atmosféricos. Las partículas minerales juegan un papel importante en la reducción de los niveles de O_3, ya que es en su superficie donde tienen lugar numerosas reacciones químicas (Adame et al. 2015). De acuerdo con esto, las SDOs, cargadas de polvo mineral, pueden llegar a afectar considerablemente las concentraciones de O_3 y otros gases atmosféricos (Dentener et al. 1996; Hanisch and Crowley, 2003).

Diversos estudios sugieren que en la interacción del ozono troposférico con la partícula de polvo mineral, debido a su elevada área superficial, se produce una absorción directa del gas en la superficie del aerosol. Esta absorción directa del gas está considerado el mecanismo principal en la reducción de las concentraciones de O_3. No obstante, el aerosol

mineral, además, puede interferir indirectamente en la formación de ozono troposférico por interacción con sus precursores. En relación a esto, Harrison et al. 2001 sugieren que el consumo de HNO_3 sobre partículas minerales puede hacer disminuir una fracción de precursores del ozono, como pueden ser los NOx, favoreciendo así una reducción en la eficiencia de la producción fotoquímica del O_3. En de Reus et al. 2000 se establece que la reducción de O_3 está principalmente asociada a la eliminación directa de O_3 por parte del material mineral y el agotamiento de precursores como el HNO_3.

Una de las grandes ventajas del estudio de estas interacciones a elevadas altitudes, es que se evidencian las SDOs con mayor nitidez. En relación a estudios centrados en la cuantificación de la reducción de O_3 en presencia de SDOs, Bonasoni et al. 2004 registran en Monte Cimone (Italia) reducciones de entre el 4 y el 21% en los niveles de O_3 durante SDOs. Así mismo, en Umann et al. 2005 se observan reducciones de O_3 del 30% en la estación de Izaña (Islas Canarias).

2. Objetivos

El objetivo general de la presente tesis es cuantificar y analizar la diferencia de concentración en n° de partículas y concentración másica (PM_1) entre emplazamientos costeros urbanos y un entorno de alta montaña, ubicados en la costa mediterránea española. Se hará hincapié en la determinación de la influencia de ciertos episodios de transporte de masas de aire sobre las concentraciones obtenidas de material particulado y O_3. Este objetivo principal se desglosa en los siguientes objetivos específicos:

- Estudio de los patrones estacionales de las concentraciones másica y del n° de partículas en los enclaves escogidos.

- Análisis en profundidad de la estación de alta montaña: caracterización de las masas de aire que llegan, composición química del PM_1 y meteorología.

- Estudio de las condiciones meteorológicas propicias para la observación del impacto sobre los niveles de material particulado en la estación de montaña debido a un episodio de alta contaminación invernal, asociado a una elevada estabilidad atmosférica.

- Cuantificación del impacto sobre el material particulado (incremento) y el O_3 (reducción) producido por las SDOs en la estación de alta montaña.

3. Área de estudio, materiales y métodos empleados

3.1. Enclaves de muestreo

El presente estudio cuenta con tres emplazamientos de muestreo que representan diferentes ambientes atmosféricos: el Monte Aitana (MS), que se corresponde con un entorno de fondo regional de montaña, un emplazamiento de fondo urbano localizado en la ciudad de Elche (US1) y, por último, una estación suburbana a las afueras de la ciudad de Alicante (US2). El periodo de estudio abarca desde octubre de 2010 hasta septiembre de 2012.

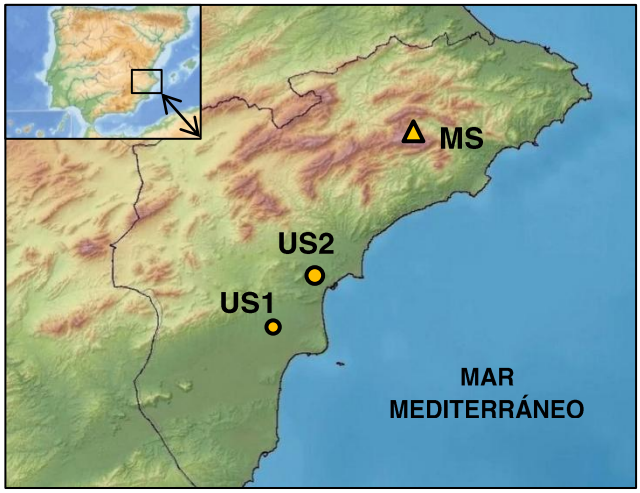

Figura 10. Localización geográfica de los emplazamientos de muestreo en la WMB.

El Monte Aitana (MS: 38°39' N; 0°16' W; 1558 msnm), enclave principal del estudio, es la cumbre más elevada de la Cordillera Bética en el sureste de la península ibérica. Ésta se encuentra a 25 km de la costa mediterránea y 300 km del punto más cercano del continente Africano. La estación de muestreo se encuentra dentro de la estación militar EVA n° 5 del Ministerio de Defensa de España. En Caballero et al. (2007) se recoge una breve descripción a nivel orográfico y geográfico de la región de estudio.

La zona se corresponde con un entorno de fondo regional de alta montaña caracterizado por una práctica ausencia de actividad antropogénica (ver figura 11). Su localización en la WMB y proximidad a África hacen de ella un enclave susceptible de verse afectada por diferentes episodios diferenciales tales como intrusiones de polvo sahariano y episodios de recirculación. La estación del Monte Aitana forma parte de la red de estaciones de monitorización del programa ACTRIS-2.

El segundo enclave de muestreo (US1: 36°16' N; 0° 41' W; 95 msnm) se corresponde con un ambiente de fondo urbano en la ciudad de Elche. La estación está ubicada en el tejado de un edificio de la Universidad Miguel Hernández, a una altura de 15 metros sobre el suelo y situado a 200 y 500 metros de dos vías de tráfico principales.

El tercer emplazamiento de muestreo (US2: 38°21' N; 0°30' W; 20 msnm) se trata de la estación de Rabassa (Alicante), la cual pertenece a la Red de Vigilancia de Contaminación Atmosférica y Calidad del Aire de la Comunidad Valenciana (RVCCA). Este emplazamiento se encuentra a las afueras de la ciudad de Alicante, próximo a una de las vías de entrada al núcleo urbano y a 2 km de la costa.

Figura 11. Estación MS emplazada en la cima del Monte Aitana.

3.2. Monitorización de PM, O_3 y variables meteorológicas

En el presente apartado se recoge una breve descripción de la instrumentación de medida, las herramientas informáticas empleadas y las fuentes de información de utilidad para la identificación de los distintos episodios diferenciales estudiados.

3.2.1. Medición de material particulado

La medida de concentraciones de PM en n° de partículas se ha llevado a cabo empleando dos contadores ópticos por dispersión de luz GRIMM modelo 190 (figuras 12 y 13) en la estación MS y modelo 365 en el emplazamiento US1. Éstos llevan a cabo una medición en continuo de partículas en aire y clasificación en función del diámetro aerodinámico de partícula.

El espectrómetro puede registrar la concentración de partículas en cuentas (n° partículas·m^{-3}, en función del diámetro de partícula), en concentración másica (µg·m^{-3}, en función del diámetro de partícula) o en fracciones PM_1, $PM_{2.5}$ y PM_{10} (µg·m^{-3}).

Los contadores de partículas utilizan una fuente de luz de alta intensidad (un láser), un flujo de aire controlado (volumen de visualización) y detectores de acumulación de luz altamente sensibles (un fotodetector). El sistema almacena medidas de concentración de partículas

cada 6 segundos. Las partículas son registradas en 31 canales o rangos de partículas distintos que van desde 0,25 a más de 32 µm. En las figuras 12 y 13 se puede observar el contador de partículas GRIMM 190, localizado en la estación MS.

Figuras 12 y 13. Contador de partículas GRIMM 190 y su entrada y sensores meteorológicos en la estación de Aitana.

La captación de material particulado (PM_1) en la estación MS se llevó a cabo mediante un captador de partículas de alto volumen MCV CAV-A/MSb con un cabezal PM_1-CAV (figuras 14 y 15), el cual selecciona el conjunto de partículas con diámetro inferior a 1 µm. Es un sistema de captación compuesto por un conjunto de aspiración con bomba centrífuga y circuitería de control electrónico del sistema. La estructura externa es de poliéster-fibra de vidrio. Las muestras de 24 horas quedan recogidas en filtros de fibra de cuarzo Pallflex de 150 mm de diámetro. La masa de material particulado contenido en el filtro es determinada posteriormente a partir del análisis gravimétrico.

Figuras 14 y 15. Captador de alto volumen MCV CAV-A/MSb y cabezal PM_1 en la estación de Aitana.

En relación al emplazamiento US2, la concentración de material particulado (PM_1) se ha determinado mediante el empleo de un contador de partículas GRIMM modelo 180A.

3.2.2. Medición de ozono

En relación al emplazamiento MS, la concentración de O_3 se ha determinado por fotometría UV, empleando un analizador de ozono en continuo Dasibi modelo 1008 UV (figura 16). El principio de medida se basa en la determinación de la radiación ultravioleta atenuada por parte del ozono contenido en la muestra de aire. El instrumento consta de una lámpara de luz UV, un detector, una célula o cámara de absorción, bomba(s) y válvula(s) de absorción, un medidor de flujo y accesorios y tuberías de teflón o PVDF. El flujo de bombeo es de 2 $L \cdot min^{-1}$. El analizador almacena valores de concentración de O_3 cada 10 segundos.

Figura 16. Analizador de Ozono Dasibi 1008 UV.

3.2.3. Meteorología

Las estaciones meteorológicas MS y US2 proporcionan datos de temperatura, velocidad y dirección de vientos, radiación solar, precipitaciones, presión y humedad relativa. En relación a la estación US1, por un lado, la temperatura, presión y humedad relativa son obtenidas a partir del contador de partículas y, por otro, la radiación solar, velocidad y dirección de viento son facilitadas por la estación "Polígono Agroalimentari" (38°40' N, 0°41' W, 44 msnm) de la RVVCA, situada 2 km al sur del punto de muestreo.

3.3. Análisis de muestras de partículas atmosféricas

Los filtros empleados en el muestreo de partículas atmosféricas se someten posteriormente a análisis gravimétrico, cromatográfico y termo/óptico con el objetivo de determina la concentración másica y composición química del PM_1. A continuación, se recoge las técnicas empleadas.

3.3.1. Gravimetría

La concentración másica del PM_1 se ha obtenido por análisis gravimétrico empleando una balanza electrónica Ohaus modelo AP250D con una sensibilidad de 10 µg. Todos los filtros han sido previamente condicionados durante al menos 24 horas a una humedad relativa del

50 ± 5% y temperatura de 20 ± 1°C. Tras la medida, los filtros fueron almacenados en un refrigerador a 4°C hasta su extracción y análisis químico.

3.3.2. Cromatografía iónica

De cada filtro, se ha tomado dos porciones circulares de 15 mm de diámetro y extraído con 15 mL de agua miliQ durante 20 minutos mediante sonificación. Las muestras líquidas son analizadas por cromatografía iónica para la determinación de los aniones (Cl^-, NO_3^-, SO_4^{2-}, $C_2O_4^{2-}$) y cationes mayoritarios (Na^+, NH_4^+, K^+, Mg^{2+}, Ca^{2+}).

La determinación de aniones y cationes se ha realizado por separado, empleando dos cromatógrafos. El cromatógrafo iónico empleado para la determinación de los aniones es un Dionex DX-120 equipado con una columna AS11-HC 250x4mm y un supresor químico ASRS-300 4 mm y KOH 15 mM como eluyente. La determinación de cationes se ha realizado a partir de un cromatógrafo iónico Dionex ICS-1100 equipado con una columna CS12A 4x250 mm, un supresor CSRS-300 4 mm y ácido metanosulfónico (CH_4O_3S) 20 mM como eluyente. El límite de detección empleado se calculó como el valor triple de la desviación estándar de los blancos.

3.3.3. Análisis termo/óptico

El OC y EC fueron determinados por análisis termo/óptico empleando un Analizador de Carbono de Sunset Laboratory, siguiendo el protocolo NIOSH 5040 (Birch y Cary, 1996). La técnica presenta un límite de detección de 0,2 $\mu g \cdot m^{-3}$ y una precisión de ±5%.

3.4. Modelos predictivos y bases de datos empleados

En el proceso de identificación de distintos eventos se emplean varios modelos predictivos. Estas herramientas nos permiten estimar la magnitud de numerosos fenómenos que se dan en todo momento a distintas escalas, como es el caso del comportamiento de las masas de aire a nivel local, regional o global. A continuación, se recogen las distintas herramientas informáticas y bases de datos utilizadas en el proceso de identificación y evaluación de los distintos eventos. Muchas de las empleadas están contempladas en la metodología para la identificación y cuantificación de la contribución de las intrusiones de polvo sahariano (Querol et al. 2006), desarrollada en España y Portugal.

3.4.1. Modelo NAAPS-NRL

Se han empleado mapas de aerosoles de la Marine Meteorology Division del Naval Research Laboratory, USA (NRL) (http://www.nrlmry.navy.mil/aerosol). El NAAPS consiste en un sistema global de modelado y análisis multicomponente que pronostica concentraciones de polvo mineral, sulfato y materia carbonosa en superficie y espesor óptico en la troposfera. Éste sistema combina datos reales de satélites con información relativa a predicciones y simulaciones.

Entre los servicios que se ofrecen en la página web, se destacan las opciones de observaciones de aerosoles, simulaciones de aerosoles, análisis vía satélite y modelado de condiciones atmosféricas.

3.4.2. Modelo BSC-DREAM

El modelo BSC-DREAM8b v2.0 (Basart et al. 2012) es un modelo diseñado para simular o predecir el ciclo atmosférico del polvo mineral. Pertenece a la División de Ciencias de la Tierra del Centro Nacional de Supercomputación de Barcelona BSC-CNS. La página web a partir de la cual se puede acceder al modelo es:

http://www.bsc.es/projects/earthscience/BSC-DREAM/

El BSC-DREAM consiste en un modelo euleriano tridimensional en cuyas celdas se resuelve la ecuación de continuidad de la masa en derivadas parciales no lineales para la determinación de la concentración de polvo. El cálculo de los flujos de inyección de polvo se realiza en las celdas del modelo declaradas como desiertos. La trayectoria del polvo es determinada asumiendo el transporte turbulento en las primeras fases del ciclo, cuando el polvo se eleva desde el suelo hasta niveles sinópticos. Posteriormente, el transporte de material particulado a otras zonas se ve gobernado por la circulación de los vientos dominantes modelados.

Este modelo ofrece la posibilidad, entre otros servicios, de realizar predicciones sobre concentración de materia particulada en superficie, deposición de polvo atmosférico, concentración de material particulado en la sección vertical, carga de polvo y nubosidad.

3.4.3. Modelo HYSPLIT

El sistema HYSPLIT (Draxler and Rolph, 2015) es un modelo de simulación de procesos de dispersión y deposición empleado para modelar el transporte de masas de aire. Es un servicio del Laboratorio de Recursos Atmosféricos (Air Resources Laboratory - ARL) de la Administración Nacional Oceánica y Atmosférica (National Oceanic and Atmospheric Administration - NOAA) de los Estados Unidos. Este sistema surge como resultado de un esfuerzo conjunto entre la NOAA y la Oficina de Meteorología de Australia. Se puede acceder a este modelo desde la página del NOAA-ARL: http://www.ready.noaa.gov

El modelo de cálculo es un híbrido entre aproximaciones eulerianas y langragianas, donde los cálculos asociados a procesos de advección y difusión se hacen bajo un entorno langragiano mientras que las concentraciones de contaminantes se calculan sobre retículas fijas (modelo euleriano).

Este producto ofrece la posibilidad de realizar predicciones de trayectorias y retrotrayectorias de masas de aire, la estimación de concentración de contaminantes, su emisión, transformación, transporte y deposición, así como la representación de diferentes parámetros meteorológicos.

3.4.4. Reanálisis NCEP/NCAR

Se ha hecho uso de mapas meteorológicos procedentes de la Agencia Estatal de Meteorología (AEMET) y del National Centers for Environmental Prediction – NCEP. El NCEP-NCAR Reanalysis (Kalnay et al. 1996) consiste en una base de datos en continua actualización sobre diferentes parámetros meteorológicos y predicciones de modelo climáticos globales. Se puede acceder al modelo desde la página web del Earth System Research Laboratory (ESRL) del NOAA: http://www.esrl.noaa.gov

Este sistema permite realizar predicciones sobre alturas geopotenciales, presión atmosférica al distintas alturas, presión a nivel del mar, velocidad de vientos a distintas alturas, temperatura y precipitaciones.

3.4.5. Modelo ECMWF

El análisis meteorológico se ha apoyado, además, en los mapas de predicción meteorológica del modelo numérico europeo ECMWF (Woods, 2006), desarrollado por el *European Centre for Medium-Range Weather Forecasts* (ECMWF), asociación intergubernamental independiente compuesta por 34 países. Se puede acceder a este modelo a partir de la página web de la Comunidad Portuguesa de Meteorología, Climatología e Medio Ambiente: http://www.meteopt.com

3.4.6. Modelo SKIRON

A partir del modelo SKIRON (Kallos et al. 1997) se han obtenido mapas de concentración de aerosoles cada 12 horas y predicciones de hasta 72 horas. Se puede acceder al modelo a partir de la página web del grupo de Predicción Meteorológica de la Universidad de Atenas: http://forecast.uoa.gr/

3.4.7. Boletines periódicos sobre episodios diferenciales

A nivel nacional se elaboran boletines en los que se recogen la predicción de episodios africanos, episodios europeos y combustión de biomasa que puedan afectar a los niveles de partículas en suspensión en las diferentes Comunidades Autónomas. Vinculada al proyecto Calima (Caracterización de AerosoLes originados por Intrusiones de Masas de aire Africanas) encontramos una gran base de datos de episodios diferenciales ocurridos.

Los organismos que dirigen las líneas de investigación vinculadas al proyecto Calima son el CSIC (a través del Instituto de Diagnóstico Ambiental y Estudios del Agua (IDAEA), la AEMET (a través del Centro de Investigación Atmosférica de Izaña), el CIEMAT (a través del Instituto de Medio Ambiente), el Instituto de Salud Carlos III, la Universidad de Extremadura, la Universidad Politécnica de Cartagena y la Universidad de Huelva. La página a partir de la cual se puede acceder al proyecto Calima es: www.calima.ws.

En esta página se pueden encontrar predicciones relacionadas con episodios de intrusión de masas de aire procedentes del Norte de África, episodios europeos (intrusión de masas de aire cargadas de Sulfatos procedentes del Norte de Europa) y quema de biomasa.

4. Resultados y discusión

La función de esta investigación en su conjunto se centra en dos líneas de actuación: 1) la determinación de la concentración de fondo del PM en el área de estudio y 2) el análisis de la influencia de los transportes de masas de aire, tanto a nivel sinóptico como mesoescalar, sobre el PM y el O_3. Ambas líneas pivotan sobre un elemento común: la instalación de una estación de alta montaña ubicada en la costa mediterránea occidental.

El resultado de estas investigaciones se presenta en los siguientes 4 trabajos:

T1. **Impacts on particles and ozone by transport processes recorded at urban and high-altitude monitoring stations**
Autores: Nicolás, J. F., Crespo, J., Yubero, E., **Soler, R.,** Carratalá, A., Mantilla, E.
Referencia: *Science of the Total Environment* **466-467**, pp. 439-446, 2014.

T2. **Chemical characterization of PM_1 at a regional background site in the Western Mediterranean**
Autores: Galindo, N., Yubero, E., Nicolás, J. F., Crespo, J., **Soler, R.**
Referencia: *Aerosol and Air Quality Research*, **16**, pp. 530–541, 2016.

T3. **PM_1 variability and transport conditions between an urban coastal area and a high mountain site during the cold season**
Autores: Nicolás, J. F., Galindo, N., Yubero, E., Crespo, J., **Soler, R.**
Referencia: *Atmospheric Environment* **118,** pp. 127-134, 2015.

T4. **Depletion of tropospheric ozone associated with mineral dust outbreaks**
Autores: Soler, R., Nicolás, J. F., Caballero, S., Yubero, E., Crespo, J.
Referencia: *Environmental Science and Pollution Research* **23**(19), pp. 19376-19386.

Con el desarrollo de dichos trabajos se ha determinado la concentración de fondo en el área de estudio, tanto en concentración másica (PM_1) (T2) como en número de partículas (T1; T3). Además, se ha obtenido la composición química del PM_1 (T2). Por su parte, el análisis de los procesos de transporte y su influencia en la estación de montaña ha permitido determinar la conectividad existente entre entornos urbanos a nivel del mar y la estación de montaña (T3). Así mismo, se ha observado cómo estos transportes influyen en los niveles de partículas y su especiación (T1; T2; T4), así como en el O_3 troposférico (T1; T4). A continuación, se expone un resumen de los principales resultados de estos artículos:

4.1. Impacts on particles and ozone by transport processes recorded at urban and high-altitude monitoring stations

El objetivo de este trabajo es cuantificar y evaluar la diferencia de concentración del n° de partículas existente entre dos emplazamientos que representan ambientes atmosféricos diferentes: MS y US1. Así mismo, se analiza la influencia que presentan distintos episodios diferenciales sobre la concentración de partículas y los niveles de O_3. El estudio se llevó a cabo entre octubre de 2011 y septiembre de 2012. En el análisis sobre el material particulado se diferencia entre partículas finas (d_{ae}<1 µm) y gruesas (d_{ae}>1 µm).

Con respecto a las partículas finas cabe destacar que, en promedio, la concentración registrada en MS (55 cm^{-3}) fue prácticamente la mitad de la obtenida en el entorno urbano (112 cm^{-3}). Por lo que la diferencia entre ambas puede atribuirse, aunque de forma aproximada, pues existen otros factores a tener en cuenta, a la actividad antropogénica propia del entorno urbano. La mayor diferencia a nivel temporal entre ambos enclaves se produjo durante los meses de invierno, posiblemente debido a que la estación de montaña reside en la troposfera libre durante gran parte de los meses más fríos. Así mismo, mostraron concentraciones anuales muy similares de partículas gruesas ≈ 0,3 cm^{-3}. Sin embargo, aunque en ambos emplazamientos los máximos se produjeron durante los meses más cálidos (julio y agosto), en MS fueron sustancialmente superiores (prácticamente el doble) debido a un mayor impacto de las SDOs sobre la MS, ya que el polvo mineral suele ser transportado a elevadas alturas y su incidencia en la localización urbana es menor.

Los efectos sobre el PM debidos a episodios de elevada estabilidad atmosférica acontecidos durante los meses más fríos del año han podido evidenciarse en ambos enclaves. No obstante, su incidencia en MS requiere de unas condiciones atmosféricas particulares: condiciones de brisa y la permanencia del punto de muestreo dentro de la PBL. En este tipo de episodios, y bajo estas condiciones, el transporte de partículas, principalmente finas (0,5-2 µm) es factible. Además, se puede se puede evidenciar un incremento en los niveles de O_3 en la estación de montaña. Este aumento puede ser consecuencia del transporte de óxidos de nitrógeno desde los enclaves urbanos que, junto a la elevada radiación solar que caracteriza este tipo de episodios, facilita la formación fotoquímica de O_3.

Durante los meses más cálidos se detectaron episodios de quema de biomasa y recirculación de masas de aire, característicos del mediterráneo occidental. En ambos casos se pudo constatar incrementos de partículas finas en la MS, sin embargo la US1 no se vio afectada. Si bien a lo largo de todo el año se detectan SDOs, es sin duda ente marzo y octubre cuando tienen lugar con mayor frecuencia. Este transporte de polvo mineral (principalmente entre 0,5 y 5 µm) tiene una importante incidencia sobre los niveles de O_3 registrados en MS, ya que al contrario de los episodios de recirculación y biomasa, durante las SDOs se produce una reducción sustancial de la concentración de O_3 troposférico, llegándose a registrar decrecimientos de hasta un 17% respecto a su valor medio.

4.2. Chemical characterization of PM_1 at a regional background site in the Western Mediterranean

Este artículo presenta como principal objetivo analizar y cuantificar el PM_1 y sus principales componentes químicos (EC, OC, Cl^-, SO_4^{2-}, NO_3^-, Na^+, NH_4^+, K^+, Mg^{2+}, Ca^{2+} y $C_2O_4^{2-}$) en el enclave MS y su comparación con otros emplazamientos de características similares. Este trabajo, además, evalúa el efecto de las SDOs sobre los compuestos analizados. La campaña de muestreo abarca desde febrero de 2011 hasta septiembre de 2012.

La concentración media de PM_1 para todo el periodo de estudio fue 4,6 $\mu g \cdot m^{-3}$. Esta concentración es similar a la registrada en Montsec e inferior a las observadas en Montseny y los Montes Cimone y Martano. No obstante, los niveles son superiores a los registrados en la estación alpina de Jungfraujoch y puy de Dôme.

Con respecto a la composición química, los principales compuestos de PM_1 fueron la materia orgánica (3,1 $\mu g \cdot m^{-3}$) y el sulfato de amonio (1,2 $\mu g \cdot m^{-3}$), siendo responsables de más del 60 y 26% de la masa total, respectivamente. Las similitudes con los niveles registrados en Montsec sugieren la existencia de una concentración de fondo de sulfato de amonio de 0,9-1,0 $\mu g \cdot m^{-3}$ en la cuenca oeste mediterránea. El nitrato, sin embargo, ha resultado ser un contribuyente minoritario al PM_1, debido principalmente a la limitada presencia de precursores como los NOx (reducida actividad antropogénica) y a la inestabilidad y descomposición del NH_4NO_3 debido a las elevadas temperaturas que tienen lugar en la cuenca oeste mediterránea en verano.

En cuanto a los patrones estacionales, las concentraciones de PM_1 y la mayoría de sus compuestos químicos presentaron un ciclo estacional similar, caracterizado por máximas concentraciones en verano y mínimas en invierno. No obstante, el nitrato registró una concentración residual en verano, difiriendo con los resultados obtenidos en otras estaciones de alta montaña. La variación estacional presentada por los niveles de material particulado se debe a varios motivos: durante parte del periodo frío, la dirección de vientos predominante no favorecen un transporte efectivo de contaminantes hacia la cima. Además, la cumbre reside parte del tiempo en la troposfera libre, inaccesible para masas de aire que puedan transportar contaminantes por debajo de la capa límite de mezcla. Durante el periodo cálido, las concentraciones de PM_1 son mayores debido a que la deposición húmeda es menor, se da un aporte más intenso de material particulado debido a una mayor frecuencia de SDOs y las elevadas temperaturas y radiación solar favorecen la emisión biogénica y la formación de aerosoles secundarios.

Durante las SDOs se evidenció un aumento en los niveles de PM_1 (25%), OC (20%) y SO_4^{2-} (~35%). La proximidad al continente africano parece ser un factor decisivo que justifica la mayor incidencia sobre los niveles de PM_1 respecto a otras estaciones más alejadas de África. El incremento en los niveles de OC y sulfato amónico puede deberse, por un lado, a la formación secundaria en la masa de aire (generación de compuestos orgánicos secundarios y oxidación de SO_2^- a H_2SO_4 y reacción posterior con el amoniaco) y, por otro, a la posible incorporación de estos contaminantes secundarios por el paso de las SDOs a través de zonas tras episodios de recirculación en el oeste mediterráneo. El incremento de amonio (20%), inferior al esperado, puede deberse a la pérdida parcial del NH_4^+ por la descomposición del NH_4NO_3 ante el incremento de temperatura experimentado (40%) durante las SDOs.

4.3. PM_1 variability and transport conditions between an urban coastal area and a high mountain site during the cold season

En este trabajo se ha evaluado el incremento que presentan episodios de alta contaminación (WREG), asociados a periodos de elevada estabilidad atmosférica, sobre el material particulado en dos entornos de elevado contraste: MS y US2. Así mismo, se ha determinado las condiciones meteorológicas que propician un transporte efectivo de contaminantes atmosféricos desde zonas urbanas costeras hasta MS durante los WREG. El estudio tuvo lugar entre octubre de 2010 y febrero de 2011.

Para el periodo de análisis, el promedio de concentración de PM_1 en MS (3,6 ± 1,0 $\mu g \cdot m^{-3}$) fue inferior al registrado en el entorno urbano (10,5 ± 6,4 $\mu g \cdot m^{-3}$). Así mismo, cabe

mencionar que la variabilidad en las concentraciones de PM_1 fue inferior en la estación de montaña, donde sólo se registraron aumentos sustanciales en los niveles en meses en los que tuvieron lugar SDOs.

Los ciclos diarios del PM_1 durante los meses más fríos del año en ambos entornos presentaron claras diferencias. Por un lado, los niveles de PM_1 en MS fueron considerablemente constantes a lo largo del día, con máximos en el periodo de máxima radiación solar (14:00-17:00 UTC). Esto coincide con el típico ciclo diurno de PM_1 en entorno de fondo regional en la cuenca oeste mediterránea en el periodo frío, donde, durante el día, la circulación de brisas dominantes, debido al aumento de insolación, propicia un flujo ascendente de masas de aire que arrastra los contaminantes acumulados en zonas urbanas costeras hacia MS. Sin embargo, durante la noche, se produce una reducción en los niveles de partículas debido a la prevalencia de vientos descendentes desde MS y una reducción en la altura de capa de mezcla. Por otro lado, el ciclo diurno del PM_1 en US2 estuvo dominado por el tráfico rodado, registrando dos picos de concentración: un máximo absoluto entre las 20:00 y 21:00 UTC, asociado al tráfico tras la jornada laboral y a una disminución en la altura de capa de mezcla y otro relativo a las 9:00 UTC, vinculado al tráfico de incorporación al trabajo.

Los episodios de elevada estabilidad atmosférica presentaron mayor impacto sobre los niveles de partículas en US2 que en MS, tanto en la cantidad de días afectados respecto al periodo total de WREG, como en al aumento en las concentraciones de PM_1, llegando a alcanzar máximos de concentración en MS y US1 de 47 y 11,6 $\mu g \cdot m^{-3}$, respectivamente. Sin embargo, el incremento porcentual de los niveles de partículas a nivel horario fue mayor a todas horas en MS que en US2. La concentración de PM_1 en la estación urbana, durante los WREG, presentó valores relativamente constantes a lo largo del día y un máximo absoluto (20:00-21:00 UTC). Esto está posiblemente asociado a un aumento de las emisiones de tráfico rodado y una reducción en la altura de capa de mezcla y temperatura que favorece la acumulación de contaminantes y condensación de compuestos semivolátiles. Mientras que el incremento relativo porcentual en US2 se mantuvo relativamente constante a lo largo del día, en la estación MS se caracterizó por un claro máximo a mediodía. Esto fue debido principalmente al transporte de contaminantes desde las zonas urbanas colindantes y a la formación fotoquímica de aerosoles secundarios durante este transporte.

Durante los episodios de elevada estabilidad atmosférica, el transporte de contaminantes desde las zonas urbanas costeras hacia la estación de montaña se ve dificultado por la compleja orografía del terreno. Sin embargo, se ha observado que puede tener lugar un transporte efectivo si se dan determinadas condiciones: fuertes incrementos en los niveles de partículas en las zonas urbanas costeras junto con brisas marinas consistentes y la permanencia de la cima dentro de la capa límite planetaria.

4.4. Depletion of tropospheric ozone associated with mineral dust outbreaks

El objetivo del presente artículo es evaluar y cuantificar la reducción en la concentración de O_3 troposférico asociado a su interacción con las partículas minerales transportadas por las SDOs a su paso por el Monte Aitana entre mayo y septiembre de 2012. Para ello, se ha

caracterizado previamente el O_3 y las partículas gruesas en presencia y ausencia de SDOs. El análisis se ha realizado a nivel horario, lo que permite suprimir las fluctuaciones diarias intrínsecas del ciclo del O_3 asociadas a la radiación solar y aislar el efecto de elementos aleatorios como las SDOs.

En relación a la variación temporal del O_3, se registró una concentración media de 57,7 ± 0,2 ppb para el periodo de estudio. La influencia de las SDOs sobre los niveles de O_3 se puede intuir comparando éstos en agosto y septiembre. La concentración media de O_3 en el mes de agosto (54,1 ppb) fue inferior a la de septiembre (58,9 ppb), contrario a la tendencia típica del O_3 en verano. Esto podría estar vinculado a una menor producción fotoquímica de O_3 debido a una menor radiación solar. Sin embargo, la inferior radiación solar en septiembre sugiere que debe haber otro factor responsable de los reducidos niveles de O_3 registrados en agosto, las SDOs. Con respecto a las partículas gruesas, la concentración media para el periodo de medida fue de 0,45 ± 0,05 cm^{-3}, más del doble registrado en otras estaciones de montaña similares. Esto es posiblemente debido a la elevada frecuencia de SDOs que tuvo lugar en el periodo de estudio.

La evolución horaria del O_3, caracterizada por menores oscilaciones a lo largo del día y valores superiores respecto a entornos de menor altitud, respondió al comportamiento típico del O_3 observado en estaciones de alta montaña. Sin embargo, la concentración máxima horaria de O_3 se dio a las 19:00 UTC, con un cierto desfase respecto a los máximos de insolación y producción fotoquímica del O_3. Éste desfase pudo ser debido a que el máximo absoluto responde a la llegada de O_3 que, producido fotoquímicamente junto a otros contaminantes secundarios, fue transportado desde las zonas costeras hasta la cima por medio de brisas marinas. El perfil de evolución horaria del material particulado alcanza valores máximos entre las 11:00 y 16:00 UTC y empiezan a decrecer a las 20:00 UTC.

En relación a la caracterización de las SDOs, cabe destacar que abarcaron el 50% de los días del periodo de estudio, distribuidos en 15 episodios diferentes, y que no implicaron necesariamente elevadas concentraciones de partículas. La concentración media de partículas gruesas para el conjunto de SDOs (0,72 cm^{-3}), fue más del doble de la concentración media del total de días en ausencia de SDOs (0,35 cm^{-3}). Cabe mencionar que para evaluar el efecto de las SDOs sobre los niveles de material particulado, se determinó la variación horaria de los valores de la mediana (N-median: siendo el valor que ocupa el lugar central del conjunto de datos ordenados de menor a mayor), media (N-mean, correspondiéndose con la media de los valores de una muestra) y percentiles 25 y 75 (N-P25 y N-P75: definidos como los valores bajo los cuales quedan el 25 y 75% del conjunto de medidas ordenadas de menor a mayor) de la concentración de partículas durante las SDOs.

Con respecto al impacto de las SDOs sobre los niveles de O_3, se observó que la reducción de los niveles de O_3 no fue homogénea a lo largo de éstas. La reducción del O_3 se produjo de manera simultánea con el inicio del aumento en los niveles de partículas, presentado un gradiente de reducción de O_3 medio de 0,39 $ppb \cdot h^{-1}$ para el conjunto de SDOs. No obstante, a pesar de que las concentraciones de partículas se mantienen elevadas durante el transcurso de las SDOs, se evidenció una saturación en la reducción de O_3 y una tendencia a la recuperación. Así mismo, en promedio, se dio una reducción de O_3 más efectiva entre las 18:00 y 23:00 UTC, fracción horaria en la que el N-mean y el N-P75 alcanzan valores máximos.

En cuanto a la cuantificación de la reducción de O_3, se observó que la caída en las concentraciones de O_3 fue estadísticamente significativa cuando la concentración de partículas gruesas es superior al valor de la mediana (N-median), obteniendo un descenso medio del 5,5% en los niveles de O_3 para el conjunto de SDOs. No obstante, se llegan a observar reducciones porcentuales de O_3 superiores al 15% en el análisis de SDOs a nivel individual. Así mismo, del estudio de las SDOs a nivel horario, se llegaron a registrar descensos medios horarios por encima del 20%.

5. Conclusiones y líneas de investigación futuras

A continuación se detallan las principales conclusiones a las que se ha llegado en este trabajo:

La contribución antropogénica a la concentración en número de partículas finas en la estación urbana (US1) es de aproximadamente el mismo valor de concentración total de partículas registrado en el enclave de montaña (~55 cm^{-3}). Sin embargo, en términos de partículas gruesas, ambas localizaciones muestran una concentración similar. En ambos tipos de partículas, las evoluciones estacionales difieren en estos entornos. Frente a la evolución típica observada en ambientes urbanos, caracterizada por concentraciones superiores en el periodo invernal, la evolución del nº de partículas (finas y gruesas) en la estación de montaña (tendencia que también se observa en la fracción PM_1) presenta un claro máximo que se extiende durante los meses más cálidos. Ésta está condicionada por varios factores: la alta frecuencia de intrusiones de polvo sahariano (SDOs) que tiene lugar durante el periodo estival, la permanencia de la estación dentro de la capa límite planetaria (PBL) durante estos meses, la escasa precipitación y, por último, la mayor formación de aerosoles secundarios asociada al incremento en la radiación solar.

En cuanto a la concentración másica de PM_1, la mayor parte de sus componentes químicos presenta una evolución temporal idéntica a la anteriormente citada. No obstante, el nitrato registra una concentración mínima durante los meses más cálidos debido a la descomposición del NH_4NO_3 por las altas temperaturas veraniegas. Los principales constituyentes de la fracción PM_1 en el pico Aitana son la materia orgánica (con una contribución superior al 65% de la masa total) y el sulfato (20%). En contraposición, las concentraciones registradas de carbono elemental (0,12 $\mu g \cdot m^{-3}$) fueron muy bajas, como corresponde a un entorno libre de emisiones antrópicas.

Los trabajos realizados han revelado el gran impacto que tienen ciertos episodios diferenciales, asociados a distintos procesos de transporte de masas de aire tanto a nivel mesoescalar como sinóptico, sobre las concentraciones registradas en la estación de montaña. Estos episodios pueden llegar a modular las variaciones estacionales del PM. De esta forma, la coincidencia de determinados factores meteorológicos puede propiciar que episodios de polución urbanos, asociados a situaciones de elevada estabilidad atmosférica durante los meses más fríos, puedan llegar a incidir sobre las concentraciones de partículas en puntos de alta montaña. A pesar de que este fenómeno se ve dificultado por la compleja orografía, se ha observado que este transporte de contaminantes es efectivo cuando se dan fuertes incrementos de PM en las zonas urbanas costeras, acompañados de brisas marinas y de montaña consistentes y la permanencia de la cumbre dentro de la PBL.

Aunque tienen lugar a lo largo de todo el año, es desde el final de la primavera hasta el otoño cuando las SDOs presentan una mayor frecuencia en el área de estudio. Podemos verificar que este tipo de transporte presenta un importante impacto sobre el PM_1, contrariamente a lo que pudiese pensarse debido a la granulometría predominantemente gruesa del material transportado durante la intrusión. De los resultados de la especiación química realizados durante estos eventos, podemos concluir que se produce una formación de compuestos secundarios durante el transporte de la masa de aire, lo que se traduce en incrementos de PM, carbono orgánico y sulfatos. Además, se ha estimado un importante impacto sobre los niveles de ozono (O_3) debido a su interacción con el polvo mineral

transportado durante estos episodios. En la reacción ozono-partícula mineral se observa que, pasado un tiempo de interacción, se produce una saturación en la reducción del O_3 y, posteriormente, su recuperación. Se ha determinado que las SDOs dan lugar a una reducción media en la concentración de O_3 de ~5,5%. No obstante, de manera individual, estos episodios de intrusiones pueden llegar a registrar reducciones de O_3 medias superiores al 15%.

5.1. Líneas futuras de investigación

Por último, se establecen las líneas de investigación futuras:

- Caracterización cualitativa y cuantitativa de las distintas fuentes de emisión que influyen en los niveles de material particulado en la estación de alta montaña mediante técnicas como la PCA (Principal Components Analysis) o la PMF (Positive Matrix Factorization).
- Mejora del modelo de series temporales y aplicación a la base de datos de O_3 con el fin de obtener en mayor profundidad la componente estacional en la evolución de los niveles de O_3 en MS.
- Recopilar información sobre el O_3 y precursores en su formación fotoquímica con el objetivo de discernir y cuantificar la reducción de O_3 por consumo por parte de las partículas y por inhibición en su producción.
- Caracterización físico-química del material particulado transportado por las distintas masas de aire que llegan a la estación de Aitana, en función de su procedencia.

6. Conclusions and future research directions

In this section, a summary of the main conclusions obtained from this study is presented:

The anthropogenic contribution to the fine particle number concentration at the urban station (US1) is approximately the same as the total particle concentration registered at the high-mountain station (~55 cm^{-3}). However, the coarse particle number concentration is quite similar at both urban and high-mountain stations. The seasonal patterns of both the fine and coarse particles also show clear differences at each station. Given the typical aerosol trend found at urban stations characterized by greater particle concentrations in winter, the evolution of both fine and coarse particle concentration at the mountain station shows a clear maximum throughout the warmer months. This trend is also observed in particle mass concentration, PM_1. This can be attributed to several reasons: the high frequency of Saharan dust outbreaks (SDOs) that take place in summer; the continued presence of the summit within the planetary boundary layer (PBL) during a great part of the winter period; scarce precipitation and a greater secondary aerosol formation due to an increase in solar radiation.

Regarding PM_1 mass concentration, the main chemical compounds show the same temporary variations as those previously described. However, minimum concentrations of nitrate were registered during the warmest months due to the thermal decomposition of NH_4NO_3 favoured by high summer temperatures. The main constituents of PM_1 at MS were organic matter, (accounting for more than 65% of the total mass) and sulphate (~20%). Furthermore, elemental carbon concentrations (0.12 $\mu g \cdot m^{-3}$) were very low, as is expected in an environment with a lack of human activity.

A major environmental issue revealed by this study is the impact that several atmospheric episodes, associated with mesoscale and synoptic mass air transports, have on particulate matter and ozone concentrations at the high-mountain station. These episodes can alter the seasonal PM variations. Under specific meteorological conditions, severe urban pollution episodes caused by stagnant weather conditions during the winter months could affect the pollutant concentrations at MS. Although this phenomenon is considered uncommon due to the complex orography, we observed that it could become effective when there is a significant increase in PM concentrations in the urban coastal areas, accompanied by consistent sea and mountain breezes and provided that the mountain summit remains within the PBL.

Although SDOs can take place at any time, it is mainly from late winter to autumn that a great number of them occur in the study area. It has been confirmed that SDOs have a significant impact on PM_1 concentrations, which is unexpected if we consider that the granulometry of the particulate matter transported during these outbreaks is mainly coarse. Regarding PM_1 chemical speciation during these episodes, it can be concluded that a secondary aerosol formation takes place during their transport from urban coastal areas inland to the MS, leading to increases in PM_1, organic carbon and sulphate concentrations. In addition, a reduction in ozone levels has been associated with its interaction with mineral dust transported by SDOs. Moreover, it was observed that after a certain time period of interaction, a saturation of the ozone reduction process took place, which ultimately leads to its recovery, even though the particle levels remained high. During SDOs, an average value

of the ozone percentage reduction of 5.5% for the whole study period was established. Nevertheless, this value can rise beyond 15% if an isolated SDO is considered.

6.1. Future research directions

The study has identified the following research directions:

- Performing a qualitative and quantitative characterization of the different sources that affect the particulate matter concentrations at MS, by means of receptor models and tools such as Positive Matrix Factorization (PMF) and Principal Components Analysis (CPA).
- Improving the time series model so a deeper study of the O_3 data series' seasonal component at MS can be carried out.
- Collecting ozone and its photochemical precursors' data in order to investigate what percentage of O_3 depletion is due to its direct uptake in coarse particles and what is caused by the inhibition of the O_3 production.
- Performing a physical and chemical characterization of particulate matter transported by different air masses, classified according to their origin and nature.

7. Bibliografía

Adame, J. A., Córdoba-Jabonero, C., Sorribas, M., Toledo, D., Gil-Ojeda, M., 2015. Atmospheric boundary layer and ozone-aerosol interactions under Saharan intrusions observed during AMISOC summer campaign. *Atmospheric Environment* **104**, pp. 205–216.

Alastuey, A., Querol, X., Castillo, S., Escudero, M., Avila, A., Cuevas, E., Torres, C., Romero, P. M., Exposito, F., García, O., Diaz, J. P., Van Dingenen, R., Putaud, J. P., 2005. Characterisation of TSP and $PM_{2.5}$ at Izaña and Sta. Cruz de Tenerife (Canary Islands, Spain) during a Saharan Dust Episode (July 2002). *Atmospheric Environment* **39**(26), pp. 4715–4728.

Alonso, R., Bermejo, V., Elvira, S., Aguirre Alfaro, A., Sanz, J., Herce Garraleta, M.D., González Fernández, I., Fernández Patier, R., Gimeno, B.S., 2009. La contaminación atmosférica en la sierra de Guadarrama. Riesgos potenciales para la vegetación. VI Jornadas Científicas del Parque Natural de Peñalara y del Valle de El Paular. Comunidad de Madrid, pp 63–86.

Ariola, V., D'Alessandro, A., Lucarelli, F., Marcazzan, G., Mazzei, F., Nava, S., Garcia-Orellana, I., Prati, P., Valli, G., Vecchi, R., Zucchiatti, A., 2006. Elemental characterization of PM_{10}, $PM_{2.5}$ and PM_1 in the town of Genoa (Italy), *Chemosphere* **62**, pp. 226–232.

Ashmore, M., 2015. Ozone depletion and related topics-surface ozone effects on vegetation. reference module in earth systems and environmental sciences. *Encyclopedia of Atmospheric Sciences* (Second Edition) 2015, pp. 389–396

Basart, S., Pérez, C., Nickovic, S., Cuevas, E. & Baldasano, J.M., 2012. Development and evaluation of the BSC-DREAM8b dust regional model over Northern Africa, the Mediterranean and the Middle East. *Tellus B* **64**, pp. 1–23.

Bauer, S. E., Balkanski, Y., Schulz, M., Hauglustaine, D.A., 2004. Global modeling of heterogeneous chemistry on mineral aerosol surfaces: influence on tropospheric ozone chemistry and comparison to observations. *Journal of Geophysical Research* **109**, D02304. DOI: 10.1029/2003JD003868

Birch, M.E., Cary, R.A., 1996. Elemental carbon-based method for monitoring occupational exposures to particulate diesel exhaust. *Aerosol Science and Technology* **25**(3), pp. 221–241.

Bonasoni, P, Cristofanelli, P, Calzolari, F, Bonafé, U, Evangelisti, F, Stohl, A., Zauli Sajani, S., van Dingenen, R., Colombo, T., Balkanski, Y., 2004. Aerosol–ozone correlations during dust transport episodes. *Atmospheric Chemistry and Physics* **4**, pp.1201–1215.

Bourcier, L., Sellegri, K., Chausse, P., Pichon, J.M., Laj, P., 2012. Seasonal variation of water-soluble inorganic components in aerosol size-segregated at the puy de Dôme station (1,465 m a.s.l.), France. *Journal of Atmospheric Chemistry* **69**, pp. 47–66.

Bromberg, P. A., 2016. Mechanisms of the acute effects of inhaled ozone in humans. *Biochimica et Biophysica Acta (BBA) - General Subjects* **1860**(12), pp. 2771–2781.

Caballero, S., Galindo, N., Pastor, C., Varea, M., Crespo, J., 2007. Estimated tropospheric ozone levels on the southeast Spanish Mediterranean coast. *Atmospheric Environment* **41**, pp. 2881–2886.

Carbone, C., Decesari, S., Paglione, M., Giulianelli, L., Rinaldi, M., Marinoni, A., Cristofanelli, P. Didiodato, A., Bonasoni, P., Fuzzi, S., Facchini, M.C., 2014. 3-year chemical composition of free tropospheric PM_1 at the Mt. Cimone GAW global station – South Europe – 2165 m a.s.l. *Atmospheric Environment* **87**, pp. 218–227.

Cass, G. R., Druzik, J.R., Grosjean, D., Nazaroff W. W., Whitmore, P. M., Wittman, C. L., 1989. Protection of works of art from atmospheric ozone. *Atmospheric Environment*. Part A. General Topics, **25** (2), pp. 441–451.

Chevalier, A., Gheusi, F., Delmas, R., Ordoñez, C., Sarrat, C., Zbinden, R., Thouret, V., Athier, G., Cousin, J.-M., 2007. Influence of altitude on ozone levels and variability in the lower troposphere: a ground-based study for Western Europe over the period 2001-2004. *Atmospheric Chemistry and Physics* **7**, pp. 4311–4326.

Coury, Ch., Dillner, A.M., 2009. ATR-FTIR characterization of organic functional groups and inorganic ions in ambient aerosols at a rural site. *Atmospheric Environment* **43**, pp. 940–948.

Cozic, J., Verheggen, B., Weingartner, E., Crosier, J., Bower, K.N., Flynn, M., Coe, H., Henning, S., Steinbacher, M., Henne, S., Collaud Coen, M., Petzold, A., Baltensperger, U., 2008. Chemical composition of free tropospheric aerosol for PM_1 and coarse mode at the high Alpine site Jungfraujoch. *Atmospheric Chemistry and Physics* **8**, pp. 407–423.

Dentener, F.J., Carmichael G.R., Zhang, Y., Lelieveld, J., Crutzen, P.J., 1996. Role of mineral aerosol as a reactive surface in the global troposphere. *Journal of Geophysical Research* **101** (D17), pp. 22869–22889.

de Reus, M., Dentener, F., Thomas, A., Borrmann, S., Ström, J., Lelieveld, J., 2000. Airborne observations of dust aerosol over the North Atlantic Ocean during ACE 2: Indications for heterogeneous ozone destruction. *Journal of Geophysical Research* **105**(D12), pp. 15263–15275.

Dickerson, R. R., Kondragunta, S., Stenchikov, G., Civerolo, K. L., Doddridge, B. G., Holben, B. N.,1997. The impact of aerosol on solar ultraviolet radiation and photochemical smog. *Science* **278**, 827.

Draxler, R. R., Rolph, G. D., 2015. HYSPLIT (HYbrid Single-Particle Lagrangian Integrated Trajectory). Model access via NOAA ARL READY Website: https://ready.arl.noaa.gov/HYSPLIT_traj.php

Druzik, J. R., 1985. Ozone: The intractable problem. *Wacc Newsletter* **7**(3), pp. 3–9.

Eliseev, A.V., 2015. Impact of tropospheric sulphate aerosols on the terrestrial carbon cycle. *Global and Planetary Change* **124**, pp. 30–40.

EPA, 2002. Third external review draft of air quality criteria for particulate matter. US-EPA.

EPA, 2016a. Particulate matter (PM) pollution. Health and environmental. Effects of particulate matter (PM). https://www.epa.gov/pm-pollution/health-and-environmental-effects-particulate-matter-pm

EPA, 2016b. EPA's Air Quality Guide for Ozone. https://www.airnow.gov/index.cfm?action=pubs.aqiguideozone

Escudero, M., Querol, X., Avila, A., Cuevas, E., 2007. Origin of exceedances of the European daily PM limit value in regional background areas of Spain. *Atmospheric Environment* **41**, pp. 730–744.

Freney, E.J., Sellegri, K., Canonaco, F., Boulon, J., Hervo, M., Weigel, R., Pichon, J.M., Colomb, A., Prévôt, A.S.H., Laj, P., 2011. Seasonal variations in aerosol particle composition at the puy-de-Dôme research station in France. *Atmospheric Chemistry and Physics* **11**, pp. 13047–13059.

Fuzzi, S., Baltensperger, U., Carslaw, K., Decesari, S., Denier van der Gon, H., Facchini, M. C., Fowler, D., Koren, I., Langford, B., Lohmann, U., Nemitz, E., Pandis, S., Riipinen, I., Rudich, Y., Schaap, M., Slowik, J. G., Spracklen, D. V., Vignati, E., Wild, M., Williams, M., Gilardoni, S., 2015. Particulate matter, air quality and climate: lessons learned and future needs. *Atmospheric Chemistry and Physics* **15**, pp. 8217–8299.

Hanisch, F., Crowley, J. N., 2003. Ozone decomposition on Saharan dust: an experimental investigation. *Atmospheric Chemistry and Physics* **3**, pp. 119–130.

Harrison, S. P., Kohfeld, K. E., Roelandt, C., Claquin, T., 2001. The role of dust in climate changes today, at the last glacial maximum and in the future. *Earth-Science Reviews* **54**(1-3), pp. 43–80.

Horemans, B., Cardell, C., Bencs, L., Kontozova-Deutsch, V., De Wael, K., Van Grieken, R., 2011. Evaluation of airborne particles at the Alhambra monument in Granada, Spain. *Microchemical Journal* **99**(2), pp. 229–438.

IPCC, 2013. Climate Change 2013: The physical science basis. In *Contribution of Working Group I to the Fifth Assessment Report of the Intergovernmental Panel on Climate Change*. (Eds.), Cambridge University Press, Cambridge, United Kingdom and New York, NY, USA.

Jorba, O., Pandolfi, M., Spada, M., Baldasano, J. M., Pey, J., Alastuey, A., Arnold, D., Sicard, M., Artiñano, B., Revuelta, M. A., Querol, X., 2013. Overview of the meteorology and transport patterns during the DAURE field campaign and their impact to PM observations. *Atmospheric Environment* **77**, pp. 607–620.

Kallos, G., Kotroni, V., Lagouvardos, K., 1997. The regional weather forecasting system SKIRON: an overview. Proceedings of the symposium on regional weather prediction on parallel computer environments. University of Athens, Greece, pp. 109–122.

Kalnay, E., Kanamitsu, M., Kistler, R., Collins, W., Deaven, D., Gandin, L., Iredell, M., Saha, S., White, G., Woollen, J., Zhu, Y., Leetmaa, A., Reynolds, B., Chelliah, M., Ebisuzaki, W., Higgins, W., Janowiak, J., Mo, K. C., Ropelewski, C., Wang, J., Jenne, R., Joseph, D., 1996. The NCEP/NCAR 40-year reanalysis project. *Bulletin of the American Meteorological Society* **77**, pp.437–471.

Liu, Y. J., Zhang, T. T., Liu, Q. Y., Zhang, R. J., Sun, Z. Q., Zhang, M. G., 2014. Seasonal variation of physical and chemical properties in TSP, PM_{10} and $PM_{2.5}$ at a roadside site in Beijing and their influence on atmospheric visibility. *Aerosol and Air Quality Research* **14**, pp. 954–969.

Marenco, F., Bonasoni, P., Calzolari, F., Ceriani, M., Chiari, M., Cristofanelli, P., D'Alessandro, A., Fermo, P., Lucarelli, F., Mazzei, F., Nava, S., Piazzalunga, A., Prati, P., Valli, G., Vecchi, R., 2006. Characterization of atmospheric aerosols at Monte Cimone, Italy, during summer 2004: source apportionment and transport mechanisms. *Journal of Geophysical Research* **111**(D24). DOI: 10.1029/2006JD007145

Marinoni, A., Cristofanelli, P., Calzolari, F., Roccato, F., Bonafè, U., Bonasoni, P., 2008. Continuous measurements of aerosol physical parameters at the Mt. Cimone GAW Station (2165 m asl, Italy). *Science of the Total Environment* **391**(2–3), pp. 241–251.

Mészáros, E., 1999. *Fundamentals of Atmospheric Aerosol Chemistry*. Akadémiai Kiado.

Millán, M., Salvador, R., Mantilla, E., Artiñano, B., 1996. Meteorology and photochemical air pollution in Southern Europe: experimental results from EC research projects. *Atmospheric Environment* **30**, pp. 1909–1924.

Millán, M., Sanz, J., Salvador, R., Mantilla, E., 2006. Atmospheric dynamics and ozone cycles related to nitrogen deposition in the western Mediterranean. *Environmental Pollution* **118**, pp. 167–186.

Mills, G., Harmens, H., Wagg, S., Sharps, K., Hayes, F., Fowler, D., Sutton, M., Davies, B., 2016. Ozone impacts on vegetation in a nitrogen enriched and changing climate. *Environmental Pollution* **208**(B), pp. 898–908.

Moroni, B., Castellini, S., Crocchianti, S., Piazzalunga, A., Fermo, P., Scardazza, F., Cappelletti, D., 2015. Ground-based measurements of long-range transported aerosol at the rural regional background site of Monte Martano (Central Italy). *Atmospheric Research* **155**, pp. 26–36.

Paoletti, E., 2006. Impact of ozone on Mediterranean forests: a review. *Environment Pollution* **144**(2), pp. 463–474.

Pateraki, S., Assimakopoulos, V.D., Bougiatioti, A., Kouvarakis, G., Mihalopoulos, N., Vasilakos, C., 2012. Carbonaceous and ionic compositional patterns of fine particles over an urban Mediterranean area. *Science of the Total Environment* **424**, pp. 251–263.

Pérez, N., Pey, J., Castillo, S., Viana, M., Alastuey, A., Querol, X., 2008. Interpretation of the variability of levels of regional background aerosols in the Western Mediterranean. *Science of the Total Environment* **407**(1), pp. 527–540.

Pey, J., Pérez, N., Querol, X., Alastuey, A., Cusack, M., Reche, C., 2010a. Intense winter atmospheric pollution episodes affecting the Western Mediterranean. *Science of the Total Environment* **408**(8), pp. 1951–1959.

Pey, J., Querol, X., Alastuey, A., 2010b. Discriminating the regional and urban contributions in the North-Western Mediterranean: PM levels and composition. *Atmospheric Environment* **44**(13), pp. 1587–1596.

Pope III, C. A., Dockery, D. W. 2006. Health effects of fine particulate air pollution: lines that connect. *Journal of the Air & Waste Management Association* **56**(6), pp. 709–742.

Prospero, J. M., Schmitt, R., Cuevas, E., Savoie, D. L., Graustein, W. C., Turekian, K. K., Volz-Thomas, A., Díaz, A., Oltmans, S. J., Levy II, H., 1995. Temporal variability of summer-time ozone and aerosol in the free troposphere over the eastern North Atlantic. *Geophysical Research Letters* **22**(21), pp. 2925–2928.

Putaud, J.P., Van Dingenen, R., Raes, F., 2002. Submicron aerosol mass balance at urban and semirural sites in the Milan area (Italy). *Journal of Geophysical Research*. Atmospheres **107**, 4777.

Querol, X., Alastuey, A., Pey, J., Escudero, M., Castillo, S., Gonzalez, A., Pallares, M., Jiménez, S., Cristóbal, A., Ferreira, F., Marques, F., Monjarino, J., Cuevas, E., Alonso, S., Artiñano, B., Salvador, P., de la Rosa, J., 2006. Spain and Portugal Methodology for the identification of natural African dust episodes in PM_{10} and $PM_{2.5}$, and justification with regards to the exceedances of the PM_{10} daily limit value. Ministerio de Medio Ambiente, Medio Rural y Marino (Spain) and Ministério do Ambiente, Ordenamento do Territorio e Desenvolvimento Regional (Portugal). 32 pp.

Querol, X., Alastuey, A., Pey, J., Cusack, M., Pérez, N., Mihalopoulos, N., C. Theodosi, C., Gerasopoulos, E., Kubilay, N., Koçak, M., 2009. Variability in regional background aerosols within the Mediterranean. *Atmospheric Chemistry and Physics* **9**, pp. 4575–4591.

Ripoll, A., Pey, J., Minguillón, M.C., Pérez, N., Pandolfi, M., Querol, X., Alastuey, A., 2014. Three years of aerosol mass, black carbon and particle number concentrations at Montsec (Southern Pyrenees, 1570 m a.s.l.). *Atmospheric Chemistry and Physics* **14**, pp. 4279–4295.

Ripoll, A., Minguillón, M. C., Pey, J., Pérez, N., Querol, X., Alastuey, A., 2015a. Joint analysis of continental and regional background environments in the Western

Mediterranean: PM_1 and PM_{10} concentrations and compositions. *Atmospheric Chemistry and Physics* **15**, pp. 1129–1145.

Ripoll, A., Minguillón, M. C., Pey, J., Jiménez, J. L., Day, D.A., Sosedova, Y., Canonaco, F., Prévôt, A.S.H., Querol, X., Alastuey, A., 2015b. Long-term realtime chemical characterization of submicron aerosols at Montsec (Southern Pyrenees, 1570 m a.s.l.). *Atmospheric Chemistry and Physics* **15**, pp. 2935–2951.

Rodriguez, S., Querol, X., Alastuey, A., Mantilla, E., 2002. Origin of high summer PM_{10} and TSP concentrations at rural sites in Eastern Spain. *Atmospheric Environment* **36**, pp. 3101–3112.

Salvador, P., Alonso-Pérez, S., Pey, J., Artíñano, B., de Bustos, J. J., Alastuey, A., Querol, X., 2014. African dust outbreaks over the western Mediterranean Basin: 11-year characterization of atmospheric circulation patterns and dust source areas. *Atmospheric Chemistry and Physics* **14**, pp. 6759–6775.

Scheel, H., Areskoug, H., Geiss, H., Gomiscek, B., Granby, K., Haszpra, L., Klasinc, L., Kley, D., Laurila, T., Lindskog, A., Roemer, M., Schmitt, R., Simmonds, P., Solberg, S., Toupance, G., 1997. On the spatial distribution and seasonal variation of lower-troposphere ozone over Europe. *Journal of Atmospheric Chemistry* **28**, pp. 11–28.

Segura, S., Estellés, V., Esteve, A.R., Marcos, C.R., Utrillas, M.P., Martínez-Lozano, J.A., 2016. Multiyear in-situ measurements of atmospheric aerosol absorption properties at an urban coastal site in western Mediterranean. *Atmospheric Environment* **129**, pp. 18–26.

Seinfeld, J.H., Pandis, S.N., 1998. Atmospheric Chemistry and Physics: From air pollution to climate change. John Wiley & Sons, Inc.

Sellegri, K., Laj, P., Dupuy, R., Legrand, M., Preunkert, S., Putaud, J.P., 2003. Size-dependent scavenging efficiencies of multicomponent atmospheric aerosols in clouds. *Journal of Geophysical Research* **108** (D11), 4334.

Singh, S., Elumalai, S.P., Pal, A. K., 2016. Rain pH estimation based on the particulate matter pollutants and wet deposition study. *Science of the Total Environment* **563–564**, pp. 293–301.

Sjogren, S., Gysel, M., Weingartner, E., Alfarra, M. R., Duplissy, J., Cozic, J., Crosier, J., Coe, H., Baltensperger, U., 2008. Hygroscopicity of the submicrometer aerosol at the high-alpine site Jungfraujoch, 3580 m a.s.l., Switzerland. *Atmospheric Chemistry and Physics* **8**, pp. 5715–5729.

Umann, B., Arnold, F., Schaal, C., Hanke, M., Uecker, J., Aufmhoff, H., Balkanski, Y., Van Dinengen R., 2005. Interaction of mineral dust with gas phase nitric acid and sulfur dioxide during the MINATROC II field campaign: first estimate to the uptake coefficient gamma (HNO_3) from atmospheric data. *Journal of Geophysical Research* **110**, D22306. DOI:10.1029/2005JD005906.

Van Dingenen, R., Putaud, J. P., Martins-Dos Santos, S., Raes, F., 2005. Physical aerosol properties and their relation to air mass origin at Monte Cimone (Italy) during the first MINATROC campaign. *Atmospheric Chemistry and Physics* **5**, pp. 2203–2226.

Vecchi, R., Marcazzan, G., Valli, G., Ceriani, M., Antoniazzi, C., 2004. The role of atmospheric dispersion in the seasonal variation of PM_1 and $PM_{2.5}$ concentration and composition in the urban area of Milan (Italy). *Atmospheric Environment* **38**, pp. 4437–4446.

Viana, M., 2003. Niveles, composición y origen del material particulado atmosférico en los sectores Norte y Este de la Península Ibérica y Canarias. Tesis Doctoral, Universidad de Barcelona.

Warneck, P., 1988. Chemistry of the natural atmosphere. *International Geophysics Series*. **41**, p. 757. John Wiley & Sons.

Whitby, K. T., 1978. The physical characteristics of sulfur aerosols. Sulfur in the Atmosphere. Proceedings of the International Symposium Held in Dubrovnik, Yugoslavia, 7–14 September 1977. pp. 135–159.

WHO, 2013a. IARC: Outdoor air pollution a leading environmental cause of cancer deaths. https://www.iarc.fr/en/media-centre/iarcnews/pdf/pr221_E.pdf

WHO, 2013b. Review of evidence on health aspects of air pollution–REVIHAAP. First Results. WHO's Regional Office for Europe, Copenhaguen.
http://www.euro.who.int/__data/assets/pdf_file/0020/182432/e96762-final.pdf

WHO, 2016. Ambient (outdoor) air quality and health – Fact Sheet. September 2016. http://www.who.int/mediacentre/factsheets/fs313/en/

Woods, A., 2006. Medium-Range Weather Prediction – The European Approach. Springer. ISBN 978-0-387-26928-3. DOI 10.1007/b138324

Yan, Z., Jin, Y., An, Z., Liu, Y., Samet, J. M., Wu, W., 2016. Inflammatory cell signaling following exposures to particulate matter and ozone. *Biochimica et Biophysica Acta (BBA) - General Subjects* **1860**(12), pp. 2826–2834.

Yubero, E., Galindo, N., Nicolás, J.F., Crespo, J., Calzolai, G., Lucarelli, F., 2015. Temporal variations of PM_1 major components in an urban Street canyon. *Environmental Science and Pollution Research* **22**, pp. 13328-13335.

Zhao, T., Yang, L., Yan, W., Zhang, J., Lu, W., Yang, Y., Chen, J., Wang, W., 2017. Chemical characteristics of $PM_1/PM_{2.5}$ and influence on visual range at the summit of Mount Tai, North China. *Science of the Total Environment* **575**, pp. 458–466

Anexo 1.

Impacts on particles and ozone by transport processes recorded at urban and high-altitude monitoring stations

Science of the Total Environment 466–467 (2014) 439–446

Contents lists available at SciVerse ScienceDirect

Science of the Total Environment

journal homepage: www.elsevier.com/locate/scitotenv

Impacts on particles and ozone by transport processes recorded at urban and high-altitude monitoring stations

J.F. Nicolás [a,*], J. Crespo [a], E. Yubero [a], R. Soler [a], A. Carratalá [b], E. Mantilla [c]

[a] Laboratory of Atmospheric Pollution (LCA), Miguel Hernández University, Av. de la Universidad s/n, Edif. Alcudia, 03202 Elche, Spain
[b] Department of Chemical Engineering, University of Alicante, P.O. Box 99, 03080 Alicante, Spain
[c] Instituto Universitario CEAM-UMH, Parque Tecnológico, C/Charles R. Darwin 14, E-46980 Paterna, Spain

HIGHLIGHTS

- Coarse particles at the mountain site are 40% higher than at the urban site in summer.
- Stagnant urban episodes can provoke particle increases at the mountain station.
- Stagnant events affect mainly particles in the 0.5–2 μm range at the mountain station.
- During Saharan outbreaks, O_3 levels at the mountain site undergo a decrease (3–17%).

ARTICLE INFO

Article history:
Received 22 April 2013
Received in revised form 28 June 2013
Accepted 17 July 2013
Available online xxxx

Editor: Xuexi Tie

Keywords:
High-altitude station
Transport aerosol
Particle number concentration
Size distribution
Ozone

ABSTRACT

In order to evaluate the influence of particle transport episodes on particle number concentration temporal trends at both urban and high-altitude (Aitana peak-1558 m a.s.l.) stations, a simultaneous sampling campaign from October 2011 to September 2012 was performed. The monitoring stations are located in southeastern Spain, close to the Mediterranean coast.

The annual average value of particle concentration obtained in the larger accumulation mode (size range 0.25–1 μm) at the mountain site, 55.0 ± 3.0 cm^{-3}, was practically half that of the value obtained at the urban station (112.0 ± 4.0 cm^{-3}). The largest difference between both stations was recorded during December 2011 and January 2012, when particles at the mountain station registered the lowest values. It was observed that during urban stagnant episodes, particle transport from urban sites to the mountain station could take place under specific atmospheric conditions. During these transports, the major particle transfer is produced in the 0.5–2 μm size range. The minimum difference between stations was recorded in summer, particularly in July 2012, which is most likely due to several particle transport events that affected only the mountain station. The particle concentration in the coarse mode was very similar at both monitoring sites, with the biggest difference being recorded during the summer months, 0.4 ± 0.1 cm^{-3} at the urban site and 0.9 ± 0.1 cm^{-3} at the Aitana peak in August 2012. Saharan dust outbreaks were the main factor responsible for these values during summer time. The regional station was affected more by these outbreaks, recording values of >4.0 cm^{-3}, than the urban site. This long-range particle transport from the Sahara desert also had an effect upon O_3 levels measured at the mountain station. During periods affected by Saharan dust outbreaks, ozone levels underwent a significant decrease (3–17%) with respect to its mean value.

1. Introduction

Interesting atmospheric studies have been made possible thanks to the installation of monitoring stations at high altitude sites in order to characterize regional background environments. The same studies would be difficult at ground level sites.

In Europe, the study of atmospheric particulate matter (PM) at these mountain stations, e.g. Jungfraujoch (Switzerland — 3580 m a.s.l.), Monte Cimone (Italy — 2165 m a.s.l.) or Montseny (Spain — 720 m a.s.l.) has allowed researchers to establish reliable PM background levels. Other studies also show the impact of both the regional and long-range transport of polluted air masses on these kind of environments (Schwikowski et al., 1995; Káiser et al., 2007; Marinoni et al., 2008; Pey et al., 2010a) and determine the main causes of the daily and seasonal variability (Henning et al., 1999; Marinoni et al., 2008; Cristofanelli and Bonasoni, 2009; Querol et al., 2009). Therefore, an important aspect of the research has been the analysis of how the

* Corresponding author. Tel.: +34 966658325; fax: +34 966658397.
E-mail address: j.nicolas@umh.es (J.F. Nicolás).

0048-9697/$ – see front matter © 2013 Elsevier B.V. All rights reserved.
http://dx.doi.org/10.1016/j.scitotenv.2013.07.060

PM generated in urban and industrial environments, under specific meteorological conditions, can contribute to the PM value registered at these regional background stations. Marinoni et al. (2008) at Monte Cimone station recorded maximum values of fine fraction particles during summer period due to the vertical transport of polluted air masses. Pey et al. (2010a) recorded PM_1 peaks during polluted episodes in winter characterized by anticyclonic synoptic scenarios. This is also partly due to secondary aerosol formation along the trajectory of air masses from urban locations to the elevated rural sites.

Due to the height and the lack of anthropogenic activity at these sampling points, remote mountain stations are suitable to determine precisely the impact of air masses from Sahara desert impact on particle concentration (Bonasoni et al., 2004; Marinoni et al., 2008) and on the tropospheric ozone decrease (Bonasoni et al., 2004). Bonasoni et al. (2004) observed an ozone concentration reduction between 4 and 21% with respect to their monthly average values during twelve Saharan dust outbreaks between June and December 2000. Similarly, Umann et al. (2005) recorded a decrease of 30% in the ozone levels at the Izaña station (2360 m a.s.l.) during a Saharan dust transport. These studies suggest that mineral dust particles may act as a reactive surface in the heterogeneous destruction of the ozone (Cristofanelli and Bonasoni, 2009).

Measuring at elevated regional environments presents another advantage, that is, to obtain concentration profiles that can help us, by subtraction, to discriminate what is the real contribution attributable to a particular anthropogenic location. A graphic example of this method can be seen in Lenschow et al. (2001). This distinction, using the chemical composition of PM, is also presented in Pey et al. (2010b).

Most of the high-mountain stations show common features, such as a lack of human activity or low concentration values for the majority of pollutants. Nevertheless, depending on where its particular geographical position is, regional background stations can be affected by different contributions of different pollutants according to the origins of the air masses in which they are transported. Both, atmospheric dynamics and the main sources of particles in each area can determine the concentration levels and the seasonal variability obtained at these sampling points.

The western Mediterranean basin, which is the study area analyzed in this work, has a peculiar atmospheric dynamic that provokes a clear temporal pattern in the levels registered at the regional background locations. In Querol et al. (2009), the main factors affecting the complex atmospheric dynamic in the western Mediterranean basin, such as the scarce summer precipitation or the influence of the Azores high-pressure system, are described. During warm periods, the atmospheric conditions characterized by the lack of advection, favors the recirculation of air masses and the occurrence of Saharan dust outbreaks. During cold periods, Atlantic air masses bring clean, fresh air removing the regional aged air masses. Furthermore, polluted air masses from central and northern Europe can reach the study area. Lastly, episodes involving the stagnation of air masses can be generated, leading to the increase of atmospheric pollution (Pey et al., 2010a).

Recently, a new regional background station has been placed on the top of mountain range. This mountain station is located in southeastern Spain, close to the Mediterranean coast. With this new elevated sampling point, it is expected to determine the following:

- the aerosol size distribution and number concentration at this regional background station (RS) and the difference when compared with the ones obtained at an urban background station (US). In doing this, an estimation of the real particles load attributable to urban sources can be obtained. Their seasonal variations will also be assessed. All of this will be discussed in Section 3.2.
- the influence that local and synoptic transports of air masses have upon aerosol parameters and tropospheric ozone at the RS. The inputs of particles at this point coming from coastal emissions and from Sahara Desert will be investigated (Sections 3.3 and 3.4).

2. Experimental

2.1. Measurement sites

The study is a general assessment of the main factors governing the total particle number concentration at the RS (N_{RS}) and the US (N_{US}). In order to achieve this, two locations whose features were the most appropriate to represent these environments inside the province of Alicante in southeastern Spain, were chosen. On a synoptic scale, this region belongs to the Western Mediterranean Basin (Fig. 1), and its local and regional meteorology characteristics have been discussed in the introduction. The study area is situated in a semiarid region with low annual precipitation levels recorded at urban sites (in general less than 300 $l \cdot m^{-2}$). A brief orographic and geographic description of the study region can be found in Caballero et al. (2007). The two main characteristics of this region are that the area is barely industrialized and that its major cities are located very close to the coast.

The first sampling location represented a regional background site. The sampling point (38°39′N; 0°16′W; 1558 m a.s.l.) was located on top of a mountain range, in a military area (EVA nº. 5) belonging to the Ministry of Defence and situated 25 km from the Mediterranean coast (see Fig. 1). The station is located specifically at the named "Aitana peak".

The second monitoring site, about 57 km southeast of the RS, represents an urban background environment. The station is located in the city of Elche (38°16′N; 0°41′W; 95 m a.s.l.), 12 km from the coast (Fig. 1). Specifically, the measurement site is placed on the roof of a building at the Miguel Hernández University, approximately 15 m above ground level in a ventilated area. The main meteorological characteristics of the urban area can be consulted in Nicolás et al. (2009).

2.2. Data collection

The study period comprised from October 2011 to September 2012. In that period particle number concentration and size distribution along with O_3 levels and meteorological parameters in the two stations aforementioned were measured.

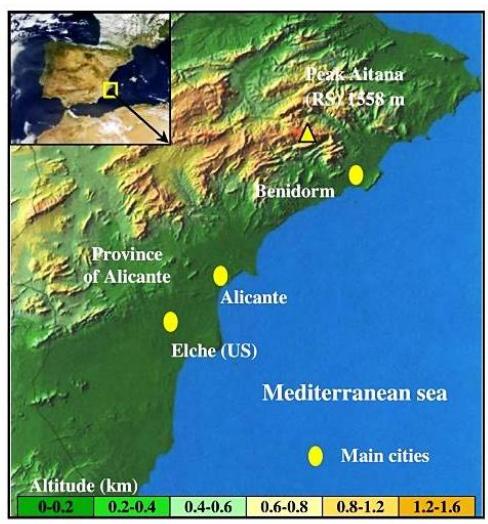

Fig. 1. Location and topography of the monitoring sites (US and RS) on the Spanish Mediterranean coast.

The instruments used to measure particle concentrations were two optical counters: Grimm 365 (US) and Grimm 190 (RS). These instruments determine particle number concentrations in 31 particle size channels from 0.25 to 32 μm. The measurements permit the determination of a fraction of fine mode and coarse mode particles with a 1 min time resolution although during the campaign a time resolution of 10 min was used. Twenty-four hour averages were subsequently calculated based on the counter data. The instrument is based on the quantification of 90° scattering of light by aerosol particles. All sizes are given as optical equivalent diameters.

At the RS site, meteorological data were obtained from a weather station located about 10 m above the ground. For the US site, the data were provided by an air quality network station belonging to Valencia regional government, located ~2 km south of the measurement site. At both stations levels of: temperature, wind velocity, wind direction, precipitation, solar radiation, atmospheric pressure and relative humidity were measured. At the US several gaseous and particulate pollutants concentrations were sampled. At the RS, levels of O_3 were registered using a Dasibi model 1008 UV absorption continuous analyzer.

NCEP meteorological maps (http://www.esrl.noaa.gov/psd/data/composites/hour/) (Kalnay et al., 1996) were checked in order to analyze the synoptic meteorological scenarios. Aerosol maps from the Marine Meteorology Division of the naval research Laboratory, USA (NRL) (http://www.nrlmry.navy.mil/aerosol); the BSC-/DREAM dust maps (http://www.bsc.es/projects/earthscience/DREAM/) (Pérez et al., 2006), and a data base containing details of Saharan dust intrusions and other differential events affecting the Iberian Peninsula and Canary Islands (http://www.calima.ws/) were also used.

To determine the CBL (Convective Boundary Layer) height the webpage (http://weather.uwyo.edu/upperair/sounding.html), provided by the University of Wyoming, where meteorological soundings are available was used. In our case, soundings which were gathered at a station located near the city of Murcia (37°59′ N; 1°7′ W; 62 m a.s.l), which is close to our urban site, were studied. For this purpose we also used the webpage (http://ready.arl.noaa.gov/READYamet.php) from the NOAA Air Resources Laboratory.

2.2.1. Intercomparison of the two optical counters

Prior to the measurement campaign, an intercomparison between the two counters was performed: $N_{365} = 1.04 \cdot N_{190} + 0.4$ (cm^{-3})/ $R^2 = 0.9993$; where N is the total particle number concentration. The optical counter located at the US measured about 5% more particles than the one located at the RS. This discrepancy will be corrected when the difference in total particle concentration between the two environments is assessed.

In order to compare the particle size distribution obtained in both environments it is necessary to carry out a calibration between the optical counter channels one by one. For this purpose, we compared the average size distributions obtained by the two optical counters at the same location (urban site) and at the same time. The values registered by the Grimm 365 were taken as a reference and the values obtained by the other counter were corrected. Once the Grimm 190 values were corrected, the average particle concentrations obtained by every channel in both counters were compared with a non-parametric test (Mann–Whitney) since the distributions obtained did not follow a normal distribution. The use and applicability of statistical tests for comparing particle size distributions which are characterized by a large number of sizing channels is a common practice (Heitbrink et al., 1990; Morawska et al., 1999). In this case, for each channel of both counters the distributions were compared with the null hypothesis (H_0): the average values obtained in the same channel of both optical counters are similar at a 95% confidence level; H_0 will be rejected if the p-value < 0.05. We obtained a p-value > 0.05 in all channels up to 1 μm. However, for larger sizes, p-values were < 0.05. This result is expected since the particle number concentration for coarse particles is <0.1 cm^{-3}.

3. Results and discussions

3.1. Particle episodes and meteorological variables

The atmospheric dynamic that takes place in the study area has a huge influence on the temporal variability of PM. It presents several meteorological scenarios, all of them with a marked seasonality. These atmospheric situations cause increases or decreases in particle number concentrations at different degrees according to their strength.

During the spring and summer months, both the urban and regional sites were affected by Saharan air masses. Up to fifteen different outbreaks took place during the sampling period. Ten of these outbreaks affected the study area given that they passed below 1500 m a.s.l. This means that 42% of summer and spring days were affected by this kind of event. Sometimes, these air mass intrusions with a high load of dust can hide the effects from recirculation episodes on PM since both scenarios can take place simultaneously.

Another significant event that occurs mainly during summer is the uncontrolled biomass burning. Wild fires, mainly due to the mass burning of dry fruit tree branches, are common in southeast Spain and in general throughout the entire Iberian Peninsula. Seven events close to the study area were identified during this period.

During autumn and winter months, only one-third of the Saharan dust outbreaks which occur during warm months were registered. Nevertheless, eleven episodes of high atmospheric stability that favored the accumulation of pollutants in the urban sites were recorded during the cold season. These events lasted between three and nine days. Specifically, one objective of our work is to find out if some PM from urban stations reaches the RS during these high stability periods.

On many of days during the cold season (50–60%) the air masses had an Atlantic origin. European episodes scarcely affected the study area.

Table 1 shows monthly average values of the main meteorological parameters registered at both stations. Precipitation data corresponds to the accumulate value.

As can be seen, the temperature at the RS was between 7 and 12 °C lower than at the US, and at both stations there was a clear division between the colder (November–April) and warmer months (May–October). Monthly variation tendency in temperature was the same at both environments. Similar behavior was observed in the levels of solar radiation, although this parameter presented higher values at the RS than at the US. This is likely due to the presence of clouds below the RS (1558 m a.s.l.) and the negative particle and gas gradients with height.

The annual accumulate precipitation at the RS was almost three times higher than the one registered at the US, in particular during the month of November at the RS. During this month, precipitations were registered on half of the days. This meteorological situation at the RS contrasts with data recorded at both stations during June and July when precipitations values were lower than 2 $l \cdot m^{-2}$.

3.2. Monthly evolution of particle number concentration at both stations

Table 2 shows monthly and global average values for the coarse and fine particles at the two environments. During autumn months only 40% of the data was valid. This was due to the high relative humidity (RH) registered at the RS during those days (RH daily average >80%). Under such conditions, it is unlikely that the counter can discriminate adequately between aerosols and small precipitating droplets or extremely small droplets that remain suspended in the atmosphere (Castro et al., 2010).

The highest levels of fine particle concentration at the US (N_{FUS}) were registered during the winter and summer months with N_{FUS} reaching its absolute peak during August. The coarse particle concentration at the US (N_{CUS}) showed a clear discontinuity between the colder months (November–March), with values below 0.20 ± 0.01 cm^{-3}, and the warmer ones, in which the concentration became three times

Table 1
Monthly average values for the main meteorological parameters recorded at US and RS.

Month	T_{US} (°C)	T_{RS} (°C)	P_{US} (l·m^{-2})	P_{RS} (l·m^{-2})	SR_{US} (W/m^2)	SR_{RS} (W/m^2)	v_{US} (m·s^{-1})	v_{RS} (m·s^{-1})
Oct-11	21.2	10.7	18.0	127.7	156.1	137.5	0.9	4.3
Nov-11	16.5	5.7	104.8	208.0	84.2	86.2	1.1	6.4
Dec-11	13.4	4.3	8.4	86.6	78.5	103.9	0.8	6.1
Jan-12	12.6	3.0	11.0	104.0	94.4	104.7	0.7	4.6
Feb-12	9.9	−0.5	6.2	97.9	149.6	160.4	1.1	7.5
Mar-12	14.1	5.1	36.2	18.0	204.5	228.5	1.1	n.d
Apr-12	17.3	5.7	50.8	45.1	222.5	221.2	1.1	8.0
May-12	21.4	13.3	0.4	75.0	293.2	330.8	1.1	4.4
Jun-12	25.8	18.8	1.6	1.3	294.4	337.6	1.2	4.5
Jul-12	26.4	19.0	0.0	0.2	273.5	309.8	1.3	3.8
Aug-12	28.2	22.2	1.2	16.8	235.8	276.7	1.1	4.7
Sep-12	24.0	15.7	73.8	59.7	191.8	232.6	1.0	4.4
Annual	19.2	10.3	312.4	840.3	189.8	210.8	1.0	5.3

T: Temperature; P: Total precipitation; v: Wind speed; SR: Solar radiation; n.d: no data.

higher, reaching its maximum in June (0.6 ± 0.1 cm^{-3}). N_{CUS} differences between the cold and warm months can be attributed to the following factors: a higher contribution with marine aerosol, lack of precipitation, greater resuspension and a higher frequency of Saharan dust outbreaks (this factor also affects the fine particles too). Winter high stability episodes have a greater influence on the fine particles than on the coarse ones (Marcazzan et al., 2002; Galindo et al., 2008). This explains the elevated values of N_{FUS} during winter.

At the RS, the fine particles showed a similar monthly trend to the one seen at the US. Fine particle concentration at the RS (N_{FRS}) obtained maximum levels during the warmer period (from July to September). Although slightly lower than in summer, N_{FRS} showed high values during February and March as well. N_{FRS} made up between 20 and 85% of N_{FUS}. This percentage varies according to the season, with minimum values in January and February and maximum values in spring and summer. The annual average was: $N_{FRS} \approx 0.5 \cdot N_{FUS}$. The coarse particle concentration at the RS (N_{CRS}) was relatively higher during summer when compared to the rest of year, reaching a peak of 0.9 ± 0.1 cm^{-3} in August. Significantly, $N_{CRS} > N_{CUS}$ during summertime. This is likely due to the fact that between June and August, 55% of days were affected by Saharan dust outbreaks and these air mass entrances affected the RS more than the US. For this reason, N_{CRS} annual average value was slightly higher than N_{CUS} one.

Global particle concentration levels measured at the RS are quite high if they are compared with ones obtained at other similar stations. For instance, the average values at Mt. Cimone (North Italian Apennines — 2165 m a.s.l.) were $N_F = 26.15$ cm^{-3} and $N_C = 0.17$ cm^{-3} (Marinoni et al., 2008). These values involve concentrations 50% lower than the ones measured at Aitana peak. Again, this is more likely due to the high frequency of dust outbreaks that took place during the sampling period of this work which was higher than in previous years. Furthermore, Aitana peak is closer to the Sahara desert than Mt. Cimone. Nevertheless, temporal concentration evolutions are quite similar at both mountain stations.

In Fig. 2 we can compare the particle size distributions obtained at the RS and the US. The distributions are calculated for the colder (December–January and February) and warmer (June–July and August) months.

In general, the size distributions at both stations during the cold period (Fig. 2a) were quite similar, although the particle number concentration up to 2 μm registered at the US was higher. During the warm

Table 2
Monthly average values of fine and coarse particles and standard deviation at RS and US.

	n	N_{FUS} (σ)	N_{FRS} (σ)	N_{CUS} (σ)	N_{CRS} (σ)
Oct-11	16	136.9 (45.4)	61.5 (25.0)	0.3 (0.2)	0.2 (0.2)
Nov-11	2	99.5 (42.3)	n.d	0.2 (0.1)	n.d
Dec-11	18	92.1 (58.9)	18.7 (12.3)	0.1 (0.1)	0.1 (0.1)
Jan-12	21	125.9 (69.4)	24.9 (7.5)	0.1 (0.1)	0.1 (0.1)
Feb-12	24	101.9 (54.6)	59.8 (21.0)	0.1 (0.1)	0.1 (0.1)
Mar-12	23	133.9 (55.4)	83.7 (34.9)	0.2 (0.1)	0.2 (0.1)
Apr-12	20	73.4 (38.0)	31.9 (16.0)	0.4 (0.2)	0.2 (0.1)
May-12	29	86.8 (44.0)	45.8 (20.0)	0.4 (0.2)	0.3 (0.2)
Jun-12	29	104.8 (33.8)	57.5 (28.9)	0.6 (0.2)	0.7 (0.6)
Jul-12	27	115.1 (29.6)	96.4 (54.5)	0.3 (0.1)	0.6 (0.4)
Aug-12	27	139.7 (44.1)	69.4 (55.6)	0.4 (0.1)	0.9 (0.3)
Sep-12	21	137.4 (44.0)	75.4 (30.0)	0.3 (0.1)	0.3 (0.1)
Annual	257	112.3 (46.6)	55.0 (27.5)	0.3 (0.1)	0.3 (0.2)

n: Valid days at RS; σ: Standard deviation (cm^{-3}); N_{FUS}: Fine particle number concentration at US (cm^{-3}); N_{FRS}: Fine particle number concentration at RS (cm^{-3}); N_{CUS}: Coarse particle number concentration at US (cm^{-3}); N_{CRS}: Coarse particle number concentration at RS (cm^{-3}); n.d: no data.

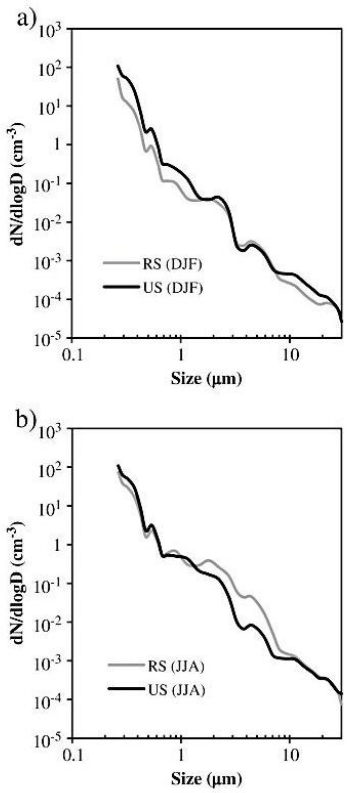

Fig. 2. Average number size distributions obtained at RS and US during: a) cold months (DJF); b) warm months (JJA).

months (Fig. 2b), two differences with respect to the distributions obtained in winter were observed. Firstly, the particle number concentration difference in the accumulation mode between the RS and the US decreased even though the concentration at the US remained slightly higher. The second difference was that the particle number concentration in coarse mode particles up to 10 μm was higher at the RS, reaching the largest difference in the 3–5 μm range.

3.3. Transport of polluted air masses during cold months from urban coastal areas to the RS

During the colder months, the daily variation in total particle concentration registered at the RS ($N_{RS}(t)$) can be attributed mainly to õAtlantic episodes (air masses from the Atlantic Ocean), and on a few occasions to the regional transport of particles from urban nuclei. Moreover and although much less frequently than in summer period, air masses from the Sahara desert can reach the RS.

The transport of particles and other pollutants during winter from urban coastal areas within the study region (see Fig. 1) to the RS takes place under specific meteorological scenarios. From the $N_{RS}(t)$ analysis it can be proven that some high stability episodes produced at these urban sites can also provoke increases in N_{RS}. In Fig. 3a an example that demonstrates this particular situation can be observed. This episode took place from 24 February 2012 to 2 March 2012. To quantify its impact upon N_{RS} values it must be remembered that during winter months the average total particle concentration values were: $N_{US} = 120 \pm 9\ cm^{-3}$ and $N_{RS} = 58 \pm 5\ cm^{-3}$ (see Table 2). On 1 March 2012 maximum values of N_{US} and N_{RS} were $275 \pm 9\ cm^{-3}$ and $124 \pm 4\ cm^{-3}$ respectively. Maximum values were also registered at both stations after several days with consecutive increases. As can be seen, O_3 levels registered at the RS experienced a similar rise.

Meteorological characteristics provoking these episodes are well-known: an anticyclonic situation, low wind velocity, high solar radiation and a decrease in the mixing layer height. Some of them have been represented in Fig. 3b. However, these features can only explain the urban particle increase. Under the aforementioned meteorological scenario, a local breeze regimen would have also been necessary to produce the N_{RS} increase. Marine breezes can collect part of settled PM at coastal urban sites, carrying it towards the mountain slopes. Subsequently, particles can be transported by mountain breezes that are channeled through the slopes until reaching the RS. A similar explanation about this sort of transport can be found in Pey et al. (2010a).

Focusing on the previous example, marine breeze circulation from 24 February 2012 to 1 March 2012 with the exception of 27 February 2012 was documented. Breeze speed was slightly low, with values ranging from 1.6 to 2.3 $m \cdot s^{-1}$. During those days between 13:00 h and 17:00 h (UTC) the wind direction oscillated within the 120–140° range. Under these conditions, the air mass flowing through the city of Alicante (see Fig. 1) at 14:00 h UTC may have reached at the RS at 20:00 h (UTC) approximately.

The ozone level increased during these episodes since the marine breeze carries nitrogen oxides from the urban sites. The high solar radiation prevailing on those days favors the O_3 formation. As such, during winter episode, a significant percentage of the O_3 measured at the RS

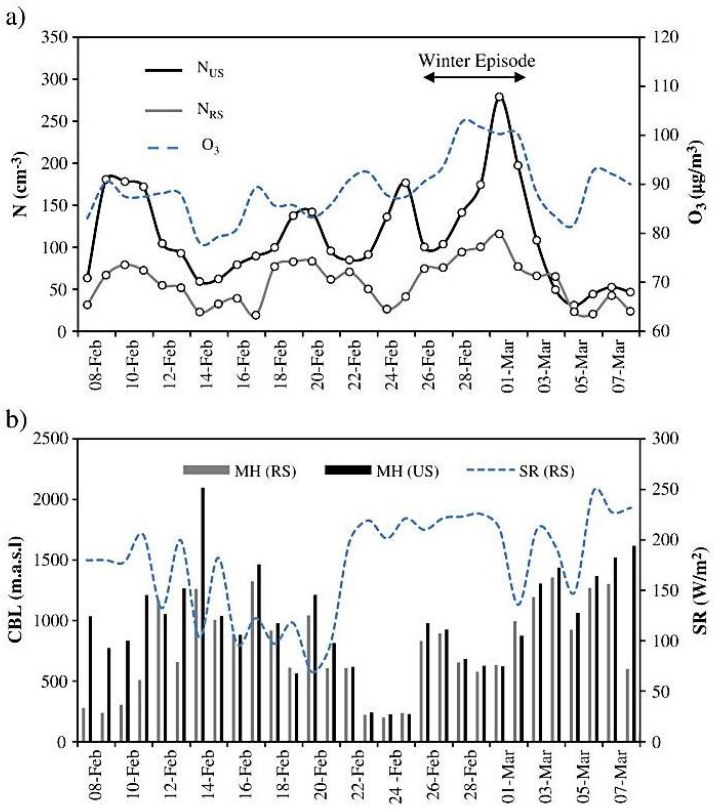

Fig. 3. Daily values obtained during a winter period of: a) total particle concentration measured at US (N_{US}) and RS (N_{RS}) along with tropospheric ozone at RS. b) Mixing layer height (MH) registered at US and RS along with solar radiation (SR) at RS.

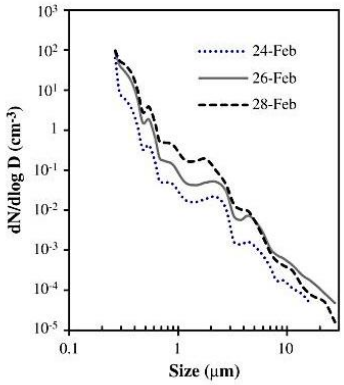

Fig. 4. Evolution of particle size distribution obtained at RS during the winter episode.

(approximately 10%) was generated along the path between coastal urban nuclei and the RS.

Fig. 4 shows the evolution in particle size distributions during the days that the winter episode at the RS lasted. As the distributions belonging to 29 February 2012 and 1 March 2012 are practically identical to that obtained on 28 February 2012, only this day was represented.

Using the size distribution obtained on 24 February 2012 as the reference, it is noted that the higher increment, in relative terms, was obtained in the 0.5–2 μm range. This is the size range where a major particle transfer from urban sites to the RS is produced. A statistical comparison (Mann–Whitney test) of particle size distributions was applied between the distribution obtained on 24 January 2012 (event start) and the one registered on 28 January 2012. The test revealed that the two distributions are not similar (p value < 0.05) up to 7.5 μm.

3.4. Transport of air masses affecting the RS and the US during warm season

The frequency of events that can influence $N_{RS}(t)$ during spring and summer periods is even greater than the one registered in cold months. An example of this can be seen in Table 3. The different events that occurred in the study area between 25 June and 6 August are presented in Table 3.

In this brief time period, up to four Saharan dust outbreaks (S) took place along with a recirculation episode (R) and one uncontrolled biomass burning episode (BB). The influence of these events upon $N_{RS}(t)$ and $N_{US}(t)$ can be observed in Fig. 5. Fig. 5 shows two features about this influence: a) the impact of these episodes did not affect fine (N_F) and coarse (N_C) particles in the same way, regardless of the kind of environment; b) some episodes (R, BB) only affect the RS.

The first affirmation can be confirmed if the different impact provoked by dust intrusions is observed. The S1 intrusion had an effect upon coarse particles at both environments, but the N_{FRS} level was hardly affected. The situation differs if the effect on particles due to S4 intrusion is checked. During S4 intrusion, a large increase in the N_{FRS}, the N_{FUS} and the N_{CRS} values was detected, however, a noticeable increment in the N_{CUS} values was not observed. The different heights of the outbreaks which reached the study area, together with the distinct previous paths that the air masses from the Sahara desert covered before arriving at the RS or the US, undoubtedly determine the different impacts upon particle concentration. In Giménez et al. (2010), we can find measurements gathered within the study area that verify this assertion. Moreover, the recirculation of air masses and the biomass burning episode only affected the regional station, and mainly fine particles.

Table 3
Dates for the PM episodes recorded between the end of June 2012 and the first days of August 2012.

Date	Event	Abbreviated name
28–30 June	Saharan dust outbreak	S1
1–3 July	Biomass burning	BB
7–11 July	Saharan dust outbreak	S2
14 July	Saharan dust outbreak	S3
21–24 July	Recirculation	R
25 July–05 August	Saharan dust outbreak	S4

Due to the high frequency of episodes registered at the RS, the variation in particle size distributions at the regional station can be observed in a short time period. This can be verified during the first week represented in Fig. 5, between 25 June 2012 and 1 July 2012. In order to check this variation, Fig. 6 shows the particle size distributions obtained during 26 June 2012 (without event), 29 June 2012 (S1) and 1 July 2012 (BB).

Using the distribution obtained on 26 June 2012 as a reference, we can check as S1intrusion affects mainly particles in the 0.5–5 μm size range. A very similar result was obtained at Monte Cimone station (Bonasoni et al., 2004). Both distributions are not statistically similar (p value < 0.05) up to 10 μm, suggesting particles of those days come from different sources. Meanwhile, BB presented a similar profile to that of the reference, with the exception of the finest particles (size <0.5 μm), which experienced a noticeable increase. This result coincides with several studies that have shown a unimodal size distribution of PM from biomass burning with a peak at 0.3–0.6 μm (Hays et al., 2005; Saarnio et al., 2010). The application of the Mann–Whitney test between the reference distribution and the one registered on 1 July 2012 (BB event) revealed that the two distributions are not similar (p value <0.05) up to 6.5 μm.

3.4.1. Variation in ozone levels at RS due to different episodes

The temporal period shown in Fig. 5 is useful for observing the ozone variations measured at the RS in relation to the air masses origin. Fig. 7 presents this variability. The figure also shows the $N_{CRS}(t)$ along with daily average values of solar radiation. Solar radiation is a meteorological parameter that can influence ozone levels measured at the RS. This was confirmed during 15 and 16 July 2012 (see Fig. 7), when both solar radiation and O_3 levels had simultaneously a clear minimum at the same time.

The recirculation episode observed between 21 and 24 July 2012 provoked a daily increment of ozone levels until reaching values higher than 110 μg/m^3. Its effect can be also observed on the N_{FRS} values (Fig. 5).

This daily increase in ozone and fine particles produced mainly in the summer and spring months at the RS was due to the transport of pollutants from urban to regional sites by means of breeze circulation (mountain and sea breezes) over several days. An explication of the accumulation process and the meteorological context under this event is developed, can be found in Rodríguez et al. (2002). Another ozone peak that we can see in Fig. 7 was produced between 2 and 4 July 2012. This maximum could be related to the biomass burning episode that took place during those days. It is known that biomass burning provided the necessary precursors for the observed ozone enhancement (Liu et al., 1999).

N_{CRS} values experienced noticeable rises during most of the dust outbreaks periods with the highest values obtained during 28 and 29 June 2012 (S1) and 27 July 2012 and 2 August 2012 (S4). As can be seen during those days, the ozone levels showed decreasing trends. On 29 June 2012, with $N_{CRS} > 3$ cm^{-3}, the minimum ozone value (80.5 μg/m^3) was measured. However, during the Saharan dust outbreak (S2) a noticeable decrease in the ozone levels was not registered. It is likely due to during S2, N_{CRS} values hardly ever increased. This result suggests that a reduction in ozone levels will be observed if the Saharan air mass carries coarse particles with it.

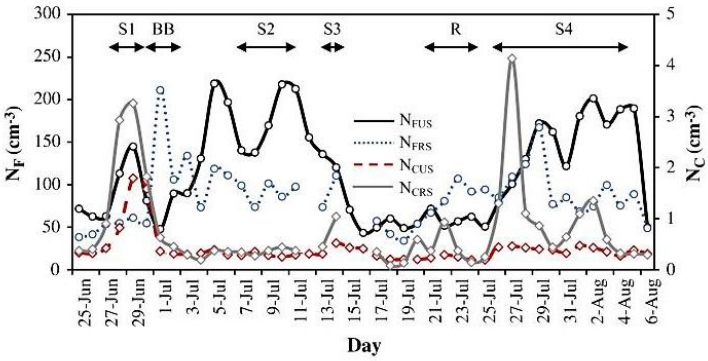

Fig. 5. Contributions of different events on the daily evolution of N_C and N_F at RS and US during a summer period.

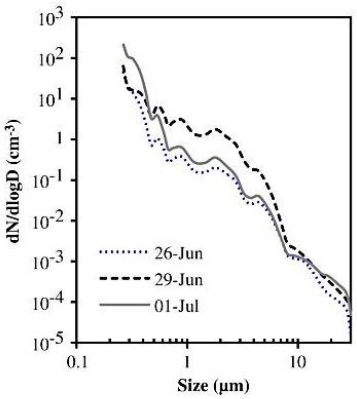

Fig. 6. Particle size distribution variation at RS during the S1and BB events (29 June 2012 and 1 July 2012) and without event (26 June 2012).

During the temporal period showed in Fig. 7 (43 days), the ozone mean value obtained was 97.3 μg/m^3. During the four periods during which Saharan outbreaks occurred (S1–S4), ozone levels decreased with respect to this value between 3 and 17%. This range is similar to the ozone decrease found by Bonasoni et al. (2004) at Mt. Cimone.

4. Conclusions

As expected, N_{US} measured was higher than N_{RS}. However, the different between both concentrations was not sustained over time and instead varied continuously throughout the year. This temporal variation is due to the regions where the stations are located are affected by a continuous succession of air mass entrances with different origins. The nature and frequency of these entrances, which involve distinct particle episodes, differ according to the season and they can affect the fine and the coarse particles in different ways.

For this reason, we have obtained as an average annual value, that $N_{FUS} \approx 2 \cdot N_{FRS}$, although with a greater difference between both concentrations during the colder months. Nevertheless, we have observed how the typical urban stagnant episodes taking place mainly in winter are capable of affecting N_{RS} under a particular atmospheric dynamic. In this way, under the influence of this sort of episode, we measured levels at the RS that doubled its average value. This rise mainly affects particles in the 0.5–2 μm range. The average annual value in coarse particles was more similar at both stations, although during the summer months, $N_{CRS} > N_{CUS}$. The high frequency of air masses from the Sahara desert contributed to this. These outbreaks rise above all particles in the 0.5–5 μm size range and mostly affect the mountain station.

The prevailing atmospheric conditions in the study area can also have effects upon the O_3 levels measured at RS. O_3 shows slight variations according to the sort of event. Thus, winter stagnant episodes, biomass burning and the air masses recirculation that took place in the spring and summer months increased the O_3 levels. However, the effect

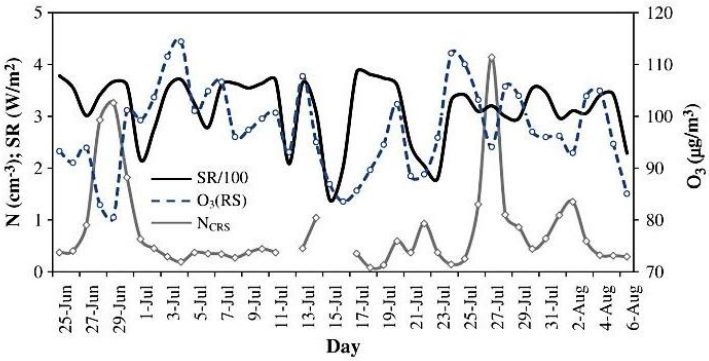

Fig. 7. Daily values measured at RS during a summer period of ozone, N_{CRS} and solar radiation (SR).

of the dust outbreaks is the opposite. During these episodes O_3 levels can be reduced up to 17% from its average value.

Conflict of interest

In this brief letter, the authors of this manuscript want to express that with the publication of this manuscript we only have a scientific objective. Thus, we do not have other goal like financial gain.

Acknowledgements

This study has been supported by the Spanish Ministry of Science and Innovation, MICINN I + D + I Program: PASSE Project, CGL2009-08036. We would like to thank the military area (EVA no. 5) for its assistance in this work. We also thank Paul Nordstrom for his support in this work.

References

Bonasoni P, Cristofanelli P, Calzolari F, Bonafé U, Evangelisti F, Stohl A, et al. Aerosol–ozone correlations during dust transport episodes 2004. Atmos Chem Phys 2004;4:1201–15.

Caballero S, Galindo N, Pastor C, Varea M, Crespo J. Estimated tropospheric ozone levels on the southeast Spanish Mediterranean coast. Atmos Environ 2007;41:2881–6.

Castro A, Alonso-Blanco E, González-Colino M, Calvo A, Fernández-Raga M, Fraile R. Aerosol size distribution in precipitation events in León, Spain. Atmos Res 2010;96:421–35.

Cristofanelli P, Bonasoni P. Background ozone in the southern Europe and Mediterranean area: influence of the transport processes. Environ Pollut 2009;157:1399–406.

Galindo N, Nicolás JF, Yubero E, Caballero S, Pastor C, Crespo J. Factors affecting levels of aerosol sulfate and nitrate on Western Mediterranean coast. Atmos Res 2008;88:305–13.

Giménez J, Pastor C, Castañer R, Nicolás JF, Crespo J, Carratalá A. Influence of Saharan dust outbreaks and atmospheric stability upon vertical profiles of size-segregated aerosols and water vapor. Atmos Environ 2010;44:338–46.

Hays MD, Fine PM, Geron CD, Kleeman MJ, Gullett BK. Open burning of agricultural biomass: physical and chemical properties of particle-phase emissions. Atmos Environ 2005;39:6747–64.

Heitbrink WA, Baron PA, Willeke K. Coincidence in time of flight aerosol spectrometers: phantom particle creation. Aerosol Sci Tech 1990;14:112–26.

Henning S, Lugauer M, Weingartner E, Nyeki S, Buchmann B, Gäggeler HM, et al. Influence of synoptic weather conditions on the aerosol size distribution at the high-alpine site Jungfraujoch. J Aerosol Sci 1999;30(Suppl. 1):579–80.

Kaiser A, Scheifinger H, Spangl W, Weiss A, Gilge S, Frcke W, et al. Transport of nitrogen oxides, carbon monoxide and ozone to the Alpine Global Atmosphere Watch stations Jungfraujoch (Switzerland), Zugspitze and Hohenpeissenberg (Germany), Sonnblick (Austria) and Mt. Krvavec (Slovenia). Atmos Environ 2007;4:9273–87.

Kalnay E, Kanamitsu M, Kistler R, Collins W, Deaven D, Gandin L, et al. The NCEP/NCAR 40-year reanalysis project. Bull Am Meteorol Soc 1996;77:437–71.

Lenschow P, Abraham HJ, Kutzner K, Lutz M, Preuß JD, Reichenbächer W. Some ideas about the sources of PM10. Atmos Environ 2001;35:S23–33.

Liu H, Chang WL, Oltmans SJ, Chan LY, Joyce MH. On springtime high ozone events in the lower troposphere from Southeast Asian biomass burning. Atmos Environ 1999;33:2403–10.

Marcazzan GM, Valli G, Vecchi R. Factors influencing mass concentration and chemical composition of fine aerosols during a PM high pollution episode. Sci Total Environ 2002;298:65–79.

Marinoni A, Cristofanelli P, Calzolari F, Roccato F, Bonafè U, Bonasoni P. Continuous measurements of aerosol physical parameters at the Mt. Cimone GAW Station (2165 m asl, Italy). Sci Total Environ 2008;391:241–51.

Morawska L, Thomas S, Jamriska M, Johnson G. The modality of particle size distributions of environmental aerosols. Atmos Environ 1999;33:4401–11.

Nicolás JF, Yubero E, Pastor C, Crespo J, Carratalá A. Influence of meteorological variability upon aerosol mass size distribution. Atmos Res 2009;94:330–7.

Pérez C, Nickovic S, Pejanovic G, Baldasano JM, Özsoy E. Interactive dust-radiation modeling: a step to improve weather forecast. J Geophys Res 2006;111(D16206). http://dx.doi.org/10.1029/2005JD006717.

Pey J, Pérez N, Querol X, Alastuey A, Cusack M, Reche C. Intense winter atmospheric pollution episodes affecting the Western Mediterranean. Sci Total Environ 2010a;408:1951–9.

Pey J, Querol X, Alastuey A. Discriminating the regional and urban contributions in the North-Western Mediterranean: PM levels and composition. Atmos Environ 2010b;44:1587–96.

Querol X, Alastuey A, Pey J, Cusack M, Pérez N, Mihalopoulos N, et al. Variability in regional background aerosols within the Mediterranean. Atmos Chem Phys 2009;9:4575–91.

Rodríguez S, Querol X, Alastuey A, Mantilla E. Origin of high summer PM10 and TSP concentrations at rural sites in Eastern Spain. Atmos Environ 2002;36:3101–12.

Saarnio K, Aurela M, Timonen H, Saarikoski S, Teinilä K, Mäkelä T, et al. Chemical composition of fine particles in fresh smoke plumes from boreal wild-land fires in Europe. Sci Total Environ 2010;408:2527–42.

Schwikowski M, Seibert P, Baltensperger U, Gaggeler HW. A study of an outstanding Saharan dust event at the high-alpine site Jungfraujoch, Switzerland. Atmos Environ 1995;29:1829–42.

Umann B, Arnold F, Schaal C, Hanke M, Uecker J, Aufmhoff H, et al. Interaction of mineral dust with gas phase nitric acid and sulfur dioxide during the MINATROC II field campaign: first estimate to the uptake coefficient gamma (HNO_3) from atmospheric data. J Geophys Res 2005;110(D22306). http://dx.doi.org/10.1029/2005JD005906.

Anexo 2.

Chemical characterization of PM_1 at a regional background site in the Western Mediterranean

Aerosol and Air Quality Research, 16: 530–541, 2016

ISSN: 1680-8584 print / 2071-1409 online
doi: 10.4209/aaqr.2015.05.0302

Chemical Characterization of PM_1 at a Regional Background Site in the Western Mediterranean

Nuria Galindo*, Eduardo Yubero, Jose F. Nicolás, Javier Crespo, Rubén Soler

Atmospheric Pollution Laboratory (LCA), Department of Applied Physics, Miguel Hernández University, Avenida de la Universidad S/N, 03202 Elche, Spain

ABSTRACT

From February 2011 to September 2012, PM_1 samples were collected at the regional background station of Mt. Aitana, located near the eastern coast of the Iberian Peninsula at 1558 m a.s.l. Samples were subsequently analyzed to determine the major chemical composition (elemental and organic carbon, secondary inorganic ions and oxalate). The seasonal patterns of the concentrations of PM_1 and its main components and the influence of long-range transport of dust from the Sahara desert were studied in this work. PM_1 was mainly composed of organic matter and ammonium sulfate, while EC and nitrate were minor components. Concentrations ranged from 3.4 μg m^{-3} in winter to 5.8 μg m^{-3} during summer. This seasonal cycle is typical of high mountain sites, which are generally above the planetary boundary layer during winter time. All the analyzed components exhibited the same seasonal pattern except nitrate, which showed minimum values in summer. This is most likely the result of the decomposition of NH_4NO_3 favored by the higher summer temperatures. Due to the close proximity to the African continent, PM_1 levels significantly increased during Saharan dust intrusions. The concentrations of sulfate were 35% higher during dust events since the formation of secondary ammonium sulfate is favored by heterogeneous reactions on the surface of mineral particles.

Keywords: PM_1; High mountain; Western Mediterranean; Secondary ions; OC; EC.

INTRODUCTION

The effects of atmospheric aerosols on human health, climate, ecosystems, visibility, and building materials are now well-established (Horemans *et al.*, 2011; Solomon *et al.*, 2012; IPCC, 2013; Liu *et al.*, 2014; Eliseev, 2015). The magnitude of the impacts is strongly linked to particle size and composition, as both size and composition determine the region of the respiratory system where the particles are deposited, as well as the chemical, toxicological and optical properties of aerosols (Cheng *et al.*, 2008; Li *et al.*, 2016).

The size and composition of particles depends on the multiplicity of emission sources, both natural and anthropogenic, the physical and chemical processes that lead to their formation, and the atmospheric transport and dispersion conditions. Since all these factors vary substantially with time and space, the complex scientific knowledge behind all these processes still contains many gaps. Regional background stations provide the opportunity to study aerosol formation and transformation processes in the lower troposphere without the interference of local anthropogenic emissions. Additionally, when these stations are located at high elevations, they are especially suitable for identifying natural and anthropogenic aerosols transported over long distances (Marenco *et al.*, 2006; Babu *et al.*, 2011; Nicolás *et al.*, 2014; Moroni *et al.*, 2015).

During the last decade, an increasing number of studies on aerosol properties have been performed at high altitude locations across Europe, such as Switzerland (Jungfraujoch, 3580 m a.s.l.; Cozic *at al.*, 2007; Sjogren *et al.*, 2007), France (puy de Dôme, 1465 m a.s.l.; Sellegri *et al.*, 2003; Freney *et al.*, 2011) or Italy (Mt. Cimone, 2165 m a.s.l.; Van Dingenen *et al.*, 2005; Marenco *et al.*, 2006). In eastern Spain, two high-altitude stations have been recently established in order to study aerosol dynamics in the western Mediterranean basin. One of them was located at Mt. Montsec (in northeastern Spain, 1570 m a.s.l.; Ripoll *et al.*, 2014), while the other was placed at Mt. Aitana, approximately 400 km south (1558 m a.s.l.; Nicolás *et al.*, 2014). To date, the study on aerosol chemical speciation at regional background sites in the western Mediterranean is limited to the works by Ripoll *et al.* (2015a, b) at the Montsec station, located 140 km from the city of Barcelona. This work is aimed at studying the factors affecting the chemical composition of PM_1 at Mt. Aitana. These data can represent the chemical composition of western Mediterranean aerosols either in

* Corresponding author.
Tel.: +34 966658581; Fax: +34 966658397
E-mail address: ngalindo@umh.es

the upper part of the planetary boundary layer (PBL) or in the lower part of the free troposphere, depending on meteorological conditions.

METHODS

Sampling Location

Mt. Aitana (38°39′N; 0°16′W; 1558 m a.s.l.) is the highest peak of the Betic Cordillera located in the southeast of the Iberian Peninsula, 16 km from the nearest Mediterranean coast (Fig. 1). The sampling station was placed within a military area (EVA no. 5) belonging to the Spanish Ministry of Defense. There are some small villages (< 100 inhabitants) spread sparsely over the mountain range. Thus, local anthropogenic emissions are very scarce. Although the most populated city (Alicante, 335,000 inhabitants) is less than 40 km south of the sampling site, the complex orography of the terrain complicates the transport of pollutants from the major coastal urban nuclei to the top of the mountain range (Nicolás *et al.*, 2015).

The study region can be considered as semi-arid, vegetation consisting mainly of some pine forests, Mediterranean scrub and areas of typical Mediterranean crops such as almond and olive trees.

Sampling and Analysis

Between February 2011 and September 2012, twenty-four hour samples were collected every three days by means of a high-volume sampler (MCV, 720 m^3 day^{-1}) equipped with a PM_1 cut-off inlet. Quartz fiber filters (150 mm; Pallflex) were used as substrates for the collection of atmospheric aerosol samples. Sampling started at 00:00 UTC each day. A total of 161 samples were collected and analyzed during the measurement period.

PM_1 mass concentrations were obtained gravimetrically using an electronic balance (Ohaus, Model AP250D) with 10-μg sensitivity. All filters were conditioned for at least 24 h prior to weighing at a relative humidity of 50 ± 5% and temperature of 20 ± 1°C. After weighing, the filters were stored in the fridge at 4°C until chemical analysis.

Two punches of 15 mm diameter of each filter were extracted with 15 mL of ultra-pure water in an ultrasonic bath for 20 min, followed by warming at 60°C for about 6 h. The extracts were subsequently analyzed by ion chromatography for the determination of major anions (Cl^-, NO_3^-, SO_4^{2-}, $C_2O_4^{2-}$) and cations (Na^+, NH_4^+, K^+, Mg^{2+}, Ca^{2+}). For Cl^-, Na^+, K^+, Mg^{2+} and Ca^{2+} a significant number of samples showed concentrations below the detection limit and therefore are not included in this paper. To determine organic and elemental carbon concentrations punches of 1.5 cm^2 area from the filters were separately analyzed with a Thermal-Optical Carbon Aerosol Analyser by Sunset Laboratory. Details of the analytical procedures are given in Yubero *et al.* (2015).

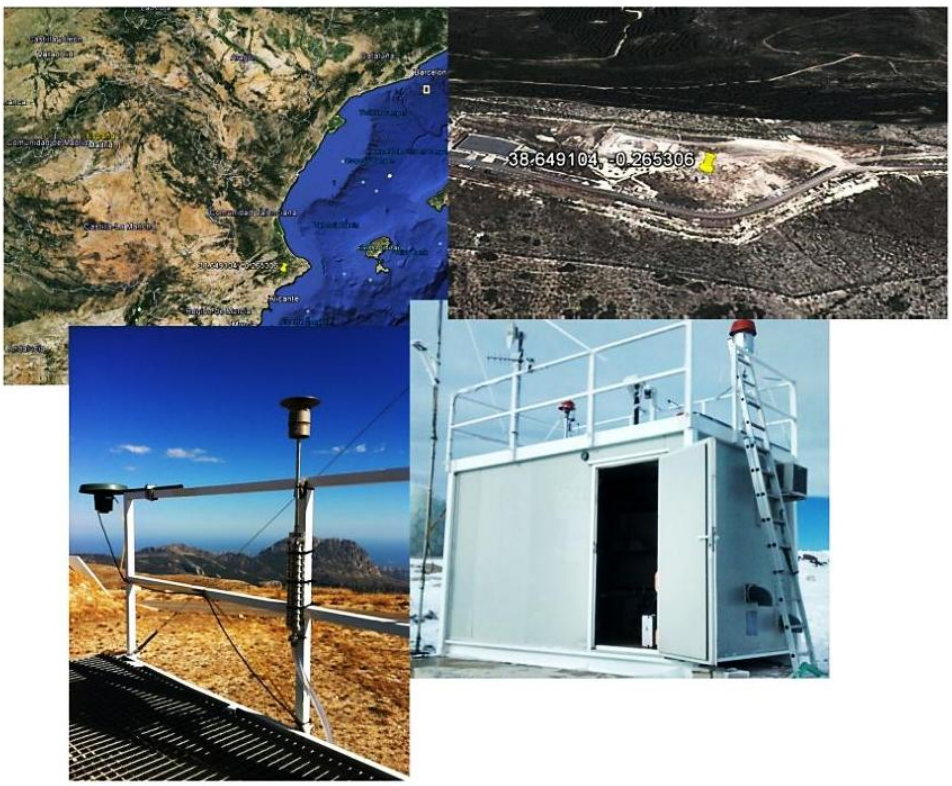

Fig. 1. Location of the sampling site in the southeast of the Iberian Peninsula.

Meteorological Data and Identification of Saharan Dust Intrusions

Temperature, solar radiation, relative humidity, rainfall, wind speed and wind direction were continuously monitored by a meteorological station located at the sampling site.

Mixing layer heights were estimated at Mt. Aitana by using the tools provided by NOAA-ARL available at: http://www.arl.noaa.gov/ready/amet.html.

The identification of African dust events was performed using different tools such as back trajectory analysis carried out using the HYSPLIT model (Draxler and Rolph, 2013). Ninety-six-hour backward trajectories ending at 1000 m above ground level were computed at an interval of every 6 hours during the study period. The forecasts of the Dust REgional Atmospheric Model (DREAM) and the Navy Aerosol Analysis and Prediction System (NAAPS) model were also used. The first is a regional model designed to simulate the atmospheric cycle of mineral dust (Nickovic *et al.*, 2001). The NAAPS model, developed by the Naval Research Laboratory (NRL) in Monterey (USA) (http://www.nrlmry.navy.mil/aerosol), is a global forecast model that predicts the concentrations of several aerosol types in the troposphere. A governmental database with information on Saharan dust episodes detected in Spain was also consulted (http://www.magrama.gob.es/es/calidad-y-evaluacion-ambiental/temas/atmosfera-y-calidad-del-aire/calidad-del-aire/gestion/anuales.aspx).

RESULTS AND DISCUSSION

Meteorological Characterization

The seasonal variation of a number of meteorological parameters is plotted in Fig. 2. Winter was from December to February, spring from March to May, summer from June to August, and fall from September to November.

Average temperatures ranged from 3°C in winter to values close to 20°C during the summer season. The highest variability was observed in spring due to the low temperatures usually registered in early spring (March), which were similar to winter values. Seasonal mean values of relative humidity were minima in summer (53%) and maxima in winter and fall (~70%). Solar radiation intensity, especially during summer (292 W m^{-2}), was higher than that measured on the coast (~270 W m^{-2}; Galindo *et al.*, 2013). Wind speed

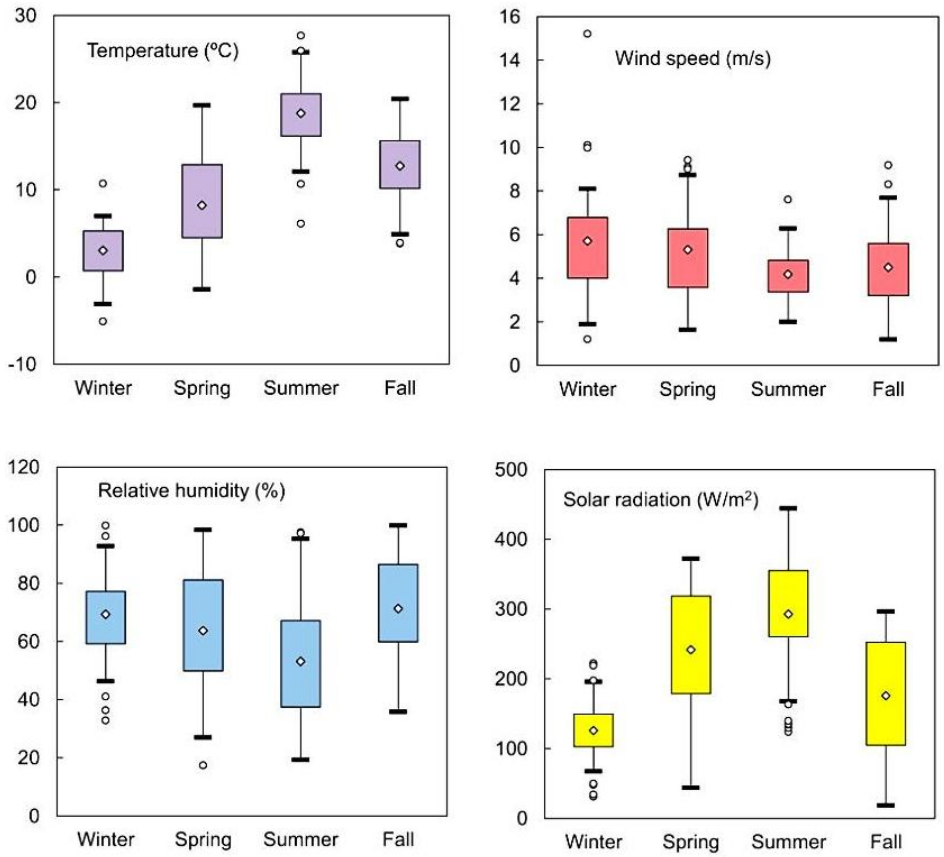

Fig. 2. Box plots of meteorological parameters at Mt. Aitana during the study period. The whiskers correspond to the 25th and 75th percentiles and the white diamond represents the mean value. Maximum and minimum concentrations are represented by dashes (–).

was lowest during summer months (4.2 m s^{-1} summer mean) and showed fewer variations than in the other seasons of the year. Seasonal wind roses generated using the *openair* package (Carslaw *et al.*, 2012) are shown in Fig. 3. During summer, local winds are mainly from the coast, while in winter winds primarily blow from the northern quarters with prevailing NNW direction. During the transient seasons (spring and fall), a change from winter to summer type conditions occurs, with the prevailing winds from the NE and SW sectors.

Accumulated precipitation during 2011 and 2012 was around 700 and 600 mm, respectively. Similar precipitation rates were obtained at another regional background site in Spain, Mt. Montsec, which is located at a similar altitude, but at a higher latitude (Ripoll *et al.*, 2014).

The diurnal variability of the mixing height calculated in the Mt. Aitana area during summer and winter is presented in Fig. 4. In the warmer months, the mountain summit is mostly within the PBL during the central hours of the day (~70% of days, Fig. 4(c)) so polluted air masses from coastal urban areas can be advected to the measurement site. In contrast, during winter the station resides most of the time in the free troposphere (~70% of days, Fig. 4(c)) and hence is much less influenced by regional pollution.

PM_1 Average Levels and Composition

Summary statistics for PM_1 and its major components are presented in Table 1. It is important to point out that there are few studies on PM_1 aerosols at high altitude sites. Additionally, sampling campaigns were not always carried out during the same period of the day or the same season of the year, making it difficult to compare measurements. For these reasons, when data on other PM fractions are available for different locations, the values have been used for comparative purposes.

The PM_1 concentration averaged for the whole study

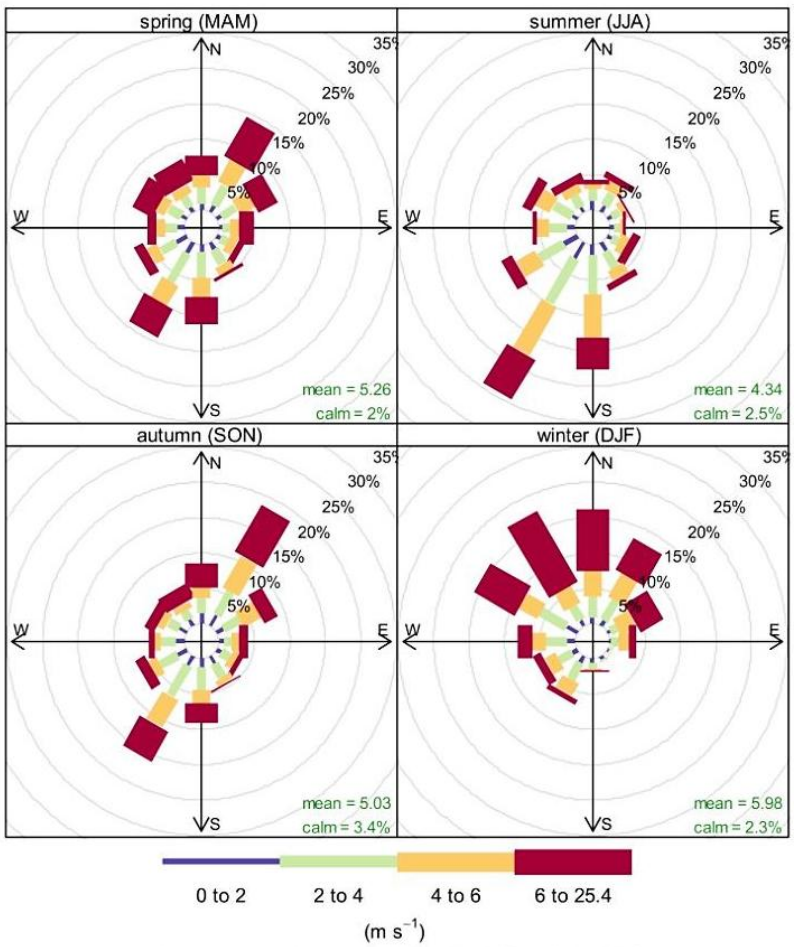

Fig. 3. Wind roses showing wind speed and direction at Mt. Aitana for seasons defined as spring (March–May), summer (June–August), fall (September–November) and winter (December–February).

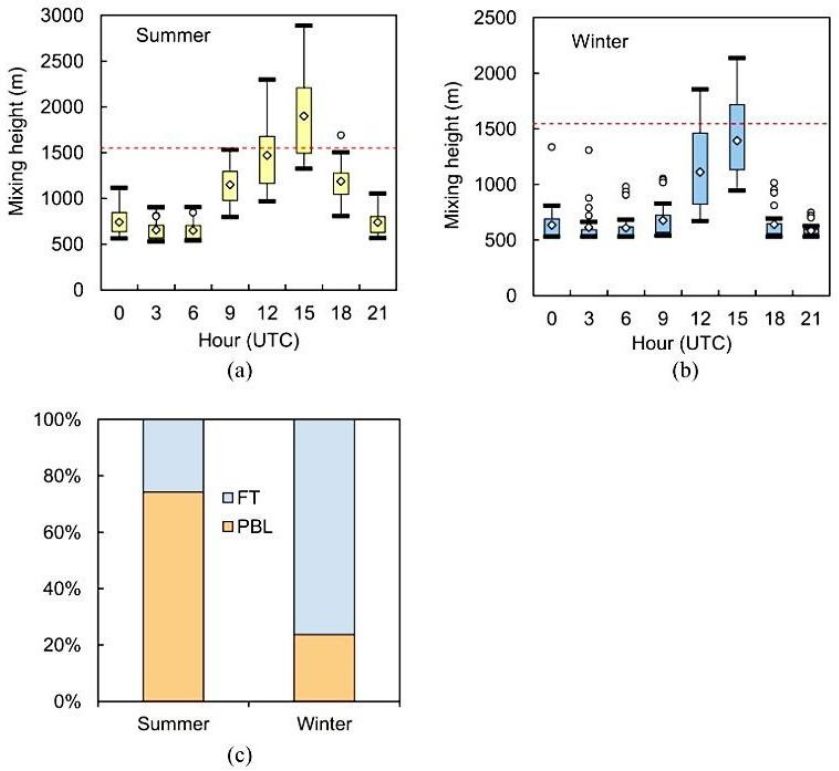

Fig. 4. Variatiation of the mixing layer height as a function of the time of day during (a) summer and (b) winter. The height of the research station is indicated with a dotted line. (c) Percentage of days that Mt. Aitana is within the planetary boundary layer (PBL) or in the free troposphere (FT) at 15 h UTC in summer and winter.

Table 1. Statistics of PM_1 and main components (μg m^{-3}) between February 2011 and September 2012.

	Mean	σ	Min	Max
PM_1	4.6	1.8	1.3	10.3
OC	1.71	0.62	0.55	4.31
EC	0.07	0.07	0.02	0.4
SO_4^{2-}	0.87	0.65	0.02	3.16
NO_3^-	0.10	0.15	0.02	1.17
$C_2O_4^{2-}$	0.06	0.04	0.00	0.22
NH_4^+	0.33	0.26	0.02	1.44

period was of the same order than that found at the Montsec site (5 μg m^{-3} three-year average) and lower than the value obtained at Montseny (8 μg m^{-3}). The Montseny Spanish station is located closer to urban areas than Montsec, as well as at a considerably lower altitude (720 m a.s.l.) and, therefore, it is commonly within the planetary boundary layer (Ripoll *et al.*, 2014). The value was also lower than that reported for other stations in central Italy like Mt. Cimone (2165 m a.s.l., 7.1 μg m^{-3} summer average; Marenco *et al.*, 2006) or Mt. Martano (1100 m a.s.l., 7.4 μg$PM_{1.3}$ m^{-3} and 9.0 μg$PM_{1.3}$ m^{-3} winter and summer averages, respectively; Moroni *et al.*, 2012). These stations are often under the influence of emissions in the Po Valley, one of the most industrialized regions in Europe. Alternatively, the mean value obtained in this study was significantly greater than PM_1 concentrations measured at sites located at considerably higher altitudes like the Jungfraujoch high alpine station (3580 m a.s.l., 1.7 μg m^{-3} and 2.5 μg m^{-3} winter and summer averages, respectively; Cozic *et al.*, 2008) or the Nepal Climate Observatory-Pyramid located in Southern Himalayas (5079 m a.s.l., 1.9 μg m^{-3}; Marinoni *et al.*, 2010). Finally, the average PM_1 concentration found at Mt. Aitana was slightly higher than that observed at puy de Dôme (3.9 μg m^{-3}, annual average), located at similar altitude in central France (Bourcier *et al.*, 2012).

The main constituent of PM_1 at Mt. Aitana was organic matter (OM, 3.1 μg m^{-3}), accounting for more than 60% of the total mass. The organic content was calculated by

multiplying OC concentrations by a factor of 1.8, as suggested in the literature for high altitude sites (Cozic *et al.*, 2008; Sandrini *et al.*, 2014). The second most abundant component was ammonium sulfate (1.20 μg m^{-3}), which contributed 26% to the average PM_1 concentration. The sulfate to ammonium mass ratio (2.56, Fig. 5(a)), very similar to the expected ratio of 2.66 for $(NH_4)_2SO_4$, indicates that all sulfate was neutralized by ammonium. The average sulfate concentration obtained in this study was comparable to the value found at Montsec (Ripoll *et al.*, 2015b), which suggest the existence of a regional background concentration of this compound of around 0.9–1.0 μg m^{-3} in the western Mediterranean basin. EC concentrations were extremely low, as expected from its exclusively anthropogenic origin. Regarding nitrate, it was also a minor contributor to PM_1 levels. Submicron nitrate aerosols are generated from the atmospheric oxidation of nitrogen oxides with OH radicals and subsequent neutralization with gaseous ammonia. Since traffic, the main source of NO_x, is extremely scarce in the surroundings of the sampling site, the formation of NH_4NO_3 is very limited, especially in summer due to the thermal instability of this compound. Additionally, the transport of pollutants from the nearest coastal urban areas is complicated due to orographic factors. This is particularly important in winter, when the mountain summit is commonly above the PBL. Oxalate, one of the most abundant water-soluble organic compounds, showed a moderate correlation with sulfate (Fig. 5(b)), suggesting an aqueous formation pathway of oxalic acid (Craham *et al.*, 2004). The average $C_2O_4^{2-}/SO_4^{2-}$ mass ratio was similar to that found in the marine atmosphere (0.05) and lower than the value characteristic of urban environments (~0.1; Anlauf *et al.*, 2006).

Seasonal Patterns of PM_1 Components

The seasonality of PM_1 and its main chemical components can be observed in in the box-and-whiskers plots shown in Fig. 6. The seasonal cycle of PM_1 concentrations at Mt. Aitana was characteristic of high altitude locations (Marenco *et al.*, 2004; Cozic *et al.*, 2008; Freney *et al.*, 2011; Bourcier *et al.*, 2012; Carbone *et al.*, 2014; Ripoll *et al.*, 2015). The highest values were recorded during summer (5.8 μg m^{-3}) while the minima were measured in winter time (3.4 μg m^{-3}). The reasons for such a variation are: (1) during winter the top of the mountain is generally outside the PBL and the aerosol is typical of the undisturbed free troposphere. In fact, the winter average concentration obtained in this study was only a little higher than the value measured at Mt. Cimone during night-time (~2.4 μg m^{-3} three-year average; Carbone *et al.*, 2014), when the site is commonly outside the influence of regional or local pollution; (2) the prevailing wind directions during winter (Fig. 3) do not favor aerosol transport from the main urban areas located on the coastline, (3) the processes of wet scavenging of aerosols from the atmosphere are hindered in summer due to the absence of precipitation; (4) the increase in temperatures and solar radiation in summer months favors biogenic emissions and the formation of secondary aerosols; and (5) in summer there is a higher frequency of occurrence of Saharan and recirculation episodes that contribute to increase PM levels in the western Mediterranean basin (Galindo *et al.*, 2011a).

All the analyzed components showed the same seasonal pattern than PM_1 levels except nitrate, whose concentrations had a summer minimum. This variation differs from that reported for many other high altitude locations in Europe (Cozic *et al.*, 2008; Freney *et al.*, 2011; Moroni *et al.*, 2012; Carbone *et al.*, 2014) and is most likely due to the greater summer temperatures at Mt. Aitana. During the summer season, especially in July and August, mean daily temperatures at the measurement location were frequently above 20°C and therefore, the decomposition of submicron ammonium nitrate into gaseous nitric acid and ammonia was promoted. Also, it is possible that a fraction of ammonium nitrate evaporated from the filters (negative artifact). The same seasonal variation has been described at the Montsec Mediterranean station (Ripoll *et al.*, 2015a, b).

For the other PM_1 major components the highest concentrations were observed in summer, when the mountain top is very often below the PBL and polluted urban air masses

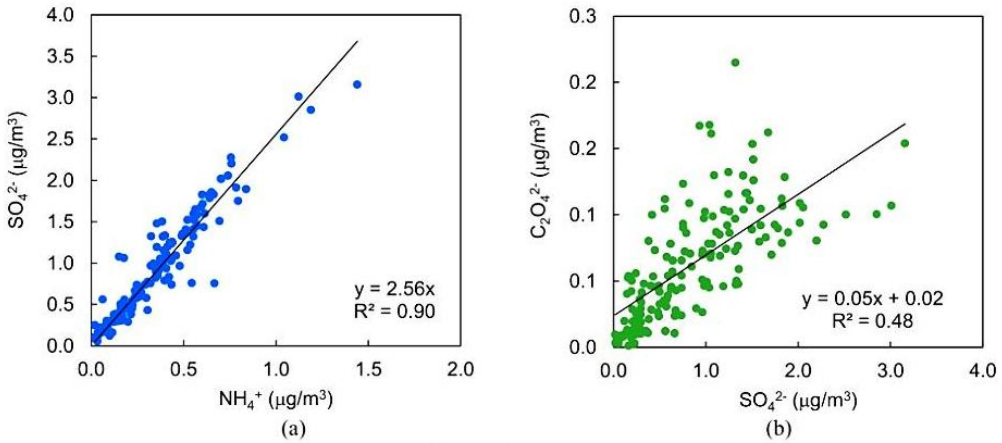

Fig. 5. Correlation between (a) sulfate and ammonium, and (b) oxalate and sulfate.

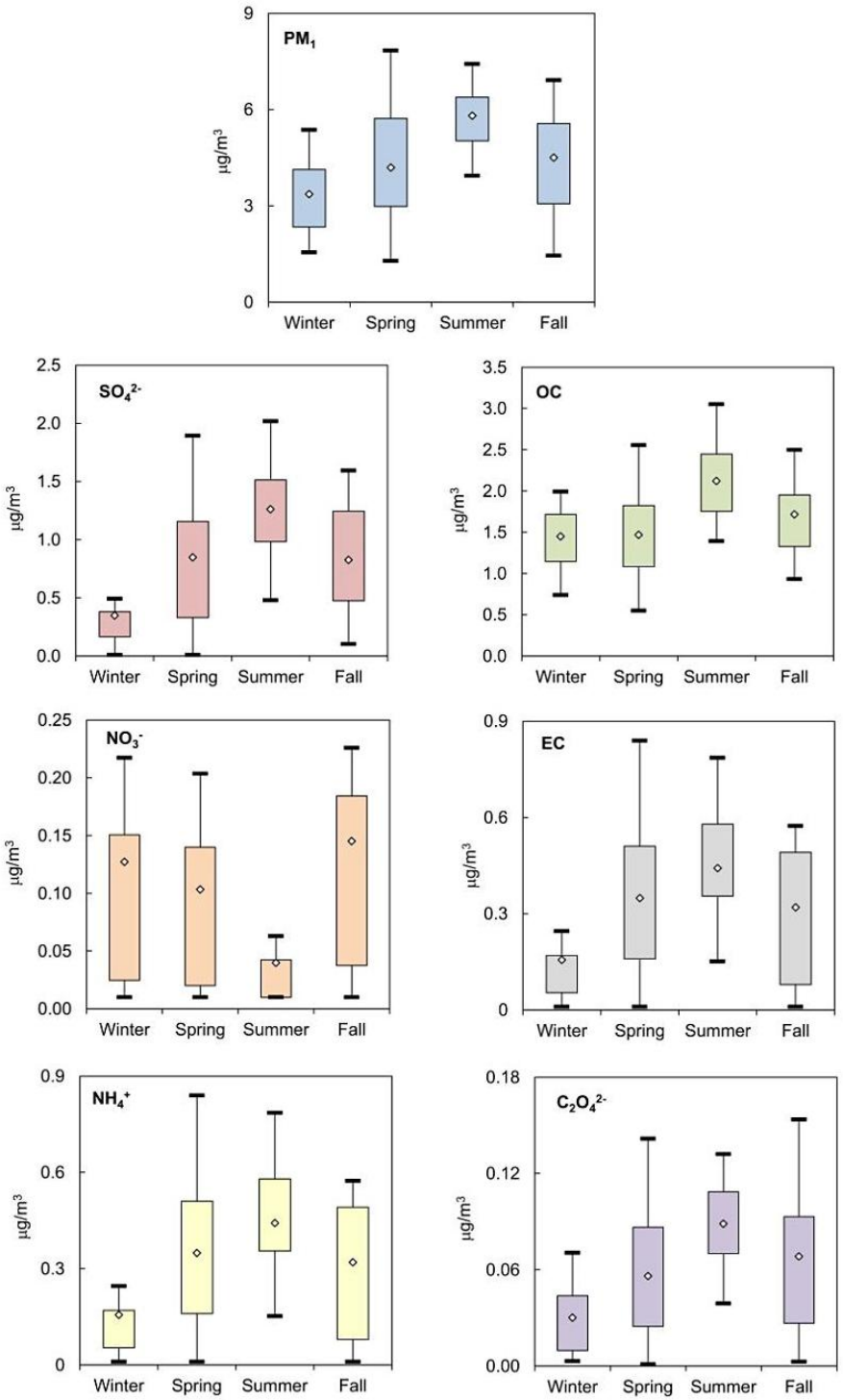

Fig. 6. Box plots of PM_1 major components at Mt. Aitana during the study period. The whiskers correspond to the 25th and 75th percentiles and the white diamond represents the mean value. Maximum and minimum concentrations are represented by dashes (–).

can be advedted to the site. Moreover, meteorological factors that affect pollutant emissions and transformation processes could also account for the observed seasonal variation. Greater SO_4^{2-} levels during summer have also been observed in nearby urban and suburban areas as a result of increased photochemical oxidation of SO_2 (Galindo *et al.*, 2011b; Yubero *et al.*, 2015). However, the seasonal variation of carbonaceous species at Mt. Aitana was different from that observed at metropolitan areas within the western Mediterranean, where the highest concentrations occurred during winter (Yubero *et al.*, 2014, 2015). This outcome points to enhanced transport from coastal urban areas in summer as the main reason for the observed seasonal variation of carbonaceous components. Actually, during the summer season pollutants may be transported from the major urban nuclei located along the Mediterranean coast inland by mesoscale winds dominated by sea-breezes (see Fig. 3). In the case of organic matter, additional factors, such as an increase in biogenic emissions and the photochemical formation of secondary organic aerosols, could also account for the higher summer concentrations (Cozic *et al.*, 2008; Ripoll *et al.*, 2015b). During winter, the site is often in the free troposphere and consequently the regional pollution does not reach the station.

The chemical composition of PM_1 at Mt. Aitana during spring, summer and autumn was quite constant compared to other elevated sites in Europe (Freney *et al.*, 2011; Carbone *et al.*, 2014). The contribution of organic matter was approximately 65%, whereas sulfate and ammonium accounted for about 20% and 8%, respectively, of the total mass of PM_1. In contrast, during winter time OM made up 78% of PM_1 while the joint contribution of sulfate and ammonium decreased to 15%. Regarding nitrate, its contribution ranged from less than 1% in summer to almost 4% in winter. The spring and summer composition of PM_1 aerosols was fairly similar to that described for other high altitude locations like Mt. Cimone (Carbone *et al.*, 2014), puy de Dôme (Freney *et al.*, 2011) or Jungfraujoch (Cozic *et al.*, 2008), except for the much lower contribution of nitrate at our sampling site. The largest divergences in the composition of PM_1 between different high altitude sites in Europe were observed in winter, as already pointed out by Carbone *et al.* (2014).

The Impact of Saharan Dust Intrusions

North African dust outbreaks are quite frequent across the Mediterranean Basin, especially at more southern sites where the occurrence is between 30 and 37% of the annual days (Pey *et al.*, 2013). These events, which have a greater impact on aerosol concentrations at higher altitudes, show a clear prevalence in the warmer seasons. Fig. 7 presents the cluster analysis of backward trajectories calculated by the HYSPLIT model for the study period. The site was exposed to air masses coming mainly from the Atlantic, central Europe and northern Africa. As expected, Saharan dust episodes were much more frequent in summer (the occurrence of air masses coming directly from northern Africa during this season was 30%). Although the coarse fraction of PM is more affected than the fine and submicron fractions, significant increases in PM_1 and $PM_{2.5}$ levels has been observed at high altitude sites during Saharan events (Collaud Coen *et al.*, 2004; Ripoll *et al.*, 2014; Moroni *et al.*, 2015). During the measurement period, 38 sampling days were under the influence of air masses coming from northern Africa and 34 of these days occurred during spring and summer. Table 2 presents average concentrations of the analyzed species and meteorological parameters during non-event days and intrusion days for the spring-summer period. In order to obtain a more accurate estimation of the influence of Saharan dust outbreaks, those days with an accumulated precipitation higher 1 mm were removed from the dataset.

The PM_1 average concentration during African events was significantly higher than the mean concentration obtained on non-event days, which is in agreement with the results obtained at Montsec (Ripoll *et al.*, 2014, 2015a, b). However, the influence of these episodes seems to be higher at the measurement location than at other elevated sites in Italy (Carbone *et al.*, 2014) and central Europe (Salvador *et al.*, 2010; Freney *et al.*, 2011). The reason could be that Mt. Aitana is closer to the African continent.

Saharan intrusions increased sulfate concentrations nearly 35%, which is the largest relative increase among the quantified species. PM_1 sulfate can actually be formed by oxidation of SO_2 on the surface of submicron dust particles and successive reaction of generated sulfuric acid with ammonia. The higher surface area of submicron particles compared to coarse particles would favor this process, as already observed in the study area (Galindo *et al.*, 2013). An additional reason for this increase in ammonium sulfate levels is that Saharan dust plumes often arrives to the western Mediterranean just after recirculation events. These episodes, characterized by air masses trapped and nearly stagnant over the sea during summer, favor the photochemical formation of secondary pollutants under strong insolation conditions (Millán *et al.*, 2002). OC and NH_4^+ showed relative increases of about 20% during Saharan events. The lower increase in ammonium concentrations relative to sulfate concentrations could be partly due to the volatilization of particulate NH_4NO_3 under warmer conditions (the average temperature was more than 40% higher on days under the influence of Saharan dust intrusions). This outcome differs from that obtained at other high altitude sites such as Montsec (Ripoll *et al.*, 2015a) and Jungfraujoch (Collaud Coen *et al.*, 2004), where an increase of PM_1 nitrate has been observed during north African episodes. Regarding organic matter, the higher values measured during these events could be due to an increase in secondary organic compounds formed by reactions during transport of the African dust plumes (Carbone *et al.*, 2014). In previous works performed at elevated sites in Europe, high concentrations of carbonaceous species such as OC and EC (Salvador *et al.*, 2010) or black carbon (Ripoll *et al.*, 2014) were associated to air masses coming from northern Africa. This has been attributed to the transport of anthropogenic pollutants emitted in the Mediterranean basin and northern Africa. At our sampling site, this appears less probable since a concurrent increase of EC and OC during Saharan events has not been observed.

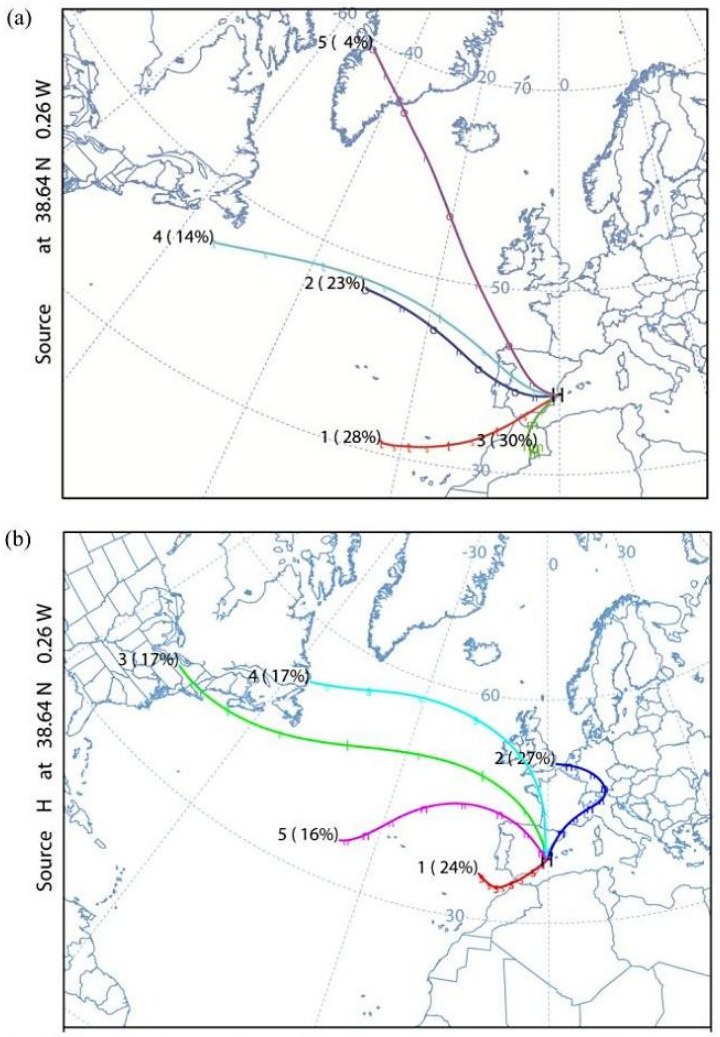

Fig. 7. Cluster analysis of back trajectories ending at Mt. Aitana for (a) summer and (b) winter. Percentage frequency of the different origins of air masses is also indicated.

Table 2. Average values on non-event days and intrusion days for the spring and summer seasons.

	Non-intrusion ($N = 55$)	Intrusion ($N = 31$)
PM_1 *	4.8	6.0
OC *	1.75	2.11
EC	0.12	0.12
SO_4^{2-} *	1.02	1.36
NO_3^-	0.10	0.09
$C_2O_4^{2-}$	0.07	0.09
NH_4^+	0.40	0.48
T (°C) *	12.9	18.6
RH (%) *	59	46
WS (m s^{-1})	4.2	4.6
Solar rad (W m^{-2})	280	303

* Average values on intrusion and non-intrusion days were statistically different at the 95% confidence level.

CONCLUSIONS

The concentrations of PM_1 measured at a high mountain location in southeastern Spain were similar to the values reported for other Spanish regional background stations (~5 μg m^{-3}) but lower than those found in elevated sites within the Po Valley, in Italy, one of the most polluted areas in Europe. This indicates that PM levels at high mountain sites are influenced by the degree of anthropogenic pollution in the region.

Organic matter and ammonium sulfate were the major contributors to PM_1 mass, while EC and nitrate, largely related to local sources, were minor components. Actually, nitrate concentrations were significantly lower than those measured at other elevated sites in Europe. The most probable reasons are, on the one hand, that pollutant transport from coastal urban areas is difficult due to the complex orography of the terrain and, on the other hand, that the thermal decomposition of ammonium nitrate is more favored at the sampling site due to higher ambient temperatures, especially during summer. This was also supported by the different seasonal cycle of nitrate concentrations compared to other European high mountain stations.

PM_1 levels showed a well-defined seasonality, with maximum values in summer and minimum during winter time. The fact that the station is most of the time outside the PBL during winter is probably the main reason for this, since the seasonal trend in OC concentrations was opposite to that found in metropolitan areas nearby the measurement station. Nevertheless, other factors such as the higher frequency of Saharan dust events during the warm months could also contribute to the higher summer concentrations. In fact, a statistically significant increase in the concentrations of PM_1 and its main components (OC and SO_4^{2-}) was observed during African episodes. This was most likely due to the formation of secondary compound during the transport of the dust plumes since a simultaneous increase in primary pollutants (EC) was not observed.

ACKNOWLEDGEMENTS

This work was supported by the Spanish Ministry of Science and Innovation CGL2009-08036 (PASSE) project and by the Spanish Ministry MINECO CGL2012-39623-C02-2 (PRISMA-AITANA) project. This study was also co-financed by the European Union, through FEDER funds. We would also like to thank the Spanish Defense Ministry (EVA n. 5) for allowing access to its facilities.

REFERENCES

Anlauf, K., Li, S.M., Leaitch, R., Brook, J., Hayden, K., Toom-Sauntry, D. and Wiebe, A. (2006). Ionic Composition and Size Characteristics of Particles in the Lower Fraser Valley: Pacific 2001 Field Study. *Atmos. Environ.* 40: 2662–2675.

Babu, S.S., Chaubey, J.P., Moorthy, K.K., Gogoi, M.M., Kompalli, S.K., Sreekanth, V., Vagare, S.P., Bhatt, B.C., Gaur, V.K., Prabhu, T.P. and Singh, N.S. (2011). High Altitude (~4520 m amsl) Measurements of Black Carbon Aerosols over Western trans-Himalayas: Seasonal Heterogeneity and Source Apportionment. *J. Geophys. Res.* 116: D24201.

Bourcier, L., Sellegri, K., Chausse, P., Pichon, J.M. and Laj, P. (2012). Seasonal Variation of Water-soluble Inorganic Components in Aerosol Size-segregated at the puy de Dôme Station (1,465 m a.s.l.), France. *J. Atmos. Chem.* 69: 47–66.

Carbone, C., Decesari, S., Paglione, M., Giulianelli, L., Rinaldi, M., Marinoni, A., Cristofanelli, P. Didiodato, A., Bonasoni, P., Fuzzi, S. and Facchini, M.C. (2014). 3-year Chemical Composition of Free Tropospheric PM_1 at the Mt. Cimone GAW Global Station – South Europe – 2165 m a.s.l. *Atmos. Environ.* 87: 218–227.

Carslaw, D.C. and Ropkins, K. (2012). *Openair* — an R Package for Air Quality Data Analysis. *Environ. Modell. Software* 27–28: 52–61.

Cheng, Y.F., Wiedensohler, A., Eichler, H., Su, H., Gnauk, T., Brüggemann, E., Herrmann, H., Heintzenberg, J., Slanina, J., Tuch, T., Hu, M. and Zhang, Y.H. (2008). Aerosol Optical Properties and Related Chemical Apportionment at Xinken in Pearl River Delta of China. *Atmos. Environ.* 42: 6351–6372.

Collaud Coen, M., Weingartner, E., Schaub, D., Hueglin, C., Corrigan, C., Henning, S., Schwikowski, M. and Baltensperger, U. (2004). Saharan Dust Events at the Jungfraujoch: Detection by Wavelength Dependence of the Single Scattering Albedo and First Climatology Analysis. *Atmos. Chem. Phys.* 4: 2465–2480.

Cozic, J., Verheggen, B., Weingartner, E., Crosier, J., Bower, K.N., Flynn, M., Coe, H., Henning, S., Steinbacher, M., Henne, S., Collaud Coen, M., Petzold, A. and Baltensperger, U. (2008). Chemical Composition of Free Tropospheric Aerosol for PM_1 and Coarse Mode at the High Alpine Site Jungfraujoch. *Atmos. Chem. Phys.* 8: 407–423.

Crahan, K.K., Hegg, D., Covert, D.S. and Jonsson, H. (2004). An Exploration of Aqueous Oxalic Acid Production in the Coastal Marine Atmosphere. *Atmos. Environ.* 38: 3757–3764.

Draxler, R.R. and Rolph, G.D. (2013). HYSPLIT (HYbrid Single-Particle Lagrangian Integrated Trajectory) Model Access via NOAA ARL READY Website (http://ready.arl.noaa.gov/HYSPLIT.php). NOAA Air Resources Laboratory, Silver Spring, MD.

Eliseev, A.V. (2015). Impact of Tropospheric Sulphate Aerosols on the Terrestrial Carbon Cycle. *Global Planet. Change* 124: 30–40.

Freney, E.J., Sellegri, K., Canonaco, F., Boulon, J., Hervo, M., Weigel, R., Picho, J.M., Colomb, A., Prévôt, A.S.H. and Laj, P. (2011). Seasonal Variations in Aerosol Particle Composition at the puy-de-Dôme Research Station in France. *Atmos. Chem. Phys.* 11: 13047–13059.

Galindo, N., Varea, M., Gil-Moltó, J., Yubero, E. and Nicolás, J. (2011a). The Influence of Meteorology on Particulate Matter Concentrations at an Urban Mediterranenan Location. *Water Air Soil Pollut.* 215: 365–372.

Galindo, N., Yubero, E., Nicolás, J.F., Crespo, J., Pastor, C., Carratalá, A. and Santacatalina, M. (2011b). Water-soluble Ions Measured in Fine Particulate Matter next to Cement Works. *Atmos. Environ.* 45: 2043–2049.

Galindo, N., Gil-Moltó, J., Varea, M., Chofre, C. and Yubero, E. (2013). Seasonal and Interannual Trends in PM Levels and Associated Inorganic Ions in Southeastern Spain. *Microchem. J.* 110: 81–88.

Horemans, B., Cardell, C., Bencs, L., Kontozova-Deutsch, V., De Wael, K. and Van Grieken, R. (2011). Evaluation of Airborne Particles at the Alhambra Monument in Granada, Spain. *Microchem. J.* 99: 229–438

IPCC (2013). Climate Change 2013: The Physical Science Basis. In *Contribution of Working Group I to the Fifth Assessment Report of the Intergovernmental Panel on Climate Change*, Stocker, T.F., Qin, D., Plattner, G.K., Tignor, M., Allen, S.K., Boschung, J., Nauels, A., Xia, Y., Bex, V. and Midgley, P.M. (Eds.), Cambridge University Press, Cambridge, United Kingdom and New York, NY, USA.

Li, Y., Henze, D.K., Jack, D. and Kinney, P.L. (2016). The Influence of Air Quality Model Resolution on Health Impact Assessment for Fine Particulate Matter and Its Components. *Air Qual. Atmos. Health* 9: 51–68.

Liu, Y.J., Zhang, T.T., Liu, Q.Y., Zhang, R.J., Sun, Z.Q. and Zhang, M.G. (2014). Seasonal Variation of Physical and Chemical Properties in TSP, PM_{10} and $PM_{2.5}$ at a Roadside Site in Beijing and Their Influence on Atmospheric Visibility. *Aerosol Air Qual. Res.* 14: 954–969.

Marenco, F., Bonasoni, P., Calzolari, F., Ceriani, M., Chiari, M., Cristofanelli, P., D'Alessandro, A., Fermo, P., Lucarelli, F., Mazzei, F., Nava, S., Piazzalunga, A., Prati, P., Valli, G. and Vecchi, R. (2006). Characterization of Atmospheric Aerosols at Monte Cimone, Italy, during Summer 2004: Source Apportionment and Transport Mechanisms. *J. Geophys. Res.* 111: D24202.

Marinoni, A., Cristofanelli, P., Laj, P., Duchi, R., Calzolari, F., Decesari, S., Sellegri, K., Vuillermoz, E., Verza, G.P., Villani, P. and Bonasoni, P. (2010). Aerosol Mass and Black Carbon Concentrations, a Two Year Record at NCO-P (5079 m, Southern Himalayas). *Atmos. Chem. Phys.* 10: 8551–8562.

Millán, M.M., Sanz, M.J., Salvador, S. and Mantilla, E. (2002). Atmospheric Dynamics and Ozone Cycles Related to Nitrogen Deposition in the Western Mediterranean. *Environ. Pollut.* 118: 167–186.

Moroni, B., Cappelletti, D. Marmottini, F., Scardazza, F., Ferrero, L. and Bolzacchini, E. (2012). Integrated Single Particle-bulk Approach for the Characterization of Local and Long Range Transport of Particulate Pollutants. *Atmos. Environ.* 50: 267–277.

Moroni, B., Castellini, S., Crocchianti, S., Piazzalunga, A., Fermo, P., Scardazza, F. and Cappelleti, D. (2015). Ground-based Measurements of Long-range Transported Aerosol at the Rural Regional Background Site of Monte Martano (Central Italy). *Atmos. Res.* 155: 26–36.

Nickovic, S., Papadopoulos, A., Kakaliagou, O. and Kallos, G. (2001). Model for Prediction of Desert Dust Cycle in the Atmosphere. *J. Geophys. Res.* 106: 18113–18129

Nicolás, J.F., Crespo, J., Yubero, E., Soler, R., Carratalá, A. and Mantilla, E. (2014). Impacts on Particles and Ozone by Transport Processes Recorded at Urban and High-altitude Monitoring Stations. *Sci. Total Environ.* 466–467: 439–446.

Nicolás, J.F., Galindo, N., Yubero, E., Crespo, J. and Soler, R. (2015). PM_1 Variability and Transport Conditions between an Urban Coastal Area and a High Mountain Site during the Cold Season. *Atmos. Environ.* 118: 127–134.

Pey, J., Pérez, N., Querol, X., Alastuey, A., Cusak, M. and Reche, C. (2010). Intense Winter Atmospheric Pollution Episodes Affecting the Western Mediterranean. *Sci. Total Environ.* 408: 1951–1959.

Pey, J., Querol, X., Alastuey, A., Forastiere, F. and Stafoggia, M. (2013). African Dust Outbreaks over the Mediterranean Basin during 2001–2011: PM_{10} Concentrations, Phenomenology and Trends, and Its Relation with Synoptic and Mesoscale Meteorology. *Atmos. Chem. Phys.* 13: 1395–1410.

Ripoll, A., Pey, J., Minguillón, M.C., Pérez, N., Pandolfi, M., Querol, X. and Alastuey, A. (2014). Three Years of Aerosol Mass, Black Carbon and Particle Number Concentrations at Montsec (Southern Pyrenees, 1570 m a.s.l.). *Atmos. Chem. Phys.* 14: 4279–4295.

Ripoll, A., Minguillón, M.C., Pey, J., Pérez, N., Querol, X. and Alastuey, A. (2015a). Joint Analysis of Continental and Regional Background Environments in the Western Mediterranean: PM_1 and PM_{10} Concentrations and Compositions. *Atmos. Chem. Phys.* 15: 1129–1145.

Ripoll, A., Minguillón, M.C., Pey, J., Jiménez, J.L., Day, D.A., Sosedova, Y., Canonaco, F., Prévôt, A.S.H., Querol, X. and Alastuey, A. (2015b). Long-term Real-time Chemical Characterization of Submicron Aerosols at Montsec (Southern Pyrenees, 1570 m a.s.l.). *Atmos. Chem. Phys.* 15: 2935–2951.

Salvador, P., Artíñano, A., Pio, C., Afonso, J., Legrand, M., Puxbaum, H. and Hammer, S. (2010). Evaluation of Aerosol Sources at European High Altitude Background Sites with Trajectory Statistical Methods. *Atmos. Environ.* 44: 2316–2329.

Sandrini, S., Fuzzi, S., Piazzalunga, A., Prati, P., Bonasoni, P., Cavalli, F., Bove, M.C., Calvello, M., Cappelletti, D., Colombi, C., Contini, D., de Gennaro, G., Di Gilio, A., Fermo, P., Ferrero, L., Gianelle, V., Giugliano, M., Ielpo, P., Lonati, G., Marinoni, A. and Massabò, D. (2014). Spatial and Seasonal Variability of Carbonaceous Aerosol across Italy. *Atmos. Environ.* 99: 587–598.

Sellegri, K., Laj, P., Dupuy, R., Legrand, M., Preunkert, S. and Putaud, J.P. (2003). Size-dependent Scavenging Efficiencies of Multicomponent Atmospheric Aerosols in Clouds. *J. Geophys. Res.* 108: 4334.

Sjogren, S., Gysel, M., Weingartner, E., Alfarra, M.R., Duplissy, J., Cozic, J., Crosier, J., Coe, H. and Baltensperger, U. (2008). Hygroscopicity of the Submicrometer Aerosol at the High-alpine Site Jungfraujoch, 3580 m a.s.l., Switzerland. *Atmos. Chem.*

Phys. 8: 5715–5729.

Solomon, P.A., Costantini, M., Grahame, T.J., Gerlofs-Nijland, M.E., Cassee, F.R., Russell, A.G., Brook, J.R., Hopke, P.K., Hidy, G., Phalen, R.F., Saldiva, P., Sarnat, S.E., Balmes. J.R.. Tager, I.B., Özkaynak, H., Vedal, S., Wierman, S.S.G. and Costa. D.L. (2012). Air Pollution and Health: Bridging the Gap from Sources to health outcomes: Conference Summary. *Air Qual. Atmos. Health* 5: 9–62.

Van Dingenen, R., Putaud, J.P., Martins-Dos Santos, S. and Raes, F. (2005). Physical Aerosol Properties and Their Relation to air mass Origin at Monte Cimone (Italy) during the First MINATROC Campaign. *Atmos. Chem. Phys.* 5: 2203–2226.

Yubero, E., Galindo, N., Nicolás, J.F., Lucarelli, F. and Calzolai, G. (2014). Carbonaceous Aerosols at an Industrial Site in Southeastern Spain. *Air Qual. Atmos. Health* 7: 263–271.

Yubero, E., Galindo, N., Nicolás, J.F., Crespo, J., Calzolai, G. and Lucarelli, F. (2015). Temporal Variations of PM_1 Major Components in an Urban Street Canyon. *Environ. Sci. Pollut. Res. Int.* 22: 13328–13335.

Received for review, May 12, 2015
Revised, July 28, 2015
Accepted, August 5, 2015

Anexo 3.

PM_1 variability and transport conditions between an urban coastal area and a high mountain site during the cold season

Atmospheric Environment 118 (2015) 127–134

Contents lists available at ScienceDirect

Atmospheric Environment

journal homepage: www.elsevier.com/locate/atmosenv

PM_1 variability and transport conditions between an urban coastal area and a high mountain site during the cold season

J.F. Nicolás*, N. Galindo, E. Yubero, J. Crespo, R. Soler

Atmospheric Pollution Laboratory (LCA), Department of Applied Physics, Miguel Hernández University, Avenida de la Universidad S/N, 03202 Elche, Spain

HIGHLIGHTS

- The impact of winter-time stagnant conditions on PM_1 levels was studied.
- Measurements were made at a coastal urban area and a high altitude site in Spain.
- Urban PM_1 increases were maxima during the evening rush hour.
- At the mountain site the maximum increase was registered in the early afternoon.
- Pollutant transport from the coast to high sites occurs under specific conditions.

ARTICLE INFO

Article history:
Received 31 March 2015
Received in revised form
29 July 2015
Accepted 30 July 2015
Available online 31 July 2015

Keywords:
High mountain station
Regional transport
PM_1
Severe pollution episode

ABSTRACT

During late autumn and winter, the western Mediterranean basin is often affected by severe pollution episodes (SPE) caused by stagnant weather conditions that produce a notable increase in particulate matter (PM) levels. The main objective of the present study is to evaluate the impact of these episodes on the variability of PM_1 concentrations at an urban and a high mountain station in the western Mediterranean. At the urban site, SPEs caused increases in PM_1 levels of up to 20 μg m^{-3} at 20:00–21:00 UTC due to a decrease in the mixing layer depth during the evening rush hour. In contrast, the highest increments at the high mountain station (~12 μg m^{-3}) were observed around midday. Since there are little anthropogenic emissions in the surroundings of the mountain station, this was most likely the result of aerosol transport from coastal urban areas and photochemical formation of secondary particles during transport. The transport of air pollutants through a complex orography occurs under specific weather conditions.

1. Introduction

It is well known that dispersion conditions, as well as short and long-range transport of pollutants, is a key factor affecting regional air quality (Monks et al., 2009; Squizzato et al., 2012). In this sense, regional background stations can provide valuable information to study the impact of these processes on the variability of pollutant concentrations (Bonasoni et al., 2004; Hinz et al., 2005; Pey et al., 2010; Uglietti et al., 2011). With this purpose, some stations have been recently settled at high altitude locations in the western Mediterranean basin (Nicolás et al., 2014; Pey et al., 2010). The particular geographic, orographic, climatic and demographic features of this region favor the occurrence of episodic events that have a significant impact on pollutant levels such as ozone and particulate matter (PM). Saharan dust outbreaks and recirculation of air masses are the most frequent events in the warm seasons, while the occurrence of stagnant conditions which trap the pollutants in the lower altitude is relatively high during late autumn and winter (Galindo et al., 2013; Gangoiti et al., 2001; Jorba et al., 2013; Nicolás et al., 2011).

The effects of stagnant weather conditions on the concentration and/or composition of urban aerosols have been studied in some previous works (Hai and Oanh, 2013; Kassomenos et al., 2011; Park et al., 2006; Vecchi et al., 2007). The majority of these works were focused on $PM_{2.5}$ and PM_{10} and there are fewer studies addressing the influence of dispersion conditions on the PM_1 fraction. This fraction, which is principally associated with anthropogenic activities, is especially sensitive to atmospheric stability conditions (Masiol et al., 2015; Galindo et al., 2011). Stagnation events are

* Corresponding author.
E-mail address: j.nicolas@umh.es (J.F. Nicolás).

http://dx.doi.org/10.1016/j.atmosenv.2015.07.042
1352-2310/

usually associated with large-scale high pressure systems with weak surface pressure gradients, resulting in light winds, low mixing heights and cloudless skies. This meteorological situation favors not only the accumulation of primary pollutants (such as elemental carbon) emitted by local sources but also the photochemical formation of secondary aerosols (Ham et al., 2010; Katzman et al., 2010; Mira-Salama et al., 2008; Strader et al., 1999; Yubero et al., 2015). Stagnation conditions can also affect PM levels at rural and regional background sites, although anthropogenic emissions are low compared with those in urban areas (Mira-Salama et al., 2008; Pey et al., 2010; Pietrogrande et al., 2014; Squizzato et al., 2012).

The main goals of the present study are: (1) to assess the impact of periods of highly stable atmospheric conditions on PM_1 concentrations at an urban coastal area in southeastern Spain and, (2) to determine the favorable conditions for aerosol transport from coastal emission sources to a high mountain location during these episodes.

2. Experimental

2.1. Study area: connectivity between the measurements sites

The study area is situated in a semi-arid region within the Spanish Mediterranean basin. The geographic location and the orographic features of the region are described in details in Caballero et al. (2007). Alternatively, a description of atmospheric dynamics and PM events in the area are presented in Nicolás et al. (2014).

The selection of the measurement sites was based on their suitability to achieve the proposed objectives. The site representative of a regional environment (high mountain site, MS) was located on top of Mt. Aitana (38°39′ N; 0°16′ W; 1558 m a.s.l.; Fig. 1a). The monitoring station was situated in a military area (EVA no. 5) belonging to the Spanish Ministry of Defense with very little anthropogenic activity. Therefore, any alteration of the normal levels of atmospheric particles can be easily detected. The second monitoring site (an urban site, US) was a station of the Regional Environmental Surveillance Network located on the outskirts of the city of Alicante (335.000 inhabitants; 38°21′ N; 0°30′ W; 20 m a.s.l.) close to an access road approximately 2 km from the coast (Fig. 1a). This site is representative of a suburban environment.

The route from Alicante to Mt. Aitana runs through valleys and mountains that rise as we approach the regional background site. Air masses passing over coastal metropolitan areas can carry urban atmospheric pollutants inland through the valleys. When the air masses reach the mountain barrier, these pollutants can be transported up-slope by mountain breezes and reach the top of the mountain range (Pey et al., 2010). However, the orographic profile between both sites (~37 km length in straight line, Fig. 1b) complicates the transport of pollutants from the coast inland.

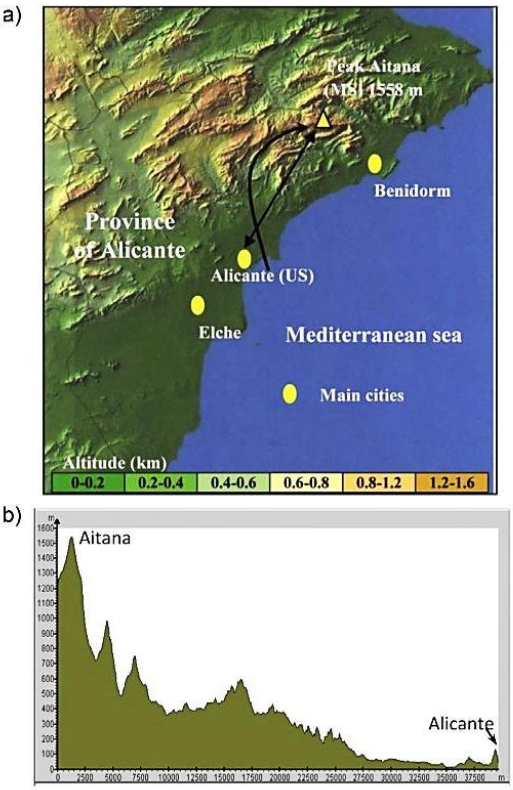

Fig. 1. (a) Location of the monitoring sites in southeastern Spain. The dashed line represents the most probable route of air masses along the orographic channels; (b) Topographic profile of the trajectory between the two monitoring sites as the crow flies.

Table 1
Meteorological parameters measured at the urban site (US) and the high mountain site (MS) during the study period.

Period	T_{US} (°C)	T_{MS} (°C)	RH_{US} (%)	RH_{MS} (%)	v_{US} (m·s^{-1})	v_{MS} (m·s^{-1})
Oct-2010	18.6	9.9	62.5	63.6	0.8	5.4
Nov-2010	14.9	4.0	56.5	81.5	1.2	7.9
Dec-2010	11.2	3.8	64.6	67.4	0.9	7.0
Jan-2011	11.5	2.4	65.5	77.9	0.8	5.9
Feb-2011	11.9	3.5	58.6	66.5	1.0	7.0
Global	13.7	4.7	61.5	71.4	0.9	6.7

T: Temperature; v: Wind speed; RH: Relative Humidity.

2.2. Meteorological differences between the measurement sites

Despite the proximity between the two monitoring sites, significant differences of meteorological parameters can be observed (Table 1). These variations are caused by the difference in altitude among the two locations. During the measurement period (from October 2010 to February 2011) the temperature at the high mountain site was on average 9 °C lower than at the urban area. The temperature gradient, quite constant during the whole study period, was approximately −6.2 °C km^{-1}. Considerable differences between wind speed and relative humidity were also found. Average wind speed was about 7 times higher at the mountain site than at the coastal urban area. As regards relative humidity, it was also higher at MS, especially in November. This was not unexpected since, as air masses coming from the sea are transported up through the valleys and mountain slopes, the decrease in ambient temperature causes an increase in relative humidity.

It is interesting to point out that solar radiation is systematically higher at the mountain site because it is frequently above the cloud layer. During the cold months differences in radiation intensity are low (119 W m^{-2} at MS against 112 W m^{-2} at US); however, variations are more significant during summer.

2.3. Data collection and analysis

As indicated in the previous section, the study period was from

October 2010 until February 2011. PM_1 concentrations at both sites were measured by means of two optical counters Grimm 190 previously calibrated. This instrument determines particle number concentrations in 31 size channels from 0.25 μm to >32 μm. The conversion to mass fractions is conducted using an internal algorithm. According to the manufacturer, the uncertainty in the determination of the mass concentration is about 10%. The measurements were made with 10 min time resolution. Hourly and daily averages were subsequently calculated based on counter data.

At the urban site, the concentrations of other pollutants (NO_x, PM_{10}) and meteorological variables (temperature, wind speed and direction, solar radiation intensity, precipitation, relative humidity and atmospheric pressure) were also measured by the Regional Environmental Surveillance Network. Meteorological data at the high mountain site were provided by a meteorological station located in the military base.

Meteorological maps from the National Center for Environmental Prediction (NCEP, http://www.esrl.noaa.gov/psd/data/composites/hour/) were checked in order to analyze the synoptic meteorological scenarios. Back-trajectory analysis (HYSPLIT model, Draxler and Rolph 2013) was used to observe the path length of air masses below the mixing layer height. The GDAS meteorological files have been used as input data. These input files have one-degree of spatial resolution.

Three-day back trajectories ending in Alicante at 500 m a.s.l. were obtained at 12 UTC for days of highly stable atmospheric conditions. A data base containing details of differential events affecting the study region (http://www.calima.ws) was also consulted. To determine the convective Boundary layer (CBL) height the webpage (http://ready.arl.noaa.gov/READYamet.php) from the National Oceanic Atmospheric Administrator (NOAA) Air Resources Laboratory was used.

The autocorrelation function (ACF) has been used in this work to elucidate diurnal patterns in pollutant concentrations. The autocorrelation function is the cross-correlation of a signal with itself at different points in time. It provides information on the similarity between observations as a function of the time lag between them. ACF is a tool for finding repeating patterns, such as the presence of a periodic signal.

2.4. Methodology applied for the identification of severe pollution episodes

Severe pollution episodes (SPEs) occurring in the urban area must be identified in order to determine whether atmospheric particulate matter accumulated over the coastal urban regions was transported to the high mountain site The evolution of the following parameters was used in order to detect this type of events:

- Convective boundary layer (CBL) height: A decrease in the CBL height (12Z) with respect to the average value must be observed. The average CBL height during this time of the year is around 900 m a.s.l.
- Pressure: During the event the persistence of a high pressure system must be detected. This situation is often accompanied by a weak pressure gradient and slow winds near the surface. Under this meteorological context, low intensity sea-breeze regimes can be established in coastal areas (Segura et al., 2013). Back trajectories of air masses below the mixing layer are normally very short during this type of episodes.
- Variation of other meteorological parameters and pollutant concentrations: The days characterized by stagnant conditions usually show a gradual increase in the concentrations of PM and other pollutants such as NO_x, as well as relative humidity.

Although this meteorological situation favors the accumulation of pollutants near the emission sources, it has to be considered that daily average concentrations of pollutants do not necessarily increase during all days with meteorological conditions characteristic of an SPE. Sometimes pollutant concentrations build-up is detected with one or two days delay. For this reason, we only considered that PM_1 levels at the urban location were influenced by atmospheric stagnant conditions when the daily average concentration was higher than the average value obtained for the whole study period. On the other hand, the analysis of SPEs will be focused on those events with time duration of at least three days. This condition was imposed because we consider that it is the minimum period required for detecting the build-up of PM_1 at both measurement sites. This criterion is particularly important at MS in order to rule out specific days with high PM_1 levels due to other reasons.

A description of the synoptic scenarios (backward trajectories and pressure maps) during the first fortnight of February 2011, when the strongest SPE took place, is shown in the Supplementary Material. The variability of the PBL height during this period has also been included.

3. Results and discussion

3.1. PM_1 temporal variations

The average PM_1 concentration obtained for the entire study period at the mountain site was 3.6 ± 1.0 μg m^{-3}. This value was low compared with those reported for other regional background sites like Mount Cimone (7 μg m^{-3} summer average, 2165 m a.s.l.; Marenco et al., 2006) or Montseny (11 μg m^{-3} annual average, 720 m a.s.l.; Querol et al., 2009). However, it was two times higher than the concentration measured at the Jungfraujoch high alpine station (1.7 μg m^{-3} winter average, 3580 m a.s.l.; Cozic et al., 2008) and also higher than the nocturnal average value obtained at Mount Cimone during winter (1.2 μg m^{-3}), when the peak constantly resides in the free troposphere (Carbone et al., 2014) Therefore, altitude and measurement period might be affecting factors that may influence PM_1 concentrations measured at this type of environment.

The mean PM_1 concentration registered at the urban location (10.5 ± 6.4 μg m^{-3}) was significantly lower than the values found in Mediterranean cities with greater number of inhabitants like Barcelona (Pérez et al., 2010), Milan (Vecchi et al., 2008) or Athens (Pateraki et al., 2014). It was also lower than that reported for an urban street canyon in the nearby city of Elche (13.3 ± 5.2 μg m^{-3}; Yubero et al., 2015) due to reduced pollutant dispersion in semi-enclosed spaces surrounded by buildings.

As shown in Fig. 2, the variability of PM_1 levels was significantly larger at the urban area than at the mountain site. Only during the months October 2010 and February 2011 a noticeable variability of PM_1 concentrations at MS was observed. Predictably, this was due to the impact of PM events occurring during several days of those months. At the beginning of October 2010 there was a Saharan dust intrusion lasting 7 days that affected the study area. The average PM_1 concentration for that period at MS was 8 μg m^{-3}. As regards the urban station, the highest value of the 75th percentile was registered in February 2011 due to a SPE of 9-days duration.

During the entire study period, the highest daily PM_1 concentrations at US and MS were, respectively, 47 and 14.5 μg m^{-3}, while the minima were 1 and <0.5 μg m^{-3}.

The average PM_1 diurnal variation between the urban and mountain sites had clear differences (Fig. 3).

PM_1 concentrations at MS were quite constant throughout the day, with a broad maximum coincident with the period of highest solar radiation (14:00–17:00 UTC). This is the typical diurnal cycle

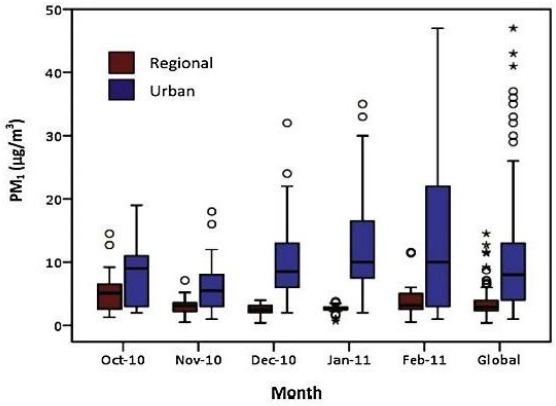

Fig. 2. Box plot of PM_1 concentrations at the urban and high mountain sites. The horizontal line inside the box is the median. The upper and lower limits of the boxes represent 25th and 75th percentiles. Maximum and minimum concentrations are represented by dashes (–). Hollow circles denote unusual values and stars indicate extreme concentrations (values higher than the 75th percentile plus three times the length of the box).

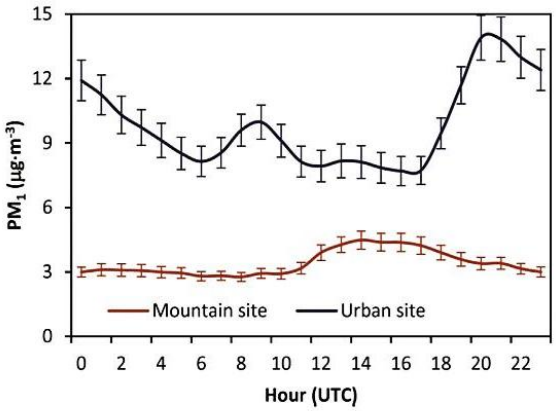

Fig. 3. Average diurnal cycle of PM_1 at the urban and high mountain sites. Error bars represent standard errors.

of PM_1 in regional background sites of the western Mediterranean basin during the autumn-winter period, which mainly depends on the dominant breeze circulation (mountain and sea breezes; Querol et al., 2009). When diurnal breeze develops due to increased insolation, pollutants accumulated in highly populated coastal regions are transported upwards to MS, increasing PM_1 levels. During the night, prevailing down-slope winds and the reduction in the mixing layer height decrease PM_1 concentrations. Instead, the urban cycle was clearly influenced by road traffic emissions, showing an absolute maximum (~14 µg m^{-3}) between 20:00 and 21:00 UTC. The peak in traffic intensity during the evening rush hour coupled with a lower mixing height at night in winter might account for this increase in PM_1 levels (Hasheminassab et al., 2014). The secondary maximum at around 9:00 UTC did not correlate with the maximum at 21:00 UTC since the autocorrelation function (Fig. 4) showed a peak positive correlation for a time lag of 24 h instead of 12 h for the urban site. This was due to the different shape of the peaks. During daytime, winds are usually stronger and a quick reduction in PM_1

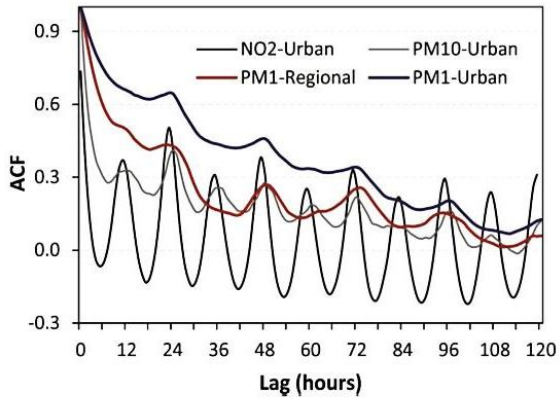

Fig. 4. Autocorrelation analysis for PM and NO_2 at the urban and high mountain stations.

concentrations was observed after the morning rush hour. In contrast, a slower reduction in PM_1 levels was detected during nighttime due to calm winds and a decrease in the mixing layer height. Autocorrelation coefficients were lower at MS than at US, indicating a weaker diurnal cycle at the high mountain site.

Fig. 4 also shows a higher association of nitrogen dioxide (used as a tracer of traffic activity; Caballero et al., 2012) with PM_{10} than PM_1 at the urban site. Both NO_2 and PM_{10} had a significant autocorrelation at a 12 h time lag. These peaks correspond to morning and evening rush hours. The former results indicate that the coarse fraction of PM_{10} was more strongly affected by traffic emissions (road dust resuspension and/or direct exhaust emissions) than the submicron fraction (Pey et al., 2008).

3.2. *Effect of severe pollution episodes on PM_1*

Table 2 presents the severe pollution episodes identified during the study period following the methodology described in Section 2.4. We considered that PM_1 levels were affected by the accumulation process associated with the stagnant meteorology when the daily average concentration at US and MS was higher than the average value obtained for the entire study period at each site.

The intensity and duration of the SPEs identified during the measurement period was variable. The longest and most intense event occurred during the first half of February. During this episode the daily average PM_1 concentration at the urban site reached a value of 47 µg m^{-3}, the highest of the whole study period. Obviously, all the SPEs affected PM_1 concentrations at the urban area, but not at the high mountain station. In fact, only 37.5% of the days with stagnant conditions had PM_1 daily concentrations above the average value at MS. The reasons will be discussed in detail in Section 3.3.

Fig. 5 shows average increases in PM_1 concentrations during this type of events at both locations. These increases were calculated by subtracting mean hourly concentrations on days not affected by SPEs from average values obtained during SPEs (9 and 24 days, respectively, at MS and US).

It is well known that the stagnation of air masses over areas of high emissions causes the accumulation of particles and other pollutants and consequently coagulation between particles. The condensation of semi-volatile species onto preexisting particles is also favored (Pey et al., 2008). These phenomena were responsible for the significant hourly increases in PM_1 levels observed at the

Table 2
Characteristics of the severe pollution episodes detected between October 2010 and February 2011. The duration of each episode is indicated in parenthesis. Mass concentrations are given in μg m^{-3}.

N	Date[a]	Days with $PM_{1\text{-Urban}}$ affected[b]	$PM_{1\text{-Urban}}$ max	Days with $PM_{1\text{-Regional}}$ affected[b]	$PM_{1\text{-Regional}}$ max
SPE 1	22-24 Oct-2010 (3)	2	19	2	9.2
SPE 2	26-29 Oct-2010 (4)	2	15	–	–
SPE 3	11-14 Nov-2010 (4)	1	18	1	4.7
SPE 4	26-29 Dec-2010 (4)	3	24	–	–
SPE 5	3-6 Jan-2011 (4)	3	16	–	–
SPE 6	12-15 Jan-2011 (4)	4	21	–	–
SPE 7	4-12 Feb-2011 (9)	9	47	6	11.6
Global	7 SPE (31)	24		9	

[a] Time period with favorable meteorological conditions to produce a SPE.
[b] Number of days during a SPE with daily PM_1 concentrations higher than the average value for the whole study period.

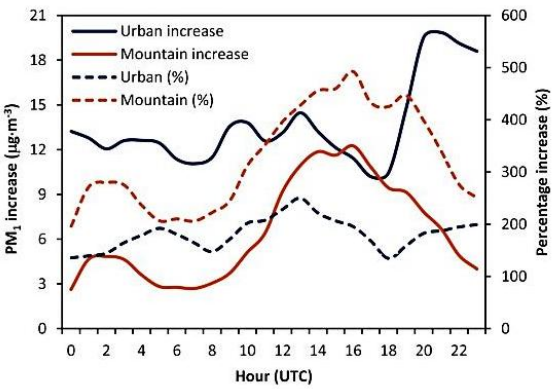

Fig. 5. Increase in PM_1 concentrations during SPEs at the urban and high mountain sites.

urban site. The increments were fairly constant throughout the day (between 12 and 15 μg m^{-3}) except for that registered at 20:00–21:00 UTC (20 μg m^{-3}). This maximum was most probably the result of an increase in traffic intensity during the evening rush hour together with a decrease in the mixing layer height and temperature, favoring the accumulation of pollutants and condensation of semi-volatile compounds.

The physical processes responsible for the increases in PM levels at the high mountain site were different. The observed increases in PM_1 concentrations during SPEs were due to pollutant transport (by marine and mountain breezes) from the accumulation areas (coastal cities) to the high mountain site. Another important process that might have caused an increase in PM_1 levels at the high mountain location, especially at midday, was the formation of secondary aerosols during transport favored by the intense solar radiation characteristic of this type of episodes. The maximum increase (~12 μg m^{-3} around 16:00 UTC) was even slightly higher than the increment observed for the urban site at the same hour. Similar results were obtained by Pey et al. (2010) at the Montseny station.

3.3. Impact of severe pollution episodes at the high mountain station

The results shown in Table 2 clearly demonstrate that many of the SPEs detected at the urban area did not impact PM_1 concentrations at the high mountain site. Next, the conditions favorable for PM transport from the coastal area to the high mountain site will be analyzed.

Table 3 shows average values of daily maximum sea-breeze velocities and CBL heights for each event. Differences between the CBL height at the mountain station and the urban site are also presented.

From the seven episodes identified during the research period, only three registered significant increases in PM_1 concentrations at the mountain station. The first condition for an effective transport of pollutants generated in urban coastal areas to the high mountain site is the development of a light coastal sea-breeze. As observed in Table 3, this situation occurred in all the events detected during the measurement campaign. However, for a further inland penetration of air masses the development of an up-slope flow is also essential. A high positive increment of the CBL height between the mountain site and the coastal area would favor a good development of mountain breezes and therefore would make the transport of pollutants to the mountain summit more effective. The three events that had a clear impact on PM_1 levels at the mountain site showed notable increases in CBL heights between MS and US. Although the increase in the CBL height was highest for SPE 5, a growth in PM_1 concentrations at MS was not recorded during this episode possible because the strong anticyclonic conditions at surface level weakened as height increased. This situation induced a synoptic wind circulation uncoupled with the surface wind during morning and midday hours, preventing PM transport to the mountain site.

Another factor that could affect the transport between both sites is the value of the CBL height. If this value is too low (for example, SPE 4) recirculation of air masses may occur due to the complex orography of the terrain (see Fig. 1) preventing pollutants from reaching the mountain top.

The meteorology of the strongest episode detected during the measurement period is analyzed in detail in Fig. 6. The hourly variation of meteorological parameters, CBL heights and PM_1 concentrations during SPE 7 is plotted for both sites. Only six out of nine days are represented (from 6 to 11 February 2011).

Table 3
Averages of daily maximum sea-breeze speeds and convective boundary layer depths for the events identified during the study period. ΔMH represents the difference between the CBL height at the mountain station and the urban site.

N[a]	v_{max} ($m \cdot s^{-1}$)[b]	$MH_{Regional}$ (m)[c]	MH_{Urban} (m)[c]	ΔMH (m)[c]
SPE 1	1.8	1208	1068	140
SPE 2	1.5	584	565	19
SPE 3	2.0	808	691	118
SPE 4	1.4	367	402	−36
SPE 5	1.8	857	637	148
SPE 6	1.6	555	547	7
SPE 7	1.6	800	692	108

[a] Events that impacted on the mountain station are shown in bold type.
[b] Average value of daily maximum sea-breeze speeds measured at the urban site.
[c] MH: Average CBL height.

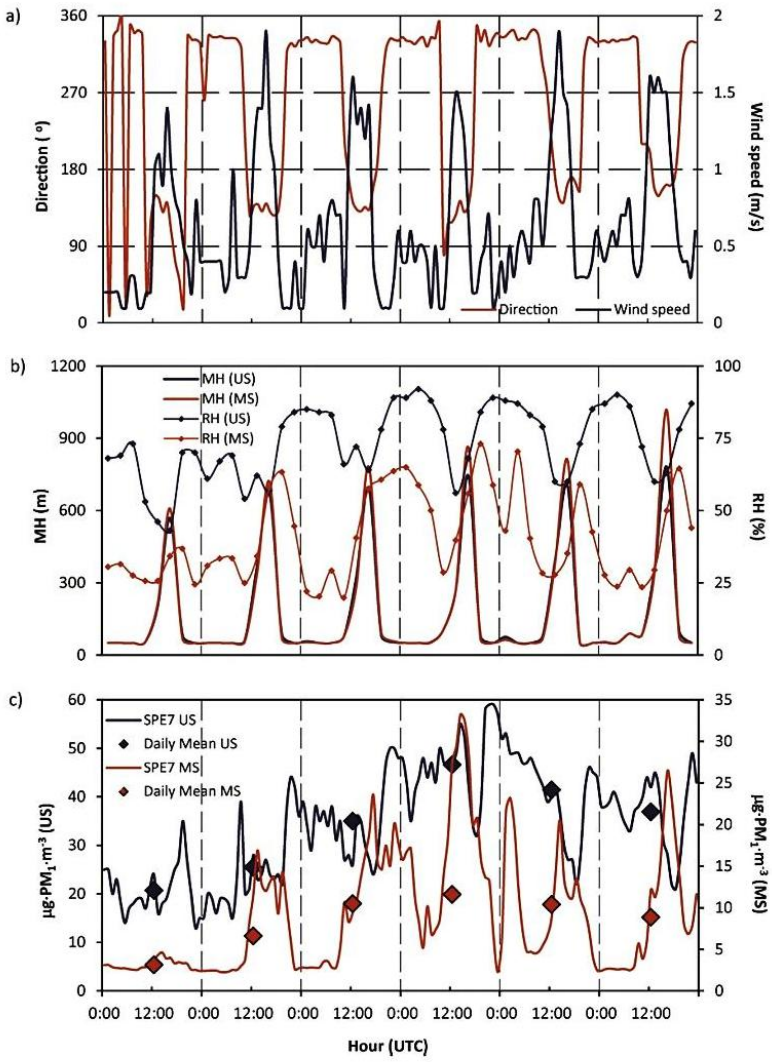

Fig. 6. Hourly average values of (a) wind speed and direction at US; (b) mixing height and relative humidity and; (c) PM_1 concentrations during SPE 7.

It can be observed that, as the episode developed, a progressive increase in PM_1 levels and relative humidity occurred. As already shown in Fig. 5, the largest increments at the urban station were observed about 20:00–21:00 UTC. The maximum hourly concentration during the event was registered on 9 February with a value of approximately 60 µg m^{-3}. It is interesting to highlight that, while at US PM_1 concentrations remained high during the night, PM_1 levels at MS fell to background values. During the night, downslope winds prevail within a fully formed valley temperature inversion sweeping pollutants away from the monitoring station. Fig. 6a shows that a weak sea breeze was established during those days since the highest wind speed during the central hours of the day was 1.9 m s^{-1} Fig. 6b compares the evolution of the mixing layer depth at both stations. Between 8 and 11 February the mixing layer height was greater (between 100 and 200 m) at the high mountain site than at the urban location during the time of maximum solar radiation. This might be the result of warming of valleys and mountain slopes favoring the development of the mountain breeze. Under these conditions, particulate matter from the coastal urban area could have been transported inland by the sea breeze and then by the mountain breeze up to the mountain summit where the monitoring site was located. At this site an evident diurnal pattern was observed, with peak hourly concentrations of almost 35 µg m^{-3} occurring between 12:00 and 18:00 UTC.

In addition to the synoptic meteorological conditions favoring a stagnation situation, local meteorological conditions as those depicted in Fig. 6a and b are required for the transport of pollutants from the coast up to the mountain summit. The fact than only on 37.5% of days with stagnant conditions PM_1 concentrations build-up at MS was noticed (Table 2) indicate that pollutant transport is difficult due to the complex orography of the terrain. The results

suggest that a significant increase in PM_1 levels at MS during a stagnant episode is observed when a combination of the following conditions occurs: (1) PM_1 concentrations at US are very high and a weak sea-breeze develops, (2) the increase in the CBL height along the route from the coast to the mountain summit is enough to favor the development of up-slope flows, and (3) the strong anticyclonic conditions at surface level remain at higher altitudes to avoid the local circulation to be decoupled from the synoptic flow above. If this does not happen, then medium-range transport is not effective. A brief description of an event in which aerosols were not transported from the coast to the mountain summit is included in the Supplementary Material).

4. Conclusions

The average PM_1 concentrations measured at a coastal urban and a high mountain site of the western Mediterranean basin between October 2010 and February 2011 were, respectively, 10.5 and 3.6 $\mu g\ m^{-3}$. During the study period, variations in daily PM_1 levels were significantly affected by severe pollution episodes (SPE) produced by stagnant weather conditions. Although not all SPEs had an impact on PM_1 levels at the high mountain site, daily concentrations considerably higher than the average values were measured at both stations during the most intense events (47 and 11.6 $\mu g\ m^{-3}$ at the urban and high mountain sites, respectively). At the urban location, the largest hourly increases with respect to the values registered on non-polluted days (20 $\mu g\ m^{-3}$) were observed around 20:00–21:00 UTC coinciding with the evening peak in traffic flow. This was due to the decrease in the mixing layer height and temperature that favor the accumulation of pollutants and the condensation of semi-volatile compounds. Instead, at the high mountain site a maximum increase of 12 $\mu g\ m^{-3}$ were registered around 16:00 UTC. The most likely explanation is that aerosols emitted in the urbanized coastal plain are carried inland by sea and mountain breezes. Additionally, the high solar radiation typical of these episodes may favor the photochemical formation of secondary aerosols during transport. For an efficient transport between both measurement sites through a complex orographic terrain, specific conditions must occur: (1) Strong increases in PM_1 concentrations at the coastal urban area in combination with a sufficient sea-breeze development, (2) a significant positive difference of the mixing layer height between the high mountain station and the coastal area to favor intense up-slope flows and, (3) a strong anticyclonic weather regime to prevent the local circulation to be decoupled from the synoptic flow above.

Acknowledgments

This work was co-financed by the Spanish Ministry of Science and Innovation under the CGL2009-08036 (PASSE) and CGL2012-39623-C02-2 (PRISMA) projects, and by the European Union through FEDER funds. We would like to thank the military base (EVA no. 5) for allowing access to its facilities.

Appendix A. Supplementary data

Supplementary data related to this article can be found at http://dx.doi.org/10.1016/j.atmosenv.2015.07.042.

References

Bonasoni, P., Cristofanelli, P., Calzolari, F., Bonafè, U., Evangelisti, F., Stohl, A., Zauli Sajani, S., van Dingenen, R., Colombo, T., Balkanski, Y., 2004. Aerosol-ozone correlations during dust transport episodes. Atmos. Chem. Phys. 4, 1201–1215.

Caballero, S., Galindo, N., Pastor, C., Varea, M., Crespo, J., 2007. Estimated tropospheric ozone levels on the southeast Spanish Mediterranean coast. Atmos. Environ. 41, 2881–2886.

Caballero, S., Esclapez, R., Galindo, N., Mantilla, E., Crespo, J., 2012. Use of a passive sampling network for the determination of urban NO_2 spatiotemporal variations. Atmos. Environ. 63, 148–155.

Carbone, C., Decesari, S., Paglione, M., Giulianelli, L., Rinaldi, M., Marinoni, A., Cristofanelli, P., Didiodato, A., Bonasoni, P., Fuzzi, S., Facchini, M.C., 2014. 3-year chemical composition of free tropospheric PM_1 at the Mt. Cimone GAW global station – South Europe – 2165 m a.s.l. Atmos. Environ. 87, 218–227.

Cozic, J., Verheggen, B., Weingartner, E., Crosier, J., Bower, K.N., Flynn, M., Coe, H., Henning, S., Steinbacher, M., Henne, S., Collaud Coen, M., Petzold, A., Baltensperger, U., 2008. Chemical composition of free tropospheric aerosol for PM_1 and coarse mode at the high alpine site Jungfraujoch. Atmos. Chem. Phys. 8, 407–423.

Galindo, N., Varea, M., Gil-Moltó, J., Yubero, E., Nicolás, J., 2011. The influence of meteorology on particulate matter concentrations at an urban Mediterranean location. Water Air Soil Pollut. 215, 365–372.

Galindo, N., Gil-Moltó, J., Varea, M., Chofre, C., Yubero, E., 2013. Seasonal and interannual trends in PM levels and associated inorganic ions in southeastern Spain. Microchem. J. 110, 81–88.

Gangoiti, G., Millán, M.M., Salvador, R., Mantilla, E., 2001. Long range transport and re-circulation of pollutants in the Western Mediterranean during the RECAPMA Project. Atmos. Environ. 35, 6267–6276.

Hai, C.D., Oanh, N.T.K., 2013. Effects of local, regional meteorology and emission sources on mass and compositions of particulate matter in Hanoi. Atmos. Environ. 78, 105–112.

Ham, W.A., Herne, J.D., Green, P.G., Kleeman, M.J., 2010. Size distribution of health-relevant trace elements in airborne particulate matter during a severe winter stagnation event: implications for epidemiology and inhalation exposure studies. Aerosol Sci. Technol. 44, 753–765.

Hasheminassab, S., Pakbin, P., Delfino, R.J., Schauer, J.J., Sioutas, C., 2014. Diurnal and seasonal trends in the apparent density of ambient fine and coarse particles in Los Angeles. Environ. Pollut. 187, 1–9.

Hinz, K.–P., Trimborn, A., Weingartner, E., Henning, S., Baltensperger, U., Spengler, B., 2005. Aerosol single particle composition at the Jungfraujoch. J. Aerosol Sci. 36, 123–145.

Jorba, O., Pandolfi, M., Spada, M., Baldasano, J.M., Pey, J., Alastuey, A., Arnold, D., Sicard, M., Artiñano, B., Revuelta, M.A., Querol, X., 2013. Overview of the meteorology and transport patterns during the DAURE field campaign and their impact to PM observations. Atmos. Environ. 77, 607–620.

Katzman, T.L., Rutter, A.P., Schauer, J.J., Lough, G.C., Kolb, C.J., Van Klooster, S., 2010. $PM_{2.5}$ and $PM_{10-2.5}$ compositions during wintertime episodes of elevated PM concentrations across the Midwestern USA. Aerosol Air Qual. Res. 10, 140–153.

Kassomenos, P.A., Kelessis, A., Paschalidou, A.K., Petrakakis, M., 2011. Identification of sources and processes affecting particulate pollution in Thessaloniki, Greece. Atmos. Environ. 45, 7293–7300.

Masiol, M., Squizzato, S., Ceccato, D., Pavoni, B., 2015. The size distribution of chemical elements of atmospheric aerosol at a semi-rural coastal site in Venice (Italy). The role of atmospheric circulation. Chemosphere 119, 400–406.

Marenco, F., Bonasoni, P., Calzolari, F., Ceriani, M., Chiari, M., Cristofanelli, P., D'Alessandro, A., Fermo, P., Lucarelli, F., Mazzei, F., Nava, S., Piazzalunga, A., Prati, P., Valli, G., Vecchi, R., 2006. Characterization of atmospheric aerosols at Monte Cimone, Italy, during summer 2004: source apportionment and transport mechanisms. J. Geophys. Res. 111, D24202.

Mira-Salama, D., Van Dingenen, R., Gruening, C., Putaud, J.–P., Cavalli, F., Cavalli, P., Erdmann, N., Dell'Acqua, A., Dos Santos, S., Hjorth, J., Raes, F., Jensen, N.R., 2008. Using Föhn conditions to characterize urban and regional sources of particles. Atmos. Res. 90, 159–169.

Monks, P.S., Granier, C., Fuzzi, S., Stohl, A., Williams, M.L., Akimoto, H., Amann, M., Baklanov, A., Baltensperger, U., Bey, I., Blake, N., Blake, R.S., Carslaw, K., Cooper, O.R., Dentener, F., Fowler, D., Fragkou, E., Frost, G.J., Generoso, S., Ginoux, P., Grewe, V., Guenther, A., Hansson, H.C., Henne, S., Hjorth, J., Hofzumahaus, A., Huntrieser, H., Isaksen, I.S.A., Jenkin, M.E., Kaiser, J., Kanakidou, M., Klimont, Z., Kulmala, M., Laj, P., Lawrence, M.G., Lee, J.D., Liousse, C., Maione, M., McFiggans, G., Metzger, A., Mieville, A., Moussiopoulos, N., Orlando, J.J., O'Dowd, C.D., Palmer, P.I., Parrish, D.D., Petzold, A., Platt, U., Pöschl, U., Prévôt, A.S.H., Reeves, C.E., Reimann, S., Rudich, Y., Sellegri, K., Steinbrecher, R., Simpson, D., ten Brink, H., Theloke, J., van der Werf, G.R., Vautard, R., Vestreng, V., Vlachokostas, Ch, von Glasow, R., 2009. Atmospheric composition change – global and regional air quality. Atmos. Environ. 43, 5268–5350.

Nicolás, J., Chiari, M., Crespo, J., Galindo, N., Lucarelli, F., Nava, S., Yubero, E., 2011. Assessment of potential source regions of PM2.5 components at a southwestern Mediterranean site. Tellus B 63, 96–106.

Nicolás, J.F., Crespo, J., Yubero, E., Soler, R., Carratalá, A., Mantilla, E., 2014. Impacts on particles and ozone by transport processes recorded at urban and high-altitude monitoring stations. Sci. Total Environ. 466–467, 439–446.

Park, S.S., Kleissl, J., Harrison, D., Kumar, V., Nair, N.P., Adam, M., Ondov, J., Parlange, M., 2006. Characteristics of PM2.5 episodes revealed by semi-continuous measurements at the Baltimore supersite at Ponca St. Aerosol Sci. Technol. 40, 845–860.

Pateraki, St, Asimakopoulos, D.N., Bougiatioti, A., Maggos, Th, Vasilakos, Ch, Mihalopoulos, N., 2014. Assessment of $PM_{2.5}$ and PM_1 chemical profile in a multiple-impacted Mediterranean urban area: origin, sources and meteorological dependence. Sci. Total Environ. 479–480, 210–220.

Pérez, N., Pey, J., Cusack, M., Reche, C., Querol, X., Alastuey, A., Viana, M., 2010.

Variability of particle number, black carbon, and PM_{10}, $PM_{2.5}$, and PM_1 levels and speciation: influence of road traffic emissions on urban air quality. Aerosol Sci. Technol. 44, 487–499.

Pey, J., Rodríguez, S., Querol, X., Alastuey, A., Moreno, T., Putaud, J.P., Van Dingenen, R., 2008. Variations of urban aerosols in the western Mediterranean. Atmos. Environ. 42, 9052–9062.

Pey, J., Pérez, N., Querol, X., Alastuey, A., Cusack, M., Reche, C., 2010. Intense winter atmospheric pollution episodes affecting the. West. Mediterr. Sci. Total Environ. 408, 1951–1959.

Pietrogrande, M.C., Bacco, D., Visentin, M., Ferrari, S., Poluzzi, V., 2014. Polar organic marker compounds in atmospheric aerosol in the Po Valley during the Supersito campaigns — part 1: low molecular weight carboxylic acids in cold seasons. Atmos. Environ. 86, 164–175.

Querol, X., Alastuey, A., Pey, J., Cusack, M., Pérez, N., Mihalopoulos, N., Theodosi, C., Gerasopoulos, E., Kubilay, N., Koçak, M., 2009. Variability in regional background aerosols within the Mediterranean. Atmos. Chem. Phys. 9, 4575–4591.

Segura, S., Estellés, V., Esteve, A.R., Utrillas, M.P., Martinez-Lozano, J.A., 2013. Analysis of a severe pollution episode in Valencia (Spain) and its effects on ground level particulate matter. J. Aerosol Sci. 56, 41–52.

Squizzato, S., Masiol, M., Innocente, E., Pecorari, E., Rampazzo, G., Pavoni, B., 2012. A procedure to assess local and long-range transport contributions to $PM_{2.5}$ and secondary inorganic aerosol. J. Aerosol Sci. 46, 64–76.

Strader, R., Lurmann, F., Pandis, S.N., 1999. Evaluation of secondary organic aerosol formation in winter. Atmos. Environ. 33, 4849–4863.

Uglietti, C., Leuenberger, M., Brunner, D., 2011. European source and sink areas of CO_2 retrieved from Lagrangian transport model interpretation of combined O_2 and CO_2 measurements at the high alpine research station Jungfraujoch. Atmos. Chem. Phys. 11, 8017–8036.

Vecchi, R., Marcazzan, G., Valli, G., 2007. A study on nighttime–daytime PM10 concentration and elemental composition in relation to atmospheric dispersion in the urban area of Milan (Italy). Atmos. Environ. 41, 2136–2144.

Vecchi, R., Chiari, M., D'Alessandro, A., Fermo, P., Lucarelli, F., Mazzei, F., Nava, S., Piazzalunga, A., Prati, P., Silvani, F., Valli, G., 2008. A mass closure and PMF source apportionment study on the sub-micron sized aerosol fraction at urban sites in Italy. Atmos. Environ. 42, 2240–2253.

Yubero, E., Galindo, N., Nicolás, J.F., Crespo, J., Calzolai, G., Lucarelli, F., 2015. Temporal variations of PM_1 major components in an urban street canyon. Environ. Sci. Pollut. Res. http://dx.doi.org/10.1007/s11356-015-4599-z **(in press).**

Anexo 4.

Depletion of tropospheric ozone associated with mineral dust outbreaks

Environ Sci Pollut Res (2016) 23:19376–19386
DOI 10.1007/s11356-016-7134-y

RESEARCH ARTICLE

Depletion of tropospheric ozone associated with mineral dust outbreaks

Ruben Soler[1] · **J. F. Nicolás**[1] · **S. Caballero**[1] · **E. Yubero**[1] · **J. Crespo**[1]

Received: 15 April 2016 / Accepted: 20 June 2016 / Published online: 4 July 2016

Abstract From May to September 2012, ozone reductions associated with 15 Saharan dust outbreaks which occurred between May to September 2012 have been evaluated. The campaign was performed at a mountain station located near the eastern coast of the Iberian Peninsula. The study has two main goals: firstly, to analyze the decreasing gradient of ozone concentration during the course of the Saharan episodes. These gradients vary from 0.2 to 0.6 ppb h^{-1} with an average value of 0.39 ppb h^{-1}. The negative correlation between ozone and coarse particles occurs almost simultaneously. Moreover, although the concentration of coarse particles remained high throughout the episode, the time series shows the saturation of the ozone loss. The highest ozone depletion has been obtained during the last hours of the day, from 18:00 to 23:00 UTC. Outbreaks registered during this campaign have been more intense in this time slot. The second objective is to establish from which coarse particle concentration a significant ozone depletion can be observed and to quantify this reduction. In this regard, it has been confirmed that when the hourly particle concentration recorded during the Saharan dust outbreaks is above the hourly particle median values (N > N-median), the ozone concentration reduction obtained is statistically significant. An average ozone reduction of 5.5 % during Saharan events has been recorded. In certain cases, this percentage can reach values of higher than 15 %.

Responsible editor: Gerhard Lammel

✉ Ruben Soler
ruben87sm@gmail.com

[1] Atmospheric Pollution Laboratory (LCA), Department of Applied Physics, Miguel Hernández University, Avenida de la Universidad S/N, 03202 Elche, Spain

Keywords O_3 reduction · Mountain station · Saharan dust outbreak · Coarse particles · Mineral dust · Seasonal component

Introduction

In the Western Mediterranean Basin (WMB), mineral particles and tropospheric ozone are two important components whose atmospheric dynamics are determined by the particular meteorological and orographic conditions that this geographical area presents.

Surface ozone is a secondary pollutant that can cause serious damage to human health, natural vegetation, crops, and materials (Paoletti 2006). Additionally, ozone acts as a potent greenhouse gas due to its ability to absorb light (IPCC 2013). Millán et al. (2000, 2002) and Caballero et al. (2007) describe in detail the complex processes responsible for the accumulation of ozone particularly during spring and summer due to orographic and human factors, and atmospheric dynamics in the WMB. The largest cities of the WMB are mostly located along the coastline, which is surrounded by mountain ranges reaching altitudes of approximately 1500 m. The populations of these cities increase during the summertime and consequently do the emissions of NO_x and other ozone precursors. On summer days, a strong vertical development of an unstable planetary boundary layer aided by the enhancement of coastal and mountain breezes facilitates the transport of these pollutants inland while strong sun insolation promotes their transformation into O_3 and other photochemical oxidants (Escudero et al. 2016). When the air masses reach the mountain barrier, whose southern and eastern slopes are strongly heated, these can act as orographic chimneys that favor the return of air masses aloft, with compensatory subsidence over the sea. This process causes the formation of stratified layers

Environ Sci Pollut Res (2016) 23:19376–19386

that act as reservoirs of aged pollutants, and the ozone in the lowest layers can be transported again by the sea breeze from the coast inland the following morning. As a result of these atmospheric re-circulations, O_3 persists along the Mediterranean basin for several days during periods of summer atmospheric stability, and its concentrations frequently exceed the European Community thresholds (Lelieveld et al. 2002; Castell-Balaguer et al. 2012; Escudero et al. 2014).

With regard to the mineral particles, the biggest contribution in the WMB is due to the frequent intrusion of air masses from northern Africa. This transport presents a seasonal trend pointing out a clear maximum during the spring and summer months (Escudero et al. 2005; Querol et al. 2009; Pey et al. 2013). Saharan dust outbreaks (SDOs) that take place during these months show a prevailing meteorological scenario that favors the transport of African dusty air masses towards the WMB. This pattern consists in the development of the North African thermal low caused by the intense heating. The dust is injected into the midtroposphere, and it is transported towards the WMB thanks to a high pressure system (850–700 hPa) (Escudero et al. 2005). Nevertheless, other meteorological patterns throughout the year can take place. These SDOs are primarily responsible for exceedances of the particulate matter (PM) limit value that occur in the regional background stations in this area (Escudero et al. 2007).

Dust particles may also play a significant role as a reactive surface on which heterogeneous chemistry can take place (Adame et al. 2015). Therefore, gaseous pollutants may interact with mineral dust varying their concentrations. Given the importance of these reactions, various studies have been carried out in an attempt to quantify this variation. These assessments have used different approaches. Laboratory experiments and the development of models have been performed (Zhang et al. 1994; Dentener et al. 1996; Zhang and Carmichael 1999; Hanisch and Crowley 2003); results obtained from models have been compared with field-observed data (de Reus et al. 2000; Bauer et al. 2004) and finally, field campaigns have been carried out to register in situ observations (Prospero et al. 1995; Bonasoni et al. 2004; Umann et al. 2005; Andrey et al. 2014; Adame et al. 2015).

These studies show that due to the interaction between mineral dust and ozone, the concentration of ozone decreases. This reduction not only takes place through direct uptake, in which O_3 is destroyed on the mineral aerosol surface and O_2 is produced (Bauer et al. 2004), but it has also been observed that heterogeneous surface reactions of several gasses on mineral aerosol may also be responsible for the tropospheric O_3 decrease. In this way, the depletion of HNO_3 and NO_3 on dust particles can remove some of the O_3 precursors (i.e., NO_x) favoring a reduction of photochemical O_3 production efficiency (Zhang and Carmichael 1999; Harrison et al. 2001). Under this premise, de Reus et al., 2000 state that both mechanisms, direct removal and heterogeneous removal of nitrogen species, mainly HNO_3, accounted for about 50 % of the total net ozone destruction. Umann et al. (2005) obtained an ozone reduction of 33 % during high dust concentration periods, and they confirmed that this decrease stops when the atmospheric HNO_3 has been completely removed. The comparison of ozone depletions observed under dust transport episodes, as can be observed during the Saharan dust outbreaks (SDOs), is complex since the timescale in which the ozone reduction is obtained differs among the different studies. In any case, apart from those already mentioned, maximum hourly reductions of 42 % with respect to monthly mean values have been obtained in Mt. Cimone (Italy) (Bonasoni et al. 2004). Depletions in the range of 13.9 to 17.7 % depending on the kind of the monitoring station have been found in southern Italy (Bencardino et al. 2011), comparing days under Saharan dust influence and days without any. On the other hand, Andrey et al. (2014) analyzed numerous ozone vertical profiles and found an ozone peak reduction (35 %) at about 4 km of altitude under Saharan dust outbreak periods in the Canary Islands.

Although it is known that the entry of air masses from the Sahara desert can rise the concentration of both, fine and coarse particles, it is also true that especially in stations located in the Mediterranean basin, the increase recorded by the coarse ones, it is more relevant (Contini et al. 2014; Nicolás et al. 2014; Brattich et al. 2015). Taking into account that the sampling point used in this study is located in the western Mediterranean, we have decided to analyze the interaction ozone-dust mineral only in the coarse fraction (particle size >1 μm) since these particles are the best indicator of SDOs and the main reason for ozone depletion (Bonasoni et al. 2004).

The aim of this work is to quantify the ozone concentrations reductions due to several SDOs detected at a mountain station. The study of interactions between ozone and coarse particles will be based on an hourly time scale allowing for a better observation of its features than with a daily time scale. Time series of ozone concentrations in which its seasonal component was removed have been used and as a result, the effect of the solar radiation on the ozone variability has been minimized. Consequently, ozone reductions shown in the manuscript have very little dependence with the variation of this meteorological variable. This approach has not been addressed in most studies that have dealt with this interaction. Moreover, a particle concentration from which the ozone depletion can be considered statistically significant will be determined.

Experimental

Monitoring site and data collection

The sampling site named "Aitana" (38°16'N; 0°41'W; 1558 m a.s.l) is on the top of a mountain range located inland

in the province of Alicante, in southeastern Spain. The station is situated 25 km from the Mediterranean coast and about 300 km from the nearest North Africa point (Fig. 1). These features make the station a good receptor of Saharan dust outbreaks. The station is placed inside a military area (EVA n° 5), but the anthropogenic activity in it is scarce. Data concentrations and temporal trends of PM at the site are reported by Nicolás et al. (2014) and Galindo et al. (2016).

The sampling site is mostly (~70 % of days) within the planetary boundary layer (PBL) during the midday in the warm period. Therefore, both particle and ozone concentrations may be affected by recirculation processes. This percentage falls to 30 % in autumn and winter seasons. A detailed characterization of the main meteorological parameters and the PBL dynamics in the study area can be consulted in Galindo et al. (2016).

The instrument used to measure particle concentration was an optical counter Grimm 190, which is able to determine particle number concentrations in 31 particle size channels from 0.25 to 32 μm with a 1-min time resolution. The instrument is based on the quantification of 90° scattering of light by particles. According to the manufacturer, the uncertainty in the particle counting determination is about 5 % and its resolution is 1 particle/liter. Previously to the campaign, the data (in mass concentration) provided by the Grimm spectrometer were verified by comparison with a gravimetric technique to ensure its correct operation. The correlation obtained, $PM_{10}(Grimm) = 1.11 \cdot PM_{10}(gravimetric)$ presented a correlation coefficient of $r = 0.84$.

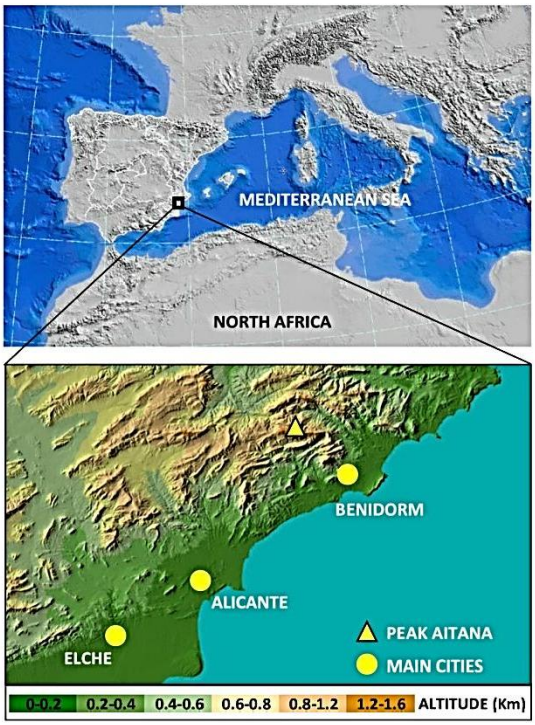

Fig. 1 Location and topography of the monitoring site on the Spanish Mediterranean coast

As aforementioned, only coarse particles (Ncoarse) have been considered in this study. Ncoarse values have been obtained as the result of the particle number concentration addition from each channel from 1 μm. Although it is known that the particles' diameters measured by Grimm change with the refractive index of the aerosol measured (Pio et al. 2014), this is not going to affect the particle number concentration. This effect should be taken into account just in the case the mass concentration is obtained from the number concentration data.

Concentrations of O_3 were registered using a Dasibi model 1008 UV absorption continuous analyzer. The analyzer has an accuracy of better than 5 % and 1-min time resolution. Meteorological data (temperature, wind velocity, solar radiation, precipitation, relative humidity) were obtained from a weather station located 10 m above the ground.

The study period comprised from May 2012 to September 2012. It is precisely during these months when the frequency of SDOs in the study area is at its highest during the year.

Removing the seasonal component of ozone data

The use of daily records to analyze the ozone-particle interaction may hide some of its features. For that reason, hourly data has been used to quantify the depletion of ozone concentrations produced by the interaction with Saharan PM. As such, to remove or at least to reduce the ozone variations due to intrinsic fluctuations, as caused by solar radiation, the hourly seasonal component in ozone data has been obtained using a time series classic model. In this additive model, time series (hourly O_3 value) can be considered the sum of three components: a trend component, a seasonal component, and an irregular component. The seasonal component informs us about the part of the ozone's daily oscillatory behavior, mainly due to meteorological variables. Although a well-defined trend component for ozone during the study period was not found, a clear hourly seasonal component was determined.

The seasonal component obtained can be seen in Fig. 2. As it can observe, ozone seasonal component attains a trough (−3.37 ppb) and a peak (+2.08 ppb) at 09:00 and 19:00 h (UTC), respectively. Possibly, this maximum shows the O_3 precursors transport from urban coastal areas to the sampling point due to breeze regimen. These hourly concentrations of the seasonal component will be subtracted from the hourly concentration of ozone throughout the whole time series to isolate the daily intrinsic fluctuations.

The hourly concentrations of ozone without this seasonal component will be used to determine a coarse particle concentration from which the ozone depletion can be considered

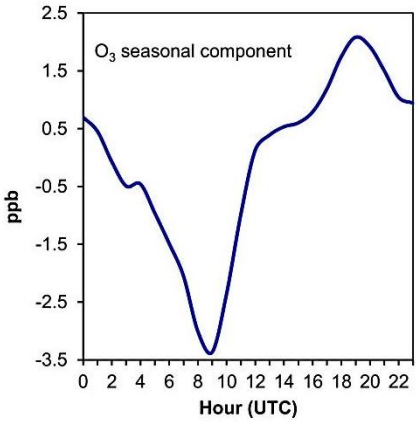

Fig. 2 Ozone seasonal component obtained from May to September 2012 and applied to hourly ozone data measured at sampling point

statistically significant (section 3.2.2) and to quantify the percentages of this depletion during SDOs (section 3.3).

SDO identification

The identification of Saharan dust events that passed through the area during the study period was checked in a governmental database (http:www.calima.ws). In that webpage, the identification of SDOs is carried out thanks to dust forecast models (NAAPS, DREAM, and SKIRON) along with a meteorological analysis based on ECMWF model. Moreover, a backtrajectory analysis (HYSPLIT model, Draxler and Rolph 2015) was used to confirm the north-African origin of the air masses during the SDOs identified. Four-day back-trajectories ending in the sampling point at 1500 and 3000 m a.s.l were obtained at 12:00 UTC for these days. The identification is validated by checking the particle concentration time series in regional background stations (RBS). This procedure is based on a methodology for the identification and quantification of the contribution of SDOs developed in Spain and Portugal (Querol et al. 2006). Information about the methodology and the use of the RBS can be consulted in http://ec.europa.eu/environment/air/quality/legislation/pdf/sec_2011_0208.pdf. The SDOs identified according to this method are shown in Table 2.

Results

Monthly and hourly ozone and coarse particles variations

Monthly average values of the main meteorological parameters obtained during the study period are shown in Table 1.

Table 1 Monthly average values for the main meteorological parameters

	T (°C)	SR (W m^{-2})	v (m s^{-1})	P (mm)	RH (%)
May-12	13.3	330.8	4.4	75.0	52.3
Jun-12	18.8	337.6	4.5	1.3	45.5
Jul-12	19.0	309.8	3.8	0.2	50.9
Ago-12	22.2	276.7	4.7	16.8	38.2
Sept-12	15.7	232.6	4.4	0.0	54.3
Global	17.8	297.8	4.4	93.3	48.0

T temperature, *SR* solar radiation, *v* wind speed, *RH* relative humidity, *P* total precipitation

The highest temperature value was registered in August, while levels of solar radiation were highest in May and June, with a decrease in September. Although the SR levels always increase from April to May, this year, the SR recorded in May was unusually high. Wind velocity was steady during the whole period. Very little precipitation was registered with most rainfall accumulated during 3 days only (two in May and one in August). Relative humidity showed low monthly average values. Nevertheless, RH can influence measurements in specific hours of day. It is known that optical instruments could be influenced by RH and that the output from these instruments increases with RH (Dinoi et al. 2016). For this reason, hourly particle data recorded with relative humidity higher than 70 % were not taken into account. We have considered this threshold since from values of RH > 70 %, particulate matter absorbs water vapor changing size and optical properties (Dinoi et al. 2016; Donateo et al. 2006). A procedure to correct the effect of RH on concentration measurements can be seen in Donateo et al. 2006.

Figure 3 shows the monthly evolution of the principal statistics parameters for coarse particles and ozone.

In Fig. 3a, it can be observed that the median value of particle concentration in August is between four and five times higher than that obtained in May. Also, the 25th percentile (P25) registered in August presents a similar value to the 75th percentiles (P75) obtained in May and September. These months, May and September, were less influenced by the Saharan dust than the others. A nearly reverse situation is produced in the ozone parameters (Fig. 3b), although the differences between months are not as clear as in the coarse particles case. The high ozone concentration obtained in May (57.5 ppb-median value) is associated with enhanced photochemical activity. An increase in solar radiation compared to April photodissociate to a greater extent the NO_2 that is accumulated during winter time (Monks 2000; Ribas and Peñuelas 2004; Escudero et al. 2016). Ozone concentration obtained in August (54.1 ppb-median value) is lower than in September (58.9 ppb-median value) and, therefore, is lower than expected considering the typical ozone trend in summer.